

APPLICATION, COMPARISON, AND IMPROVEMENT OF KNOWN
RECEIVED SIGNAL STRENGTH INDICATION (RSSI) BASED INDOOR
LOCALIZATION AND TRACKING METHODS USING ACTIVE RFID
DEVICES

A THESIS SUBMITTED TO
THE GRADUATE SCHOOL OF NATURAL AND APPLIED SCIENCES
OF
MIDDLE EAST TECHNICAL UNIVERSITY

BY

BORA ÖZKAYA

IN PARTIAL FULFILLMENT OF THE REQUIREMENTS
FOR
THE DEGREE OF MASTER OF SCIENCE
IN
ELECTRICAL AND ELECTRONICS ENGINEERING

FEBRUARY 2011

Approval of the thesis:

**APPLICATION, COMPARISON, AND IMPROVEMENT OF KNOWN
RECEIVED SIGNAL STRENGTH INDICATION (RSSI) BASED INDOOR
LOCALIZATION AND TRACKING METHODS USING ACTIVE RFID
DEVICES**

submitted by **BORA ÖZKAYA** in partial fulfillment of the requirements for the degree of **Master of Science in Electrical and Electronics Engineering Department, Middle East Technical University** by,

Prof. Dr. Canan Özgen _____
Dean, Graduate School of **Natural and Applied Sciences**

Prof. Dr. İsmet Erkmen _____
Head of Department, **Electrical and Electronics Engineering**

Dr. Arzu Koç _____
Supervisor, **Electrical and Electronics Eng. Dept., METU**

Prof. Dr. Sencer Koç _____
Co-Supervisor, **Electrical and Electronics Eng. Dept., METU**

Examining Committee Members:

Prof. Dr. Yalçın Tanık _____
Electrical and Electronics Engineering Dept., METU

Dr. Arzu Koç _____
Electrical and Electronics Engineering Dept., METU

Assoc. Prof. Dr. Çağatay Candan _____
Electrical and Electronics Engineering Dept., METU

Assoc. Prof. Dr. Ali Özgür Yılmaz _____
Electrical and Electronics Engineering Dept., METU

Haluk Karaca, M.Sc. _____
Manager, MGE0 HKSTM, ASELSAN A.Ş.

Date: 09.02.2011

I hereby declare that all information in this document has been obtained and presented in accordance with academic rules and ethical conduct. I also declare that, as required by these rules and conduct, I have fully cited and referenced all material and results that are not original to this work.

Name, Last Name: Bora Özkaya

Signature :

ABSTRACT

APPLICATION, COMPARISON, AND IMPROVEMENT OF KNOWN
RECEIVED SIGNAL STRENGTH INDICATION (RSSI) BASED INDOOR
LOCALIZATION AND TRACKING METHODS USING ACTIVE RFID
DEVICES

ÖZKAYA, Bora

M.Sc., Department of Electrical and Electronics Engineering

Supervisor: Dr. Arzu KOÇ

Co-Supervisor: Prof. Dr. Sencer KOÇ

February 2011, 151 pages

Localization and tracking objects or people in real time in indoor environments have gained great importance. In the literature and market, many different location estimation and tracking solutions using received signal strength indication (RSSI) are proposed. But there is a lack of information on the comparison of these techniques revealing their weak and strong behaviors over each other. There is a need for the answer to the question; “which localization/tracking method is more suitable to my system needs?”. So, one purpose of this thesis is to seek the answer to this question. Hence, we investigated the behaviors of commonly proposed localization methods, mainly nearest neighbors based methods, grid based Bayesian filtering and particle filtering methods by both simulation and experimental work on the same test bed. The other purpose of this thesis is to propose an improved method that is simple to install, cost effective and moderately accurate to use for real life applications. Our proposed method uses an improved type of sampling importance resampling (SIR) filter incorporating automatic calibration of propagation model parameters of log-

distance path loss model and RSSI measurement noise by using reference tags. The proposed method also uses an RSSI smoothing algorithm exploiting the RSSI readings from the reference tags.

We used an active RFID system composed of 3 readers, 1 target tag and 4 reference tags in a home environment of two rooms with a total area of 36 m². The proposed method yielded 1.25 m estimation RMS error for tracking a mobile target.

Keywords: Localization, tracking, RSSI, active RFID, nearest neighbors, Bayesian filter, particle filter

ÖZ

İÇ ORTAMDA, ALINAN SİNYAL GÜCÜ (RSSI) TABANLI, BİLİNER YER BULMA VE TAKİP YÖNTEMLERİNİN, AKTİF RFID KULLANARAK UYGULAMA, KARŞILAŞTIRMA VE GELİŞTİRİLMESİ

ÖZKAYA, Bora

Yüksek Lisans, Elektrik-Elektronik Mühendisliği Bölümü

Tez Yöneticisi: Dr. Arzu KOÇ

Ortak Tez Yöneticisi: Prof. Dr. Sencer KOÇ

Şubat 2011, 151 sayfa

Günümüzde, iç ortamlarda insanların ve eşyaların konumlandırılabilmesi ve izlenebilmesi büyük önem kazanmıştır. Gerek literatürde gerekse piyasada alınan sinyal gücü (RSSI) yöntemini kullanan birçok konum kestirme ve izleme yöntemi ortaya konulmuştur. Ancak önerilen bu yöntemleri karşılaştırarak birbirlerine göre güçlü ve zayıf yönlerini açıkça ortaya koyan bir çalışma bulunmamasının eksikliği yaşanmaktadır. Dolayısıyla “mevcut sistem gereksinimlerine en uygun yöntem hangisidir?” sorusunun cevabına ihtiyaç duyulmaktadır. Bu nedenle bu çalışmada, en sık önerilen “Nearest Neighbors” yöntemleri, Bayes filtrelemesi ve parçacık filtreleme yöntemlerini simülasyon ve deneysel gerçekleştirme kullanarak inceledik. Tezimizin bir başka amacı da günlük uygulamalar için uygulaması kolay, uygun fiyatlı ve kabul edilebilir doğrulukta geliştirilmiş bir yöntem ortaya koymaktır. Önerdiğimiz yöntem temel olarak sampling importance resampling (SIR) filtreleme yönteminin geliştirilmiş hali olmakla birlikte “log-distance path loss” dalga yayılım modelinin parametrelerinin ve RSSI ölçüm gürültüsünün, referans vericiler kullanarak otomatik olarak kalibre edilmesini içerir ve referans vericilerden elde

edilen RSSI bilgileri yardımıyla özgün bir RSSI düzgünleştirme algoritmasını kullanır.

Tez kapsamındaki uygulama çalışmaları 3 adet aktif RFID okuyucusu, 1 adet hedef tag ve 4 adet referans tag'den oluşan bir sistemle toplam 36 m² lik iki odadan oluşan bir ev ortamında gerçekleştirildi. Hareketli bir hedefin izlenmesinde, önerdiğimiz yöntem ile bu ortamda 1.25 m'lik RMS hata performansına ulaştık.

Anahtar Kelimeler: Konumlandırma, Takip, RSSI, aktif RFID, nearest neighbor, Bayes filtresi, parçacık filtresi

To My Beloved Wife

ACKNOWLEDGEMENTS

I would like to express my gratitude and deep appreciation to my supervisor Dr. Arzu Koç for her guidance and positive suggestions during this work and also during my undergraduate and graduate studies.

I would like to thank my co-supervisor Prof. Dr. Sencer Koç for his contributions and guidance especially in the electromagnetics area and the design and manufacturing of the receiver antenna used in this work.

I would like to appreciate EG Electronics Ltd. and the design engineer Erhan Turan for the RFID products used during this work.

I am also grateful to Aselsan Electronics Industries Inc. for giving me the opportunity to improve my engineering capabilities.

I also would like to thank TÜBİTAK for financial support offered throughout the thesis.

Finally, I would like to deeply appreciate my beloved wife for her love and endless support throughout this work. Also lots of thanks to my Mom, Dad and Brother for their love and support over the years. This thesis is dedicated to them.

TABLE OF CONTENTS

ABSTRACT.....	iv
ÖZ.....	vii
ACKNOWLEDGEMENTS.....	ix
TABLE OF CONTENTS.....	x
LIST OF FIGURES.....	xiv
LIST OF TABLES.....	xvi
LIST OF ABBREVIATIONS.....	xix
CHAPTERS	
1. INTRODUCTION	1
2. WIRELESS LOCALIZATION METHODS	6
2.1 TIME OF ARRIVAL (TOA) METHODS.....	6
2.2 TIME DIFFERENCE OF ARRIVAL (TDOA) METHODS.....	7
2.3 ANGLE OF ARRIVAL (AOA) METHODS.....	7
2.4 RECEIVED SIGNAL STRENGTH INDICATION (RSSI) METHODS	7
2.4.1 Literature Survey on RSSI Based Localization Methods.....	9

3. DETERMINISTIC INDOOR LOCALIZATION METHODS.....	13
3.1 NEAREST NEIGHBORS (NN) METHODS	13
3.1.1 Propagation Pattern (Empirical) Based Approach	14
3.1.2 Propagation Parameter Based Approach.....	15
3.2 LATERATION (GEOMETRY) METHOD	16
4. PROBABILISTIC INDOOR LOCALIZATION METHODS	18
4.1 APPROXIMATE GRID BASED BAYESIAN FILTERING.....	21
4.2 PARTICLE FILTERING	23
4.2.1 Sequential Importance Sampling (SIS)	24
4.2.2 Sampling Importance Resampling (SIR) Filter.....	33
5. RF SIGNAL PROPAGATION MODELS.....	38
5.1 RF SIGNAL PROPAGATION PROPERTIES	38
5.1.1 Small Scale Fading	40
5.1.2 Large Scale Fading	43
5.1.3 RSSI Pattern (Map)	49
6. RSSI CALIBRATION IN THE TARGET ENVIRONMENT	53
6.1 OFFLINE CALIBRATION OF PARAMETERS.....	54
6.2 AUTOMATIC CALIBRATION WITH REFERENCE TAGS.....	60
6.3 RSSI MAP CREATION	63
7. SIMULATIONS AND EXPERIMENTAL WORK	64
7.1 APPLIED LOCALIZATION AND TRACKING METHODS.....	64
7.1.1 Propagation Pattern Based Nearest Neighbors (NN) Method.....	64

7.1.2 Propagation Parameter Based Nearest Neighbors (NN) Method	65
7.1.3 Grid Based Bayesian Filtering.....	65
7.1.4 Sampling Importance Resampling (SIR) Particle Filtering	65
7.1.5 Additional Approaches To Conventional Localization Methods.....	66
7.1.5.1 Automatic and Online Calibration of The Propagation Parameters.....	66
7.1.5.2 Automatic and Online Calibration of Filter Measurement Noise σ	67
7.1.5.3 RSSI Smoothing By Using Reference Tags	67
7.2 SIMULATIONS.....	68
7.2.1 Simulation Setup and Models.....	70
7.2.2 Simulation Results.....	72
7.2.2.1 Parameter Based NN Method with Offline Calibration.....	72
7.2.2.2 Grid Based Bayesian Filtering	80
7.2.2.3 SIR Particle Filter.....	90
7.2.3 Analysis of Simulation Results	104
7.3 EXPERIMENTAL WORK.....	109
7.3.1 Experimental Setup	109
7.3.1.1 Experimental Environment	109
7.3.1.2 System Setup.....	110
7.3.1.3 Experimental Methods	113
7.3.2 Experimental Results.....	117
7.3.2.1 Deterministic Localization Methods	117
7.3.2.1.1 Pattern Based (Empirical) vs. Parameter Based (offline) NN Methods	117
7.3.2.1.2 Effect of k_{NN} parameter for NN methods	118
7.3.2.1.3 Effect of Automatic Online Calibration of Propagation Parameters (n, α) Using Reference Tags	119
7.3.2.2 Probabilistic Localization Methods.....	120
7.3.2.3 Effect of Automatic Online Calibration of Filter Measurement Noise Std (σ) Using Reference Tags.....	124
7.3.2.4 Effect of Online RSSI Smoothing Using Reference Tags	126

7.3.2.5 Effect of Online Calibration of σ and RSSI Smoothing Using Reference Tags	128
7.3.2.6 Using Monopole Antenna For The Readers Instead of Patch Antenna	129
7.4 ANALYSIS OF SIMULATION AND EXPERIMENTAL RESULTS	132
8. CONCLUSIONS	138
REFERENCES	137
APPENDICES	
A: CRAMER RAO LOWER BOUND (CRLB) FOR LOCALIZATION	148

LIST OF FIGURES

FIGURES

Figure 3.1. Trilateration: the estimated location corresponds to the intersection point of three circles.	17
Figure 5.1 RF Signal Propagation Mechanisms [4].....	40
Figure 5.2 Amplitude of the received signal as a function of the range [35].....	41
Figure 5.3 Propagation with and without LOS [4].....	41
Figure 5.4 Small scale fading with moving antenna [4]	43
Figure 5.5 Comparison of theoretical and empirical RSS values in outdoor [10]	44
Figure 6.1 Experimental environment.....	54
Figure 6.2 Illustration of measurement points for propagation parameter calibration	56
Figure 6.3 RSSI histograms at 1m, 2m, and 3m, respectively.	57
Figure 6.4 Measured and modeled RSSI values for Reader 1	59
Figure 6.5 Measured and modeled RSSI values for Reader 2	59
Figure 6.6 Measured and modeled RSSI values for Reader 3	60
Figure 7.1 RMS error CRLB with changing σ and number of readers.....	69
Figure 7.2 Center of grid cells with circles and reader locations with squares.....	71
Figure 7.3 Pattern Based NN method RMSE and CRLB with changing σ_0	74
Figure 7.4 RMS error and 90 percentile error with changing k_{NN} for $\sigma_0=5.2$ dB where CRLB=0.80 m.....	76
Figure 7.5 RMS error and 90 percentile error with changing k_{NN} for $\sigma_0=11$ dB, where CRLB=1.70 m.....	77
Figure 7.6 Reader configuration with half of the default reader separation	78
Figure 7.7 Estimation mean error with changing recursion time with no RSSI noise added to the target transmit power and the target is fixed	83

Figure 7.8 Recursion time for settling with changing filter process model std. D	84
Figure 7.9 Recursion time for settling with changing filter measurement model std. σ	85
Figure 7.10 Dynamic noise filtering behavior with changing D	89
Figure 7.11 Mean estimation error with changing N when the target is at a fixed point with no transmit power noise.....	92
Figure 7.12 Mean estimation error with changing rt when target location is fixed and distributed randomly.	93
Figure 7.13 Settling time with changing D	93
Figure 7.14 Settling time with changing σ	94
Figure 7.15 RMS error with varying σ_0 for a fixed target	106
Figure 7.16 RMS error with varying σ_0 for a mobile target	107
Figure 7.17 Illustration of the experimental environment	111
Figure 7.18 Active RFID products of EG Elektronik	111
Figure 7.19 Active RFID tag with JJB antenna attached.....	112
Figure 7.20 Active RFID reader and patch antenna used in the experimental work	113
Figure 7.21 Coordinate axis illustration of the experimental environment, locations of fixed target experiments, location of readers and reference tags.....	115
Figure 7.22 Target moving with constant velocity (0.5 m/rt) for mobile target experiment.....	116
Figure 7.23 Graphical illustration of NN based method vs. Bayesian filtering for target tracking.....	122
Figure 7.24 Graphical illustration of parameter based NN, grid based Bayesian and improved SIR particle filter for dynamic measurement noise experiment	123
Figure 7.25 Graphical illustration of effect of automatic calibration of σ for dynamic RSSI measurement error	126
Figure 7.26 Sample monopole antenna placement configuration.....	131
Figure 7.27 Sample patch antenna placement configuration	131

LIST OF TABLES

TABLES

Table 4.1 SIS Algorithm	27
Table 4.2 Resampling Algorithm by Systematic Resampling Scheme.....	30
Table 4.3 Generic Particle Filter	32
Table 4.4 Sampling importance resampling (SIR) Filter	34
Table 5.1 Path Loss Exponent (n) and Standard Deviation (σ) in different indoor environments for log-distance path loss model [4]	47
Table 5.2 Average Floor Attenuation Factors in dB in two different buildings [4]...	48
Table 5.3 Partition Attenuation Factors for different building materials [36]	48
Table 6.1 Propagation parameters for 3 readers.....	58
Table 6.2 Automatically calibrated propagation parameters and RSSI std.	63
Table 7.1 Error statistics for changing k_{CELL} for NN method.....	72
Table 7.2 Error statistics for changing number of readers for NN method.....	73
Table 7.3 Error statistics for changing RSSI measurement noise std. for NN method	74
Table 7.4 Error statistics for changing k_{NN} for NN method with $\sigma_0=5.2$ dB.....	75
Table 7.5 Error statistics for readers separated with half of the default separations for NN method	78
Table 7.6 Error statistics for a larger area for NN method.....	79
Table 7.7 RMS error for MAP and MMSE estimates of grid based Bayesian filtering	82
Table 7.8 Error statistics with changing number of grid cells where CRLB=0.80 m	82
Table 7.9 Error statistics for changing k_{RDR} for grid based Bayesian method.....	86
Table 7.10 Error statistics for a mobile target with changing $\sigma=\sigma_0$ values	86
Table 7.11 Error statistics for a fixed target with changing $\sigma=\sigma_0$ values	87
Table 7.12 Error statistics for different $D=D_0$ values where CRLB=0.80 m.....	88

Table 7.13 Error statistics for changing filter process model std. D where $CRLB=0.80$ m.....	88
Table 7.14 RMS Error for MAP and MMSE Estimate.....	91
Table 7.15 Error statistics of SIR filter with changing σ when target is fixed	94
Table 7.16 Error statistics of SIR filter with changing σ when target moves with Gaussian motion model with D_0	95
Table 7.17 Error statistics of SIR filter with changing $D=D_0$ where $CRLB=0.80$ m	96
Table 7.18 Error statistics of SIR filter with changing D , when the target is simulated fixed where $CRLB=0.80$ m.....	97
Table 7.19 Lack of motion information for Gaussian target motion model	98
Table 7.20 Target moving with a known speed and direction.....	99
Table 7.21 Target moving with known initial location.....	100
Table 7.22 Adding non-accessible regions for the moving target with Gaussian model.....	100
Table 7.23 Effect of smoothing w for tracking moving and fixed targets.....	102
Table 7.24 Effect of resampling when $N_{\text{eff}} < N_t$ for tracking moving and fixed targets	103
Table 7.25 Effect of w smoothing and resampling using N_{eff} for moving and fixed target cases	104
Table 7.26 Experimental results of pattern based and offline parameter based NN methods for fixed target	117
Table 7.27 Effect of k_{NN} on estimation error using offline parameter based NN method for the fixed target case	118
Table 7.28 Effect of automatic online calibration of propagation parameters for fixed target experiment.....	119
Table 7.29 Comparison of parameter based NN, grid based Bayesian and improved SIR particle filter for fixed target case.....	121
Table 7.30 Comparison of parameter based NN, grid based Bayesian and improved SIR particle filter for moving target with known velocity.....	121

Table 7.31 Error std. comparison of parameter based NN, grid based Bayesian and improved SIR particle filter for dynamic measurement noise experiment	123
Table 7.32 Effect of automatic calibration of filter measurement noise σ for fixed target case.....	124
Table 7.33 Effect of automatic calibration of σ for mobile target case	125
Table 7.34 Error std. comparison of grid based Bayesian and grid based Bayesian with automatic calibration of σ for dynamic RSSI measurement error experiment	125
Table 7.35 Effect of online RSSI smoothing using reference tags for fixed target case	127
Table 7.36 Effect of RSSI smoothing at locations near the reference tags for the fixed target case.....	127
Table 7.37 Effect of online RSSI smoothing using reference tags for mobile target case.....	128
Table 7.38 Effect of RSSI smoothing for obstructed reader case.....	128
Table 7.39 Effect of online calibration of σ and RSSI smoothing together for mobile target case.....	129
Table 7.40 Effect of reader antenna on localization accuracy: monopole antenna vs. patch antenna for mobile target case.....	130
Table 7.41 Experimental error statistics for all used localization methods for fixed target experiments where CRLB=0.76 m	133
Table 7.42 Experimental error statistics for all used localization methods for mobile target experiments where CRLB=0.76 m	134
Table 7.43 Experimental error std for all localization methods for dynamic RSSI measurement error experiments	134
Table 7.44 Mean estimation error for related localization methods for obstructed reader experiments	135
Table 7.45 Simulation results of all simulated localization methods for fixed target case where CRLB=0.80 m	135
Table 7.46 Simulation results of simulated probabilistic localization methods for mobile target case where CRLB=0.80 m	135

LIST OF ABRIVATIONS

RTLS	Real Time Locating Systems
GPS	Global Positioning System
RF	Radio Frequency
LOS	Line of Sight
RSSI	Received Signal Strength Indication
TOA	Time of Arrival
TDOA	Time Difference of Arrival
AOA	Angle of Arrival
WLAN	Wireless Local Area Network
RFID	Radio Frequency Identification
RSS	Received Signal Strength
WAF	Wall Attenuation Factor
ILS	Iterative Least-Squares
ML	Maximum Likelihood
MCL	Monte Carlo Localization
SLAM	Simultaneous Localization and Mapping
MMSE	Minimum Mean Square Error
MAP	Maximum a Posteriori
SMC	Sequential Monte Carlo
SIS	Sequential Importance Sampling
SIR	Sampling Importance Resampling
CSW	Cumulative Sum of Normalized Weights
MCMC	Markov Chain Monte Carlo
ASIR	Auxiliary Sampling Importance Resampling
RPF	Regularized Particle Filter
FAF	Floor Attenuation Factor

PAF	Partition Attenuation Factor
LS	Least Squares
RMSE	Root Mean Square Error
CDF	Cumulative Distribution Function
Std.	Standard Deviation

CHAPTER 1

INTRODUCTION

Locating objects or people close to real time with acceptable precision has always been an important part of any industry, especially in manufacturing, healthcare, and logistics. For manufacturing, the need is real time monitoring of the production process by tracking the location of semi-products and also real time tracking of the inventory. In healthcare, mobile devices in the hospital, the personnel, and the patients are usually needed to be monitored. In logistics, assets and vehicles are monitored for decreasing the time consumption and also for avoiding human faults in the visibility process. So, recently, practical, easy to deploy, cost effective, small in size real time locating systems (RTLS) and tracking systems have gained great importance. Systems that map the longitude and attitude of an object are geo-location systems and generally use the Global Positioning System (GPS) for location mapping. GPS could be used as the location determination portion of an RTLS system but GPS signals do not penetrate buildings well and thus GPS will in general not work well inside buildings and in dense areas [1]. Thus, there is a need for RTLS systems that work individually in those environments that are especially indoor environments. In order to locate objects accurately in indoor environments, a lot of work has been conducted and different solutions have been proposed over the years in the market and literature.

Different technologies have been proposed for indoor localization including infrared (IR), ultrasound, and radio frequency (RF) [2] systems. The technique selection depends on the type and scale of the environment and whether the line of sight (LOS)

is required or not. Infrared and ultrasound sensors require LOS and are short range devices. Therefore, they are not appropriate for large scale and obstacle filled environments. At this point systems using RF become popular because RF systems do not require LOS and can communicate in long ranges depending on the power of the signal. So the most popular of these localization technologies is RF systems which vary in the localization method used. The most popular of these are received signal strength indication (RSSI), time of arrival (TOA), time difference of arrival (TDOA) or angle of arrival (AOA) [3]. The main idea of all these localization methods is that, in order to localize nodes, distance of the nodes to reference points, distance between nodes or angle according to reference points need to be calculated or estimated first. However, the methods except RSSI need complicated hardware or antenna which drastically increases the system cost [4]. This leads us to use RSSI based localization methods in our work.

RSSI based location estimation and tracking problems usually make use of wireless local area network (WLAN) infrastructure, wireless sensor network (WSN) infrastructure or radio frequency identification (RFID) technology. All three technologies can be used for indoor localization and we choose to use RFID technology which is the most popular RTLS system for indoor use due to its advantages of being practical, cost effective, small in size, and easy to deploy [5], [6], [7]. RFID devices compose of transmitters (or transceivers) called tag and receivers called reader which are cost effective, small size, and low power devices. RFID systems that are developed and supplied by many different commercial enterprises are studied for localization and tracking purposes in the literature [8], [9], [2], [10], [11], [7], [12], [6], [5].

Compared with an outdoor propagation environment, indoor environments are more complex in terms of RF signal propagation. Radio signals are subject to reflections, diffractions, and scattering in complex environments. These result in multipath or shadowing effect, thus the relationship between the distance and received signal strength (RSS) in indoor environments becomes much more complicated than that in outdoor environments [2]. In RSSI based localization techniques, since location

estimation makes use of RSS – distance relationship, good modeling of the signal propagation behavior of the environment is a crucial step for decreasing the resulting location estimation error. Since RSSI measurements are prone to large errors in complicated indoor environments, range information might not be derived deterministically from the RSSI measurements [2], [5]. So, in recent years besides deterministic localization methods, probabilistic (Bayesian) localization methods taking the RSSI-range variability and a priori knowledge of the target motion into account have been proposed in the literature [5], [8], [13], [14], [15], [1], [2], [10], [9], [3] so as to improve localization performance. Investigating the localization and tracking literature on RSSI based localization and robotics, we have come up with different localization methods including deterministic and Bayesian solutions. These methods have different variations in the subcategories each having weak and strong aspects over another that are given in Chapters 3 and 4.

This work implements different deterministic and probabilistic Bayesian location estimation methods to be able to compare them and propose several improvements on the existing applications. In order to compare these methods in different aspects, the best way is to make empirical experiments on the same test bench with the same experimental variables like measurement noise, receiver position, size of the target area, experimental locations of the target etc. and to make simulations of the methods with the same simulation models. In the literature such a complete experimental or simulation comparison that runs on the same environment could not be found. So, one aim of this thesis is to supply comparisons between different localization methods that are often cited in the literature by giving both simulation and experimental results. The methods that we implemented are given in Section 7.1. The behaviors of each mentioned method with varying environmental parameters (e.g., measurement noise) and system parameters (e.g., process noise properties, grid spacing, number of particles, etc.) were also investigated for completeness.

As we stated above, since RSSI readings are not reliable measure of the distance information in complex environments, having an accurate signal propagation model of the target environment is very important to yield accurate location estimation for

any type of localization method. The RSSI modeling is done through the training phase of localization systems and several methods are proposed for this training phase. There are mainly two methods: i) deriving the propagation parameters (propagation parameter based approach) to estimate RSSI – range relation. ii) creating the RSSI pattern/map (pattern based approach) of the environment. In the first method the parameters can be derived empirically in an offline training phase or they can be calibrated automatically during the estimation steps using additional reference tags. In this work we implemented both approaches to have a comparison. Automatic calibration method [16], [5] can be very attractive for especially large target area since it does not need an extra offline training phase and it may lead to more accurate RSSI modeling by adapting the parameters to the dynamically changing (moving objects, people etc.) environment at the expense of additional system cost. We exploited automatic calibration of propagation parameters in this thesis to come up with a practical method and also it is important to note that this thesis is the only work using automatic calibration of propagation parameters for indoor localization using an RFID system.

In the second method two different approaches are found in the literature. One is creating the RSSI map with offline empirical measurements taken at discrete locations all over the target environment [17]. The other one is creating the RSSI map with an online phase by using reference tags placed at different known locations in the environment [11]. Both of these approaches are reported to give more accurate localization results but the former needs a great amount of human labor for large target area and the latter needs a large number of reference tags that is usually not practical to implement and increases the system cost. In this thesis we also implemented the offline creation of the propagation map but because of insufficient number of RFID tags we could not implement the online approach.

Another aim of this thesis is to propose a localization method that is robust and easy to deploy for practical implementations in a complex indoor environment. [5] and [9] are important studies to combine reference tag approach and Bayesian filtering algorithms and form the basis of this work. Our proposed method exploits a WAF

(wall attenuation factor) propagation model with automatic calibration of propagation parameters and measurement noise via reference tags and an improved version of SIR (sampling importance resampling) particle filtering localization method. In addition, a custom RSSI smoothing algorithm by the use of reference tags is implemented to further increase the estimation accuracy as a contribution of this work.

In this work, considering practical applicability and popularity in both literature and commercial researches, we preferred to use RFID devices exploiting RSSI measurements. Patch antenna for the RFID readers is designed and application and user interface software running localization algorithms is developed in C# language in the context of the thesis. For investigating the localization algorithms simulation work was carried out on MATLAB and empirical experiments were run in a home environment containing two rooms of a 36 m² total area with a wall between and many different furniture inside. We used 3 RFID readers, 1 target tag and 4 reference tags throughout our experimental work.

In this thesis, theory of localization methods and signal propagation issues will be given in Chapters 2-5. In Chapter 6, details of RSSI measurements taken in the target area, used signal propagation model, calibration methods of the propagation parameters will be given. Chapter 7 will detail the localization methods used from the literature and additional approaches of our work to these methods, our simulation work and the results, experimental work and the results, and the analysis of both simulation and experimental work. We will conclude with the conclusion in Chapter 8. In Appendix A Cramer Rao Lower Bound (CRLB) is derived for our localization problem.

CHAPTER 2

WIRELESS LOCALIZATION METHODS

Wireless localization methods depending on the type of the physical parameters read by the sensors can be investigated in four different categories which are received signal strength indication (RSSI), time of arrival (TOA), time difference of arrival (TDOA), and angle of arrival (AOA). In this chapter we will give brief information on TOA, TDOA, and AOA based wireless localization methods and we will give more detailed information and literature review about the RSSI based localization methods being the subject of our work.

2.1 TIME OF ARRIVAL (TOA) METHODS

The distance between a reference point and the target is proportional to the propagation time of signal [1]. TOA based systems need at least three different measuring units to perform a lateration for 2-D positioning. However, they also require that all transmitters and receivers are precisely synchronized and that the transmitting signals include time stamps in order to accurately evaluate the traveled distances.

This approach is reasonably successful in indoor environments such as with concrete walls and floors and it has a relatively high accuracy compared to other methods. But, an ideal TOA system requires costly accurate clocks because in order to attain a more precise distance measurement a timing precision up to the nanosecond scale is

a requirement, which results in a more elaborate clock synchronization system. The clock offset and clock drift corrupt the ranging accuracy [1].

2.2 TIME DIFFERENCE OF ARRIVAL (TDOA) METHODS

The principle of TDOA lies on the idea of determining the relative location of a targeted transmitter by using the difference in time at which the signal emitted by a target arrives at multiple measuring units. Three fixed receivers give two TDOAs and thus provide an intersection point that is the estimated location of the target. This method requires a precise time reference between the measuring units. Like TOA, TDOA often suffers from multipath effects which affect the time of flight of the signals. So different signal processing techniques are used to improve the accuracy of the estimation. Some of these techniques that are used for the solution of the emitter location problem include the iterative least-squares (ILS) method and the maximum likelihood (ML) estimation technique [3].

2.3 ANGLE OF ARRIVAL (AOA) METHODS

AOA consists in calculating the intersection of several direction lines, each originating from a beacon station or from the target [1]. The angle of arrival information is obtained by getting the phase difference of the source signals. At least two angles, measured with directional antenna or with an array of antennas and converted in direction lines, are needed to find the 2-D location of a target.

As TOA and TDOA methods, this technique also suffers from shadowing and multipath reflections, and it is an expensive method that requires complex and expensive equipments like antenna arrays.

2.4 RECEIVED SIGNAL STRENGTH INDICATION (RSSI) METHODS

RSSI based measurement techniques can be broadly divided into deterministic and probabilistic techniques which will be detailed in Chapters 3 and 4, respectively. In

this section first we will give brief information on the classification of these methods and then a review of the related literature that we used will be given.

In deterministic methods, lateration (geometry) based or nearest neighbor(s) (NN) (also referred to as scene analysis) approaches can be used. In lateration based approaches, distance to RSSI relation is assumed to be deterministic and the obtained distance estimation is used for triangulation solutions to estimate the location [18]. On the other hand, NN approaches assign RSSI vector signatures (fingerprints) to the equally spaced grid locations all over the target area. This can be done by empirically storing the data or by signal propagation modeling techniques. After obtaining the RSSI fingerprints, pattern matching methods are used to find the most likely grid location(s) (nearest neighbor(s)) which will lead to the location determination of the target [17].

In probabilistic positioning techniques a probability distribution of the user's location is defined over the area of the movement. In general a Bayesian belief model is established with a preset number of discretized location possibilities which will be called grid cells. The Bayesian model is established with the a priori probability distribution of a user being at a given location and by the conditional probabilities (likelihood model) with which a given RSSI is measured at that location. By using the a priori and likelihood models one can derive the conditional probabilities (and thus the a posteriori distribution over locations) of a user being at each cell given the current RSSI reading. In order to apply Bayesian filters in location estimation problems, different filtering algorithms are used which include Kalman filtering [8], [10], grid based Bayesian inference [2], [5], and sequential Monte Carlo localization (MCL) [19], [9] which is also called particle filtering.

In this thesis we will investigate and work on both deterministic and probabilistic methods to derive pros and cons of each, but our main goal is to integrate and develop both methods to obtain a novel solution to localization problems.

2.4.1 Literature Survey on RSSI Based Localization Methods

In general, RSSI based positioning includes two phases: i) the training phase where the wireless map of the environment is determined by field measurements and ii) the localization phase where location calculation is performed based on the wireless map. Note that the training phase is an offline or online process and as such it needs to be redone if there have been major changes occurred affecting the wireless propagation environment for the offline case.

Accurate modeling of the environment is crucial in the accuracy of the location estimation. For the training phase there are several approaches to model the signal propagation of the environment. We can group the modeling approaches into two main categories. One is, modeling the propagation behavior of the signal in the target area using a suitable fading model described in Chapter 5. For this approach empirical measurements or floor plan modeling techniques can be used to drive a good estimate of target to source distance from the RSSI information. This is more flexible and easy to derive but suffers from dynamic environmental changes. This modeling is usually used in lateration (geometry) based localization solutions [18]. Or it can be used to create virtual RSSI map/pattern of the environment to be used in NN or probabilistic based location estimation techniques [17], [10]. The second approach is creating the RSSI map of the environment by empirical measurements at many different locations over the target area. Details on RSSI map will also be given in Chapter 5. This method is shown to be more accurate but it needs more human labor and is less flexible since it must be redone for any changes in the environment structure or receiver position. This method can either assign deterministic RSS signature vectors (fingerprints) to each grid locations to be used for NN solutions or RSS probability distributions for each grid cell to be used for probabilistic solutions. In order to compensate dynamic changes in the environment and remove the heavy human labor in the training phase automatic parameter calibration techniques are proposed in the literature.

Among the WLAN based localization literature RADAR [17] is one of the most cited work. RADAR uses WLAN based systems for location and tracking users inside buildings. It was the first system to propose the use of an RF map of the area. RSSI for each WLAN base station is stored as a fingerprint in a database for each point in a dense grid covering the floor. When querying the database, a nearest neighbor match in the fingerprint space provides candidates for mobile's position. Two approaches for position estimation are offered: using an empirical database which is based on a large number of RSS data stored in a database, or a model of RF propagation in the floor inferred from it. In [14] wireless signal strength maps for the positioning filter are obtained by a two-step parametric and measurement driven ray-tracing approach to account for absorption and reflection characteristics of various obstacles. Location estimates are then computed using Bayesian filtering on sample sets derived by Monte Carlo sampling. [13] estimates the location of a WLAN user in a statistical approach. In this approach the physical properties of the signal propagation are not taken into account directly. Instead the location estimation is regarded as a machine learning problem in which the task is to model how the signal strengths are distributed in different geographical areas based on a sample of measurements collected at several known locations. Then a probabilistic framework for solving the location estimation problem is presented. There are many other literature using WLAN based systems to estimate position but the ones mentioned above are selected as examples which exploit different localization methods.

Due to advantages such as small size, low power and low cost, the Radio Frequency Identification (RFID) sensors are widely used for detection and tracking purposes in a large variety of sectors. With the capability of providing RSS information advanced RFID systems have become a potential candidate for mass localization. Several RFID based systems have been proposed for tracking and localization objects in indoor environments. SpotON [18] and LANDMARC [11] are two of these systems. SpotON uses an aggregation algorithm for three-dimensional localization. The tags use RSS information to obtain inter-tag distances based on empirical mapping between the two. SpotON assumes deterministic mapping between RSS and

distances and does not account for the range measurement uncertainty caused by the varying environments. LANDMARC utilizes RSS measurement information to locate objects using k_{NN} nearest reference tags. It is in a way similar to RADAR [17] scheme, except that the RF map is built by previously placed active tags. In LANDMARC, 4 readers and 16 reference tags (spaced 1 m) are used in a 40 m² single room area to give a median of 1m position estimation error. To diminish the uncertainty of the detected range caused by the varying environments, there must be a large number of reference tags distributed in the environment. This seems impractical and expensive for most of the indoor scenarios. A simultaneous localization and mapping (SLAM) system for robot navigation based on RFID tags is presented by Haehnel et al [20]. The mobile robot carries a pair of patch (directive) antennas with which it can determine the range and angular position of detected tags relative to its current position. The range – angular dependence of the RSSI is modeled statistically and then a Bayesian filter is used for position estimation. The approach in [8] also utilizes reference tags along with Kalman filtering. The first step consists of calculating the distance between each reference tag and the target tag by using RSS measurements from two readers. The location of the tag is obtained by the minimum mean squared error algorithm. The second step consists of building a probabilistic map of the error measurement for the readers' detection area. The first step is applied for each reference tag in order to calculate their corresponding error probability distribution function with the help of their estimated location and their real location. The Kalman filter is then used iteratively on this online map to reduce the effect of RSS measurement error and thus to improve the accuracy of the localization. SCOUT [5] belongs to the family of probabilistic localization techniques and uses grid based Bayesian filtering. This method also utilizes reference tags. Active tags are localized following three steps. First, the propagation parameters are calibrated using on-site reference tags. Second, the distances between the target tag and the readers are estimated with a probabilistic RSS model. Finally, the location of the tag is determined by applying Bayesian inference. Iteratively, predicted beliefs are calculated and then corrected with observations until a good model is obtained resulting in an estimation area. [9] also belongs to the probabilistic

RFID localization family and uses particle filtering method as well as the reference tag idea.

In our work we implement most of the major methods given in the literature, compare them and integrate them to have an improved method of localization.

CHAPTER 3

DETERMINISTIC INDOOR LOCALIZATION METHODS

In this chapter we will give details of deterministic indoor localization methods that do not take probabilistic behavior of RSSI observation into account. Also they do not consider the a priori knowledge of the location of the target. Nearest neighbors (NN) and lateration (geometry) methods are two main subclasses of deterministic localization methods. Geometry method is a traditional method that is usually used for GPS, AOA, TOA, and TDOA technologies and rarely for RSS based technologies [4]. NN based localization is the most used deterministic method in the literature. Therefore, we used NN based approaches in our work.

3.1 NEAREST NEIGHBORS (NN) METHODS

Nearest neighbors method, also known as scene analysis method was first introduced by J. G. Skellam [21]. The distances of the observed data set to the expected data sets are used to determine the most probable location(s). A distance function E (Euclidean distance in our case) that gives the RSS data vectors' distances is used to determine the closest vector match.

Suppose that there are m cell locations and thus m RSS pattern vectors. $R = \{R_1, R_2, \dots, R_m\}$ in which each pattern vector R_j consists of signal signatures ($R_j = \{R_{1j}, R_{2j}, \dots, R_{r_jj}\}$) at location j , ($j=1,2,\dots,m$). k_{RDR} is the number of readers

(access point, station or receiver) in the system. R_t is the target RSS vector obtained at each measurement where vector R_t consists of k_{RDR} signal signatures ($R_t = \{R_{t_1}, R_{t_2}, \dots, R_{t_r}\}$). E is calculated for the j^{th} cell's RSS data set as follows [11]:

$$E_j = \sqrt{\sum_{i=1}^{k_{RDR}} (R_{ij} - R_{t_i})^2} \quad (3.1)$$

where k_{RDR} is the number of readers, R_{t_i} is the RSS of the target measured by the reader i , and R_{ij} is the RSS of the cell j measured by the reader i . R_{ij} can be obtained either by propagation pattern based approach or by propagation parameter based approach which are explained below. E denotes the distance between each cell and the target RSSI vectors. The k_{NN} nearest cells' coordinates are then averaged to localize the target estimate (x_e, y_e) as follows [11]:

$$(x_e, y_e) = \sum_{i=1}^{k_{NN}} w_i (x_i, y_i) \quad (3.2)$$

where w_i is the weighting factor of each neighboring cell and calculated as [11]

$$w_i = \frac{1/E_i^2}{\sum_{j=1}^{k_{NN}} E_j^2} \quad (3.3)$$

[22] reported that estimation error decreases as k_{NN} increases up to a number, then the error increases.

In NN method the cells' RSS data vectors are obtained by either propagation pattern based or propagation parameter based approaches.

3.1.1 Propagation Pattern (Empirical) Based Approach

We can investigate propagation pattern based approach in two main categories. One creates the RSSI pattern in an offline phase by storing the data as in RADAR [17],

the other one obtains the pattern in an online phase by using reference transmitters located at the training grid locations as in LANDMARC [11]. For both approaches, estimation accuracy depends heavily on the density of the training grids, accuracy increases as more grid cells (i.e., the number of reference transmitters in the online approach) are used in the target area.

In the first approach the predefined cells' data sets (in our case, the RSS measurement vectors R_j) are stored previously from empirical measurements [17] which are called fingerprints. In order to obtain the training data set, cell locations are defined first (e.g., each 1 m step) and then at each cell location a certain number of training data samples are stored. Increasing number of cell locations increases the accuracy of the location estimation. This method needs a serious human labor and also suffers from flexibility since the RSS model has to be reestablished all over again in case of any change in the environment or in the locations of the readers. In [17] it is reported that the median error is 2.9 m, in a floor area of 980 m², consisting of 50 rooms.

In the second approach LANDMARC [11] introduced the concept of reference tag (transmitter) in order to establish the online pattern vector with the reference tags fixed at predefined cell locations thus removing the time consuming data storage phase. LANDMARC method is also flexible in terms of both the dynamic environmental changes and the reader positions. But it has its own drawbacks on practical implementation and system cost. The median error is about 1.8 m in an area of 20 m², in a single room, with 16 reference tags and 3 readers.

3.1.2 Propagation Parameter Based Approach

In this approach RSS pattern vectors at each cell in the concerned area are not stored empirically as in the propagation pattern based approach but instead they are created by using the signal propagation parameters and the distance d of the cell location to each reader location using the below formula [17]

$$R_{ij} = \alpha - 10 * n * \log\left(\frac{d}{d_0}\right) - c_{ij} * WAF \quad (3.14)$$

where R_{ij} is the RSS of the cell j , measured by the reader i . α and n are the parameters to be determined. d_0 is a constant dummy distance chosen in advance. WAF is the wall attenuation factor to be determined. c_{ij} is the number of walls between the j^{th} cell and the i^{th} reader. In fact [17] reports that the attenuation factor makes a difference when c_{ij} is smaller than a certain number which is found to be 4 in that paper.

In this case the parameters can be determined using two different methods: One is offline determination of the parameters as in [17]. In a training phase RSS measurements are taken at different distances from each reader with or without walls between. Then using different curve fitting algorithms, required parameters are obtained and used after the training phase. This method is simpler than the pattern based approach, more flexible but in [17] it is reported that accuracy is worse than that of the pattern based approach. The median errors are, respectively, 4.3 and 2.9 m, in a floor area of 980 m², consisting of 50 rooms. This approach is still time consuming and cannot accommodate environmental changes in the estimation phase. So another method that is automatic calibration of the parameters is proposed by several authors [16], [5].

In this work we implemented both pattern based and parameter based approaches but our main attention is on the parameter based approach. For online calibration of parameters “reference tags” or “reference access points” are used. This method eliminates the time consuming training phase and also can accommodate environmental changes up to a limit.

3.2 LATERATION (GEOMETRY) METHOD

The lateration approach, illustrated in Figure 3.1 estimates the position of the target by evaluating its distances from at least three reference points. In [18] multiple base

stations provide signal strength measurements mapping to an approximate distance. A central server then aggregates the values to triangulate the precise position of the tagged object. Finally, the computed object positions are published to client applications.

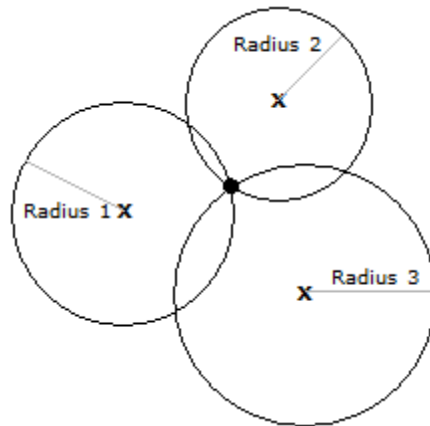


Figure 3.1. Trilateration: the estimated location corresponds to the intersection point of three circles.

[13] states that propagation based approaches are competitive against the traditional geometry method.

CHAPTER 4

PROBABILISTIC INDOOR LOCALIZATION METHODS

Probabilistic approaches' arising point is that, the propagation of RF signals in indoor environments is almost impossible to model exactly. So the relationship of RSS information with range is not deterministic. Probabilistic methods try to handle this uncertainty and errors in signal measurements. Moreover probabilistic methods incorporate the a priori knowledge about the possible/impossible locations in the interested area also taking the previous location into consideration. Probabilistic approaches use Bayesian inference which estimates the location as a probability distribution over the area of interest [1].

Bayes filters assume that the environment is Markov, that is, past and future data are (conditionally) independent if one knows the current state. The Markov assumption is stated explicitly below.

In the following formulations the notations explained below will be used.

L_t : The location of the transmitter at time t .

s_t : The sensor data (being RSSI in our problem) at time t .

$s_{1,\dots,t}$: Denotes the sensor data sequence from time 1 to time t : $\{s_1, \dots, s_t\}$

The key idea of Bayes filtering is to estimate a posterior probability density function (pdf) $p(L_t|s_{1,\dots,t})$ over the state space L_t , conditioned on the sensor measurement data $s_{1,\dots,t}$ up to time t . The initial density of the state vector is $p(L_0)$ at time zero

when there are no measurements. Then the posterior density $p(L_t | s_{1,\dots,t})$ will be obtained recursively using the previous posterior pdf $p(L_{t-1} | s_{1,\dots,t-1})$ and the most recent measurement data s_t in two stages which are prediction and update stages. Suppose that at time $t - 1$ the posterior pdf $p(L_{t-1} | s_{1,\dots,t-1})$ is available.

At the prediction stage, process model explained below is used to obtain the prior pdf (or prediction density) $p(L_t | s_{1,\dots,t-1})$ at time t via the Chapman-Kolmogorov equation [23].

$$p(L_t | s_{1,\dots,t-1}) = \int p(L_t | L_{t-1}) p(L_{t-1} | s_{1,\dots,t-1}) dL_{t-1} \quad (4.1)$$

The **process** (also called system, action, motion or mobility) **model** is [23]

$$L_t = f_{t-1}(L_{t-1}, v_{t-1}) \quad (4.2)$$

where f_{t-1} is a known function of the state L_{t-1} and the **process noise** v_{t-1} . Process noise is any mismodeling or disturbances in the process model. For example, for a moving target with constant speed c , $L_t = L_{t-1} + c + v_{t-1}$. The noise v_{t-1} is assumed to be white with known probability density function.

The transitional density $p(L_t | L_{t-1})$ in (4.1) is simplified from $p(L_t | L_{t-1}, s_{1,\dots,t-1})$ since it is a Markov process of order one. The density $p(L_t | L_{t-1})$ is defined by the process model (4.2) and the known statistics of v_{t-1} . The transitional density $p(L_t | L_{t-1})$ is sometimes called process model in the literature [14].

Update stage is applied at time step t when a measurement s_t is taken. At this stage the prior density $p(L_t | s_{1,\dots,t-1})$ is updated to form the posterior density $p(L_t | s_{1,\dots,t})$ using the Bayesian rule as [23]

$$p(L_t | s_{1,\dots,t}) = p(L_t | s_t, s_{1,\dots,t-1}) \quad (4.3)$$

$$p(L_t | s_{1,\dots,t}) = \frac{p(s_t | L_t, s_{1,\dots,t-1}) p(L_t | s_{1,\dots,t-1})}{p(s_t | s_{1,\dots,t-1})} \quad (4.4)$$

$$p(L_t | s_{1,\dots,t}) = \frac{p(s_t | L_t) p(L_t | s_{1,\dots,t-1})}{p(s_t | s_{1,\dots,t-1})} \quad (4.5)$$

$p(s_t | L_t, s_{1,\dots,t-1})$ term in (4.4) simplifies to $p(s_t | L_t)$ in (4.5) since s_t measurement only depends on the location state L_t . In (4.4) and (4.5) $p(s_t | s_{1,\dots,t-1})$ term is the normalizing constant which is [23]

$$p(s_t | s_{1,\dots,t-1}) = \int p(s_t | L_t) p(L_t | s_{1,\dots,t-1}) dL_t \quad (4.6)$$

$p(s_t | L_t)$ term in (4.5) and (4.6) is referred to as **likelihood** function which is defined by the measurement model as explained below, and the known statistics of measurement noise w_t . $p(s_t | L_t)$ is sometimes referred to as the **measurement model** in the literature [14].

The measurements are related to the location state L_t via the following **measurement (observation) model**

$$s_t = h_t(L_t, w_t) \quad (4.7)$$

where h_t is a known function and w_t is the **measurement noise** which is assumed to be white, with known probability density function. This model is generated empirically from a large set of measurements obtained in different locations in the area of interest.

Knowing the posterior density $p(L_t | s_{1,\dots,t})$ one can compute a location estimate with any criterion. Most common used ones are the minimum mean square error (MMSE) estimate and maximum a posteriori (MAP) estimate [23].

MMSE estimate is the conditional mean of L_t .

$$\hat{L}_{t|t}^{\text{MMSE}} \triangleq E\{L_t|s_{1,\dots,t}\} = \int L_t \cdot p(L_t|s_{1,\dots,t}) dL_t \quad (4.8)$$

MAP estimate is the maximum of $p(L_t|s_{1,\dots,t})$.

$$\hat{L}_{t|t}^{\text{MAP}} \triangleq \underset{L_t}{\operatorname{argmax}} p(L_t|s_{1,\dots,t}) \quad (4.9)$$

In order to implement the conceptual solution to the posterior density in (4.5) there exist several optimal or suboptimal Bayesian algorithms. The optimal algorithms can be the Kalman filters if the noise distributions are Gaussian or the grid based Bayesian method if the state space is discrete and finite. But Kalman filter typically fails when the Gaussian assumption breaks down and in a localization problem either the process noise or the measurement noise can be non-Gaussian distributions [23].

In our localization problem the state space is continuous and the motion model can be any type of distribution in real life applications. So we will use approximate or suboptimal methods. Our interest will be on approximate grid-based method (also known as Markov localization) which is a numerical approximation method, and the particle filter which is in fact sequential Monte Carlo sampling approach of Bayesian filters. Markov localization [24] and particle filters [25] are promising Bayesian filters that are also used in robot localization problems.

4.1 APPROXIMATE GRID BASED BAYESIAN FILTERING

This approach is also referred to as Markov localization in the literature [24]. In this numerical approximation of Bayesian filter, the integrals in equations (4.1) and (4.6) are solved by numerical integration where the integration is replaced by summation and the integration variables are discretized.

The continuous location space in this approach is sliced into m location cells. Then the approximate discrete posterior probability is typically called the **belief** and denoted by

$$\text{Bel}(L_t) = p(L_t | s_{1,\dots,t}) \quad (4.10)$$

where L_t is the location at time t and $s_{1,\dots,t}$ is sensor measurement data up to time t . The belief function of being at location l at time t without any assumptions is

$$\text{Bel}(L_t = l) = \frac{P(s_t | L_t = l, s_{1,\dots,t-1})P(L_t = l | s_{1,\dots,t-1})}{P(s_t | s_{1,\dots,t-1})} \quad (4.11)$$

In (4.11) using the “independence of sensor readings”, the probability $P(s_t | L_t = l, s_{1,\dots,t-1})$ simplifies to $P(s_t | L_t = l)$ and is referred to as the **measurement model** or the **likelihood function**. It states the probability of taking the measurement s_t when the target is at location l .

In (4.11) $P(L_t = l | s_{1,\dots,t-1})$ describes the probability of being at location l at time t before the sensor measurement is taken at time t . Here using the Markov assumption and conditioning on the previous state L_{t-1} we get

$$P(L_t = l | s_{1,\dots,t-1}) = \sum_{l'} P(L_t = l | L_{t-1} = l')P(L_{t-1} = l' | s_{1,\dots,t-1}) \quad (4.12)$$

$P(L_t = l | L_{t-1} = l')$ term here is called the **process model**.

By using the belief definition in (4.10), $P(L_{t-1} = l' | s_{1,\dots,t-1})$ can be written as the belief at time $t-1$ $\text{Bel}(L_{t-1} = l')$. Also we can rewrite $P(L_t = l | s_{1,\dots,t-1})$ as $P(L_t = l | L_{t-1})$ since it only depends on the previous state L_{t-1} to give

$$P(L_t = l | L_{t-1}) = \sum_{l'} P(L_t = l | L_{t-1} = l') \text{Bel}(L_{t-1} = l') \quad (4.13)$$

Integrating all the assumptions and simplifications explained above, we can rewrite (4.11) as

$$\text{Bel}(L_t = l) = \frac{P(s_t | L_t = l) P(L_t = l | L_{t-1})}{P(s_t | s_{1, \dots, t-1})} \quad (4.14)$$

The denominator here is nothing but a normalizing coefficient which supplies $\text{Bel}(L_t = l)$ sums up to one over all possible locations l in the state space. So we can rewrite

$$\text{Bel}(L_t = l) = \beta P(s_t | L_t = l) P(L_t = l | L_{t-1}) \quad (4.15)$$

where β is a normalizing coefficient.

In this method, the grids must be sufficiently dense to get a good approximation to the continuous state space. As the state space dimension increases, the computational cost of the approach and the computation time dramatically increase. However, the method can be used successfully with a moderate computational cost for localization applications that do not need much precision and that are for small area environments.

4.2 PARTICLE FILTERING

Particle filters perform sequential Monte Carlo (SMC) estimation based particle (or point mass) representation of probability densities. Detailed information can be found in [23], [1], [3], [26], [27], [28], [29]. Sequential importance sampling (SIS) which is the basic idea of SMC was introduced in 1950s [23]. But these methods had several disadvantages when implemented purely. Particle filters were made useful in

practice when the resampling step is included. Sampling importance resampling (SIR) filter is one of the filters exploiting resampling stage. In our work we used SIR filter and added several improvements on it. So in this section we will give details of the SIS approach which is the basis of SIR, the SIR filter, and improvements on SIR proposed in the literature.

4.2.1 Sequential Importance Sampling (SIS)

It is the basis for most of the SMC methods. It implements sequential Bayesian filter using MC simulations. The key idea is to represent the required posterior density function by a set of random samples with associated weights and to compute estimates based on these samples and weights. As the number of samples becomes very large, this MC characterization becomes an equivalent representation to the usual functional description of the posterior pdf, and the SIS filter approaches the optimal Bayesian estimate [23], [28].

The posterior pdf $p(L_t | s_1, \dots, s_t)$ is approximated by N discrete points of masses called **particles** $\{(L_t^j, w_t^j)\}$ as shown in (4.16) where " \approx " notation will be used to denote not equality but approximation.

$$p(L_t | s_1, \dots, s_t) \approx \{(L_t^j, w_t^j)\}, \quad j = 1, \dots, N \quad (4.16)$$

where L_t^j is the location of the j^{th} particle at time t and w_t^j is the normalized, nonnegative weight of the j^{th} particle. w_t is called the **importance factor** that approximates the distribution probability at location l . The weights are chosen using the principle of **importance sampling** which is explained below.

Suppose $p(x)$ is a probability density of a random variable x , from which it is difficult to draw samples. Instead the samples can be drawn from an arbitrary density $q(x)$ which is similar to $p(x)$ and $q(x)$ is called the **importance or proposal density**. Then a correct weighting of the sample set still makes the Monte Carlo estimation

possible. Here the similarity of $q(x)$ can be expressed by the condition: $p(x) > 0 \Rightarrow q(x) > 0$ for all x for which $p(x)$ is non zero which means that $p(x)$ and $q(x)$ have the same support. Let $x^j \sim q(x)$, $j = 1, \dots, N$ be the samples that are generated from the importance density where “ \sim ” notation is used to denote that x^j is sampled from $q(x)$, then a weighted approximation to the density $p(x)$ is given by

$$p(x) \approx \sum_{j=1}^N w^j \delta(x - x^j) \quad (4.17)$$

where

$$w^j \propto \frac{p(x^j)}{q(x^j)} \quad (4.18)$$

is the normalized weight of the j^{th} particle and “ \propto ” is used for proportionality. Returning to (4.16), if the samples L_t^j are drawn from an importance density $q(L_t | s_{1, \dots, t})$ then by using (4.18) we can write

$$w_t^j \propto \frac{p(L_t^j | s_{1, \dots, t})}{q(L_t^j | s_{1, \dots, t})} \quad (4.19)$$

Now suppose that at time step $t - 1$ we have samples forming $p(L_{t-1} | s_{1, \dots, t-1})$ and when we take a measurement s_t at time t we need to form a new set of samples approximating $p(L_t | s_{1, \dots, t})$. If the importance density is chosen to factorize such that

$$q(L_t | s_{1, \dots, t}) = q(L_t | L_{t-1}, s_t) q(L_{t-1} | s_{1, \dots, t-1}) \quad (4.20)$$

then one can obtain samples $L_t^j \sim q(L_t | s_{1, \dots, t})$ by augmenting each of the existing samples $L_{t-1}^j \sim q(L_{t-1} | s_{1, \dots, t-1})$ with the new state $L_t^j \sim q(L_t | s_t, s_{1, \dots, t-1})$. To derive the update equations the pdf $p(L_t | s_{1, \dots, t})$ is first expressed as

$$p(L_t | s_{1,\dots,t}) = \frac{p(s_t | L_t, s_{1,\dots,t-1})p(L_t | s_{1,\dots,t-1})}{p(s_t | s_{1,\dots,t-1})} \quad (4.21)$$

$$= \frac{p(s_t | L_t)p(L_t | s_{1,\dots,t-1})}{p(s_t | s_{1,\dots,t-1})} \quad (4.22)$$

$$= \frac{p(s_t | L_t)p(L_t | L_{t-1})}{p(s_t | s_{1,\dots,t-1})} p(L_{t-1} | s_{1,\dots,t-1}) \quad (4.23)$$

$$\propto p(s_t | L_t)p(L_t | L_{t-1}) p(L_{t-1} | s_{1,\dots,t-1}) \quad (4.24)$$

By substituting (4.24) and (4.20) into (4.19) the weight update equation can be written as

$$w_t^j \propto \frac{p(s_t | L_t^j)p(L_t^j | L_{t-1}^j) p(L_{t-1}^j | s_{1,\dots,t-1})}{q(L_t^j | L_{t-1}^j, s_t)q(L_{t-1}^j | s_{1,\dots,t-1})} \quad (4.25)$$

$$w_t^j \propto w_{t-1}^j \frac{p(s_t | L_t^j)p(L_t^j | L_{t-1}^j)}{q(L_t^j | L_{t-1}^j, s_t)} \quad (4.26)$$

Using the weights w_t^j the filtered posterior density $p(L_t | s_{1,\dots,t})$ can be approximated as

$$p(L_t | s_{1,\dots,t}) \approx \sum_{j=1}^N w_t^j \delta(L_t - L_t^j) \quad (4.27)$$

Here δ is the Dirac delta function. So filtering via SIS consists of recursive propagation of importance weights and the particle locations. The pseudo code for SIS algorithm is given in Table 4.1.

A common problem with the SIS particle filter is the **degeneracy** phenomenon, where after a few iterations, most of the particles will have negligible weight. It is stated in [28] that the variance of the importance weights can only increase over time, and thus, it leads to the degeneracy phenomenon which has a harmful effect on the accuracy. This degeneracy implies that a large computational effort is devoted to updating particles whose contribution to the approximation $p(L_t | s_{1,\dots,t})$ is almost zero. A suitable measure of degeneracy of the algorithm is the **effective sample size** N_{eff} [28] and can be approximated as

$$N_{\text{eff}} = \frac{1}{\sum_{j=1}^N (w_t^j)^2} \quad (4.28)$$

Hence $N_{\text{eff}} \leq N$ and large weight results in small N_{eff} which indicates severe degeneracy and vice versa. Considering extreme cases: if the weights are uniform, i.e., $w_t^j = \frac{1}{N}$ for all j , $N_{\text{eff}} = N$. If one of the weights is “1” but all others are “0” then $N_{\text{eff}} = 1$.

Table 4.1 SIS Algorithm

Algorithm: SIS Particle Filter
$[\{L_t^j, w_t^j\}_{j=1}^N] = \text{SIS}[\{L_{t-1}^j, w_{t-1}^j\}_{j=1}^N, s_t]$
FOR $j=1:N$
Draw $L_t^j \sim q(L_t L_{t-1}^j, s_t)$
Assign the particle a weight w_t^j according to (4.26)
END FOR
Normalize the weight coefficients.

One approach to reducing degeneracy effect is to use a very large N . This is often impractical; therefore, we rely on other two methods: good choice of importance density and use of resampling.

In **choice of importance density**, the first method involves choosing the importance density to minimize the variance of the weights so that N_{eff} is maximized. The optimal importance density function that minimizes the variance of the true weights conditioned on L_{t-1}^j and s_t is given to be [28]

$$q(L_t|L_{t-1}^j, s_t)_{\text{opt}} = p(L_t|L_{t-1}^j, s_t) \quad (4.29)$$

$$= \frac{p(s_t|L_t, L_{t-1}^j)p(L_t|L_{t-1}^j)}{p(s_t|L_{t-1}^j)} \quad (4.30)$$

Thus substituting (4.30) into (4.26) the weight is

$$w_t^j \propto w_{t-1}^j p(s_t|L_{t-1}^j) \quad (4.31)$$

$$w_t^j = w_{t-1}^j \int p(s_t|L_t)p(L_t|L_{t-1}^j) dL_t \quad (4.32)$$

But it is usually not easy to sample from the density $p(L_t|L_{t-1}^j, s_t)$ and to evaluate the integral in (4.32). So it is often more convenient to use the importance density as the prior density

$$q(L_t|L_{t-1}^j, s_t) = p(L_t|L_{t-1}^j) \quad (4.33)$$

Substituting (4.33) into (4.26) gives

$$w_t^j \propto w_{t-1}^j p(s_t|L_t^j) \quad (4.34)$$

This would seem to be the most common choice of importance density since it is intuitive and simple to implement. However, there are many other densities that can be used.

The second method by which the effects of degeneracy can be reduced is to use resampling whenever a significant degeneracy is observed (i.e., when N_{eff} falls below some N_t threshold). The basic idea of resampling is to eliminate particles that have small weights and to concentrate on particles with large weights. The resampling step involves generating a new set $\{L_t^i\}_{i=1}^N$, where i denotes the new index of the new resampled particle, by resampling (with replacement) N times from an approximate discrete representation of $p(L_t|s_{1,\dots,t})$ given by

$$p(L_t|s_{1,\dots,t}) \approx \sum_{j=1}^N w_t^j \delta(L_t - L_t^j) \quad (4.35)$$

The resulting sample is in fact an i.i.d. sample from the discrete density (4.35) therefore the weights are now reset to $w_t^i = 1/N$.

A direct implementation of a resampling would consist of generating N i.i.d. variables from the uniform distribution, sorting them in an ascending order and comparing them with the cumulative sum of normalized weights (CSW). The best sorting algorithm has a complexity of $O(N \log N)$ and this is the major limit in practical implementations. However, it is possible to implement this resampling procedure in $O(N)$ operations by sampling N ordered uniform variables using an algorithm based on order statistics [28]. It must be noted that other efficient (in terms of reduced MC variation) resampling schemes such as stratified sampling and residual sampling [28], may be applied as alternatives to this algorithm. Systematic resampling is the scheme often preferred in the literature since it is simple to implement, it takes $O(N)$ operations and minimizes the MC variation. Its operation is described in Table 4.2 [28].

Although the resampling step reduces the effects of the degeneracy problem, it introduces other practical problems. First, it limits the opportunity to parallelize since all the particles must be combined.

Table 4.2 Resampling Algorithm by Systematic Resampling Scheme

```

Algorithm: Resampling Algorithm
 $[\{L_t^i, w_t^i\}_{i=1}^N] = \text{RESAMPLE}[\{L_t^j, w_t^j\}_{j=1}^N]$ 
Initialize the CDF(cumulative density function):  $c_1 = 0$ 
FOR j=2:N
    Construct CDF:  $c_j = c_{j-1} + w_t^j$ 
END FOR
Start at the bottom of the CDF: j=1
Draw a starting point:  $u_1 \sim U[0, \frac{1}{N}]$  // sample
// $u_1$  from the uniform distribution  $U[0, \frac{1}{N}]$  on the interval  $[0, \frac{1}{N}]$ 
FOR i=1:N
    Move along the CDF:  $u_i = u_1 + \frac{1}{N} * (i - 1)$ 
    WHILE ( $u_i > c_j$ )
        j=j+1
    END WHILE
    Assign new sample:  $L_t^i = L_t^j$ 
    Assign weight to the new sample :  $w_t^i = \frac{1}{N}$ 
END FOR

```

Second, the particles that have high weights are statistically selected many times. This leads to a loss of diversity among the particles as the resultant sample will contain many repeated points. This problem, which is known as **sample**

impoverishment, is severe in the case of small process noise. In fact, for the case of very small process noise, all particles will collapse to a single point within a few iterations. If the process noise is zero, then using a particle filter is not entirely appropriate. Particle filtering is a method well suited to the estimation of dynamic states. If static states, which can be regarded as parameters, need to be estimated then alternative approaches are necessary. Third, since the diversity of the paths of the particles is reduced, any smoothed estimates based on the particles' paths degenerate. Schemes exist to counteract this effect. One approach considers the states for the particles to be predetermined by the forward filter and then obtains the smoothed estimates by recalculating the particles' weights via a recursion from the final to the first time step [30]. Another approach is to use the Markov Chain Monte Carlo (MCMC) [31] method.

There have been some systematic techniques proposed recently to solve the problem of sample impoverishment. One such technique is the resample move algorithm. Although this technique draws conceptually on the same technologies of importance sampling resampling and MCMC sampling, it avoids sample impoverishment [28]. It does this in a rigorous manner that ensures the particles asymptotically approximate samples from the posterior and, therefore, it is the often used method in the literature. An alternative solution to the same problem is regularization [28]. Also by introducing an additional noise to the samples the impoverishment problem can be reduced. This technique is called jittering or roughening [32].

After describing SIS, choice of importance density and resampling, we can now define a generic particle filter algorithm which is given in Table 4.3 [28].

Table 4.3 Generic Particle Filter

Algorithm: Generic Particle Filter
$[\{L_t^j, w_t^j\}_{j=1}^N] = \text{PF}[\{L_{t-1}^j, w_{t-1}^j\}_{j=1}^N, s_t]$
<p>FOR j=1:N</p> <p style="padding-left: 40px;">Draw particle samples $L_t^j \sim q(L_t L_{t-1}^j, s_t)$ // sample from the importance //density $q(\cdot)$.</p> <p style="padding-left: 40px;">Assign the particle L_t^j a weight w_t^j according to (4.26)</p> <p>END FOR</p>
<p>Normalize w_t^j</p> <p>Calculate N_{eff} using (4.28)</p> <p>IF $N_{\text{eff}} < N_t$ // N_t being a user defined threshold</p> <p style="padding-left: 40px;">Resample using:</p> <p style="padding-left: 80px;">$[\{L_t^j, w_t^j\}_{j=1}^N] = \text{RESAMPLE}[\{L_t^j, w_t^j\}_{j=1}^N]$</p> <p>END IF</p>

First we initialize the particles by drawing samples from the initial distribution $p(L_t | s_{1, \dots, t-1})$ thus sample $L_0^j \sim p(L_0)$ with uniform weights ($w_0^j = 1/N$), where $t=0$, and there is no measurements. In the following iterations we draw the samples from an appropriate importance density ($L_t^j \sim q(L_t | L_{t-1}^j, s_t)$) where the particles will be $\{L_t^j, w_t^j\}_{j=1}^N$ approximating the prior density $p(L_t | s_{1, \dots, t-1})$ when there is no measurement data (s_t). This step is also called the prediction step. Then we update

the weights using the measurement s_t by the likelihood function $p(s_t|L_t)$ via (4.26). The result here is a discrete set of particles $\{L_t^j, w_t^j\}_{j=1}^N$ which approximates the posterior density $p(L_t|s_1, \dots, s_t)$. Then go on with the resampling step if $N_{\text{eff}} < N_t$ where N_t can be chosen as $2N/3$ [32]. Or resampling may be run in every iteration as in sampling importance resampling (SIR) filter. Here particles still approximate the posterior. At this step one can estimate the location using (4.8) or (4.9). Then iterate to the time step $t+1$ starting with the prediction step.

There are many types of particle filters which mainly rely on SIS approach but differ especially in the choice or modification of importance sampling density and the resampling step. Most widespread of those are sampling importance resampling (SIR) filter, auxiliary sampling importance resampling (ASIR) filter, and regularized particle filter (RPF). Note that these filters can be combined or altered. We will explain here the basic one, SIR filter, in detail and give brief information on the other types which are in fact modified versions of SIR filter.

4.2.2 Sampling Importance Resampling (SIR) Filter

The SIR filter was first proposed under the name “Bayesian bootstrap filter” which is very close in spirit to the sampling importance resampling (SIR) filter developed independently in statistics by different researchers, with a slight difference on the resampling scheme [33]. So bootstrap and SIR filters are treated as the same class. The key idea of SIR filter is to introduce the resampling step between two importance sampling steps. The resampling step is aimed to eliminate the samples with small importance weights and duplicate the samples with large weights. The generic principle of SIR proceeds as in Table 4.4 [28].

Table 4.4 Sampling importance resampling (SIR) Filter

Algorithm: SIR Filter
$[\{L_t^j, w_t^j\}_{j=1}^N] = \text{SIR}[\{L_{t-1}^j, w_{t-1}^j\}_{j=1}^N, s_t]$ <p>FOR j=1:N</p> <p style="padding-left: 40px;">Draw particle samples $L_t^j \sim p(L_t L_{t-1}^j)$ from the importance density that is chosen as the prior density $p(L_t L_{t-1}^j)$</p> <p style="padding-left: 40px;">Assign the particle L_t^j a weight: $w_t^j = p(s_t L_t^j)$ using the likelihood</p> <p>END FOR</p> <p>Normalize w_t^j</p> <p>Resample using:</p> $[\{L_t^j, w_t^j\}_{j=1}^N] = \text{RESAMPLE}[\{L_t^j, w_t^j\}_{j=1}^N]$

Here the resampling scheme can be chosen of any type according to the system needs. The constraints of using the SIR filter are very weak. The process and measurement model functions need to be known, and it is required to be able to sample realizations from the process noise distribution of v_{t-1} and from the prior distribution. Also, the likelihood function $p(s_t | L_t^j)$ needs to be available for pointwise evaluation. The SIR algorithm can be easily derived from the SIS algorithm by an appropriate choice of the importance density and applying the resampling step at every time index. In SIR the importance density is chosen to be the prior density (also called the transitional density) $p(L_t | L_{t-1}^j)$. For this particular choice of importance density, using (4.26) it is evident that the weights are

$$w_t^j \propto w_{t-1}^j p(s_t | L_t^j) \quad (4.36)$$

But, since resampling is applied at every time index w_{t-1}^j will be $1/N$ for all j and since w_t^j is normalized as they sum up to 1 for all $j:1$ to N , (4.36) simplifies to

$$w_t^j = p(s_t | L_t^j) \quad (4.37)$$

As the importance sampling density for the SIR filter is independent of measurement, the state space is explored without any knowledge of the observations. Therefore, this filter can be inefficient and is sensitive to outliers for some cases. Also in an SIR filter, as resampling is applied at every iteration, this can result in rapid loss of diversity in particles. However, the SIR method does have the advantage that the importance weights are easily evaluated and that the importance density can be easily sampled. By simple modifications on the importance sampling and resampling stages, the weaknesses of the SIR filter can be improved.

Improvements on SIR Filters:

In the literature, many efforts have been devoted to improving the particle filters' performance (see [33] for a detailed list of literature). Here, we only focus on the improved schemes on efficient sampling/resampling and variance reduction which include the ASIR and RPF type particle filters.

In order to alleviate the sample impoverishment problem, three simple strategies were proposed by Gordon et al. which are jittering, prior boosting and prior editing [33]. In **jittering**, the main idea is to add a random noise (namely, Gaussian) to the state of each particle after sampling from the posterior before it is propagated to the next time step. As a result, if replicas of particles with high weights exist they will be replaced by different but similar particles so as to decrease the effect of sample impoverishment. Note that this would be a very important contribution if the process noise is small. Jittering is in fact adding an extra noise to the process model at each

time step and the variance of the added jitter can be chosen by the user taking the system model into consideration.

In **prior boosting** algorithm [33], in the sampling from the importance density step, one can increase the number of simulated samples drawn from the importance, such that draw $M > N$ samples; but in the resampling step, only N particles are preserved. The idea behind this adaption is that by increasing the number of particles in the prior samples, the probability of resampling replicas will be smaller. However, in [33] it is shown that standard SIR filter with M particles (not N) will give more accurate results.

Prior editing algorithm [33] is also a modification on the prior samples. After the samples are drawn from the proposal distribution, particles with small weights are rejected and another sample for each rejected particle is generated from the same distribution instead. As a result, the samples better approximate the posterior density. Thus more than N samples may be generated. Its effect is very similar to the prior boosting but it is more efficient in terms of computational cost.

In another approach suggested to improve SIR filter, the original particle set $\{L_t^j, w_t^j\}_{j=1}^N$ is replaced by a new particle set $\{L_t^i, w_t^i\}_{i=1}^N$ in resampling stage, which is generated as follows [33]:

- For $i=1, \dots, N$, L_t^i replaces L_t^j with probability proportional to a^j ,
- The associated new weights are updated as $w_t^i = w_t^j / a^j$,

where the selection of a^j is flexible and can be chosen to be $a^j = \sqrt{w_t^j}$ in order to prevent the sample impoverishment problem.

Auxiliary SIR (ASIR) filter is another improvement that was proposed as a variant of the standard SIR filter. Compared with the SIR filter, the advantage of the ASIR filter is that it naturally generates points from the sample at $t-1$, which, conditioned on the current measurement, are most likely to be close to the true state. If the process noise is small then ASIR is often not so sensitive to outliers as SIR.

However, if the process noise is large, a single point does not characterize $p(L_t | L_{t-1}^j)$ well and in such scenarios, the use of ASIR then degrades performance [28].

Regularized particle filter (RPF) which is again a modified version of SIR filter was proposed as a potential solution to the sample impoverishment problem. The RPF is identical to the SIR filter, except for the resampling stage. The RPF resamples from a continuous approximation of the posterior density, whereas the SIR resamples from the discrete approximation. Specifically, in the RPF, samples are drawn from the approximation which uses Kernel density. When the process noise is small, RPF's performance is better than that of the SIR [28].

CHAPTER 5

RF SIGNAL PROPAGATION MODELS

In this chapter we will give details on RF signal propagation properties along with propagation modeling equations and parameters and also creation of RSSI map of the environment which are important to understand and model to have a favorable location estimation. We can divide RSS propagation modeling into two main categories which are small-scale and large-scale fading models. Large scale fading predicts the mean signal strength usually for large receiver-transmitter separation distances. Small scale fading explains the fluctuating characteristics of propagation over short distances where signals are usually affected by multipath phenomenon.

In location estimation applications usually large scale fading models, which include log-distance path loss model and floor attenuation path loss model, are used to model the signal propagation. They are simple and successful in estimating the average value of RSSI for a given range or vice versa.

5.1 RF SIGNAL PROPAGATION PROPERTIES

RSS is a measure of the power received by the receiver from a transmitter and provides information about the distance of the object carrying it. According to Friis' formula, RSS is expressed in the following form [5]:

$$Pr = Pt - PL(d) + Gr + Gt \quad (5.1)$$

where P_r is the received signal power (dBm), P_t is the transmitted signal power (dBm), $PL(d)$ is the path loss (dB), and G_r and G_t are receiving and transmitting antenna gains, respectively. So the RSS information at the receiver is affected by the antenna types, orientation of the receiver-transmitter antennas, transmitted power and the path loss which is almost impossible to model in indoor complex environments.

The propagation is greatly affected by the environment between the source and destination. So in indoor environments, furniture, electrical devices, metal objects, machinery, shelves, walls result in multipath effects which make the indoor position estimation very challenging. Multipath effect is caused by the signal reaching the destination via multiple paths as the signal reflects, diffracts or scatters on the path. Multipath causes fluctuations in the received signal envelope and phase. Thus the signal components arriving from direct and indirect paths are combined to produce a distorted version of the transmitted signal [17].

The propagation of the radio wave mainly depends on the obstacles' properties (surface roughness, size, shape, material) on or around the propagation path as well as the antenna and signal wavelength properties. Obstacle's size is one of the most important factors that affect the propagation. When obstacle's size is larger than the wavelength, reflections (change of direction) could occur when the radio wave impinges on the surface of the obstacle.

When there is an obstacle which usually has sharp irregularities and with size larger than the wavelength, blocking the LOS between the transmitter and the receiver, diffraction may occur. Diffraction is the bending of the signal around the obstacle or the spreading out from an opening. The secondary waves resulting from the obstructive surface are present throughout the space and even behind the obstacle, even when an LOS path does not exist between the transmitter and the receiver. At high frequencies, diffraction, like reflection, depends more upon the geometry of the object, as well as the amplitude, phase and polarization of the incident wave at the point of diffraction [4].

If there are objects with size on the order of wavelength or smaller, the signal may radiate in many different directions around the object. This is called scattering. These mechanisms are illustrated in Figure 5.1.

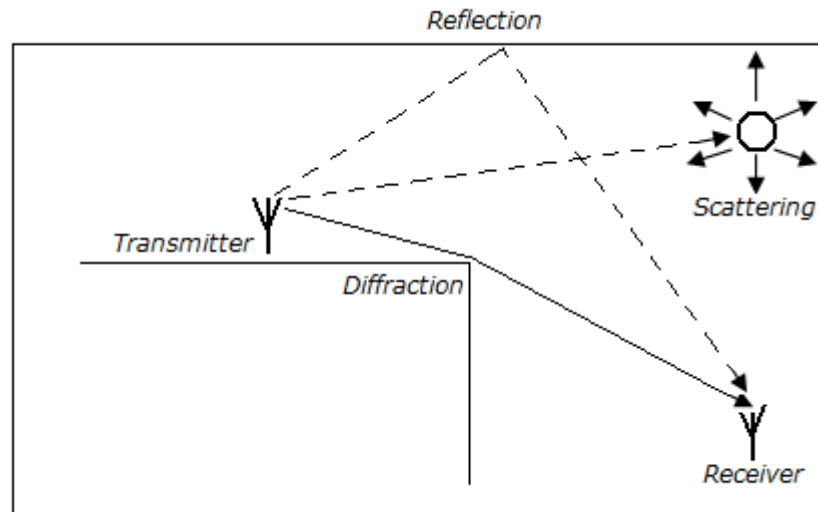


Figure 5.1 RF Signal Propagation Mechanisms [4]

5.1.1 Small Scale Fading

Small scale fading is explained by the fact that, the instantaneous received signal strength is a sum of many contributions coming from different directions due to many reflections of the transmitted signal reaching the receiver [34]. Since the phases are random, the sum of contributions varies widely. The amplitude of the received signal obeys a Rayleigh or Rician fading distribution. In small-scale fading, the received signal power may vary by as much as three or four orders of magnitude (30 or 40 dB) when the receiver is moved on the order of only a fraction of a wavelength. In Figure 5.2 a particular example of measured signal in a multipath environment is given [35]. In this example the signal frequency is 910 MHz and the wavelength is about 33 cm. Over distances as small as half the wavelength, 20 dB RSS variation can be observed due to multipath effects.

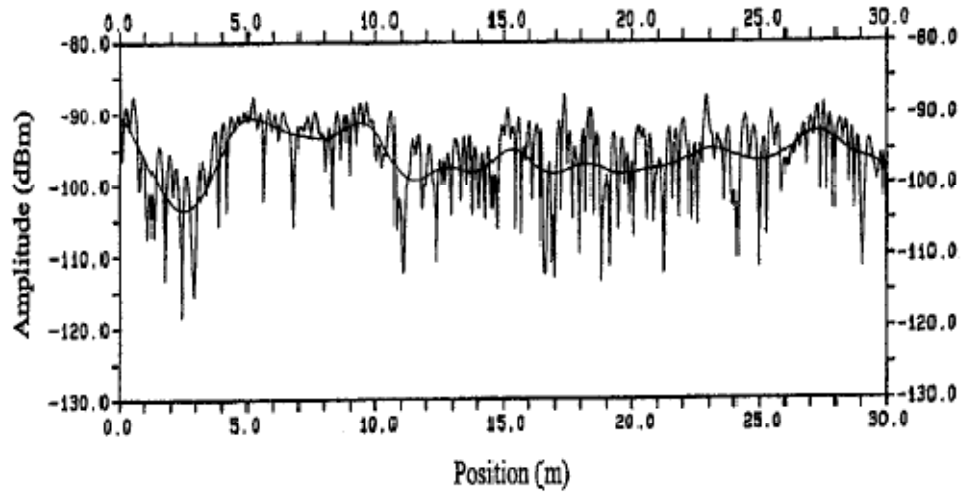


Figure 5.2 Amplitude of the received signal as a function of the range [35]

There are two important small-scale fading models: Rayleigh fading and Rician fading. Rayleigh distributions are used to model dense scatterers without an LOS component, while Rician distributions model small scale fading with stronger LOS component [4]. In Figure 5.3 the small scale fading follows Rician distribution for receiver 2, where it follows Rayleigh distribution for receiver 1.

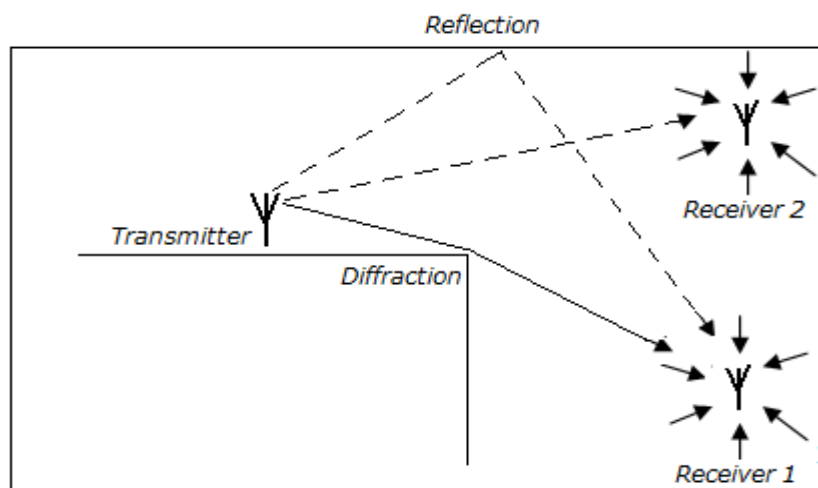


Figure 5.3 Propagation with and without LOS [4]

Rayleigh fading model was first proposed in a comment paper written by Lord Rayleigh in 1889, describing the resulting signal if many violinists in an orchestra play in unison, long before its application to mobile radio reception was recognized. The basic model of Rayleigh fading assumes a received multipath signal consisting of a large number (theoretically infinite) of reflected waves with independent and identically distributed in phase and quadrature amplitudes [17]. The mobile antenna receives a large number, say N , reflected and scattered waves. Because of wave cancellation effects, the instantaneous received power seen by a moving antenna becomes a random variable, dependent on the location of the antenna. Thus both the in phase and quadrature components, $I(t)$ and $Q(t)$, respectively, can be interpreted as the sum of many (independent) small contributions. Each contribution is due to a particular reflection, with its own amplitude and phase. For sufficiently many reflections (large N), the Central Limit Theorem now says that the in phase and quadrature components tend to a Gaussian distribution of their amplitude. $I(t)$ and $Q(t)$ appear to be independent and identically distributed (i.i.d). If there is no dominant component arriving at the receiver, the process will have zero mean with phase evenly distributed between 0 and 2π . The envelope of the channel response will therefore be Rayleigh distributed [4].

A sample of a Rayleigh fading signal is given in Figure 5.4 which shows signal amplitude (in dB) versus distance for an antenna moving at a constant velocity. Notice the deep fades that occur occasionally. Although fading is a random process, deep fades have a tendency to occur approximately every half a wavelength of motion.

In Rician fading, the amplitude gain is characterized by a Rician distribution. The Rician distribution occurs when a strong path exists in addition to the low level scattered path [17]. This strong component may be the LOS path or a path that encounters much less attenuation than others. The Rayleigh distribution is a special case of the Rician distribution; when the strong path is eliminated, the amplitude distribution becomes Rayleigh. While the model is intuitively appealing, it is very

difficult to determine the model parameters (i.e., the local mean of the scattered power and the power of the dominant component) precisely as this requires physically isolating the direct wave from the scattered components.

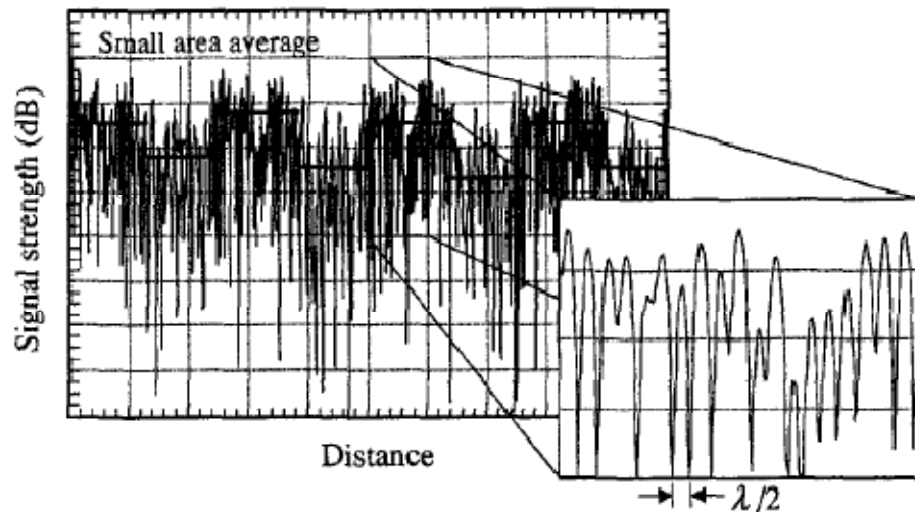


Figure 5.4 Small scale fading with moving antenna [4]

5.1.2 Large Scale Fading

Large scale fading is explained by the gradual loss of received signal power (since it propagates in all directions) with transmitter-receiver separation distance. To have an insight into large-scale fading, the first natural step is to consider propagation in free space, i.e., a medium that has no obstructions [4]. The free space propagation model is used to predict received signal strength when the transmitter and receiver are separated by a medium that has absolutely no obstacles. As such, it has been found that this model also holds when the transmitter and receiver have a clear, unobstructed LOS path between them. Satellite communication systems and microwave LOS radio links typically undergo free-space propagation [34]. Friis free space formula is given as [10]

$$P_r = P_t - 10 \log \left(\frac{4\pi d}{\lambda} \right)^2 + G_r + G_t \quad (5.2)$$

where P_r is the received signal power (dBm), P_t is the transmitted signal power (dBm), $10 \log \left(\frac{4\pi d}{\lambda} \right)^2$ is the path loss which will be denoted as $PL(d)$ (dB), G_r and G_t are receiving and transmitting antenna gains, respectively, d is the distance between receiver and transmitter antennas and λ is the wavelength of the signal transmitted. In Figure 5.5 theoretical RSS values vs. measurement values in an outdoor environment are given [10]. Free space assumption is used for the calculated RSS values. It is seen that measured RSSI data in outdoor environment fits quite well to the free space propagation model.

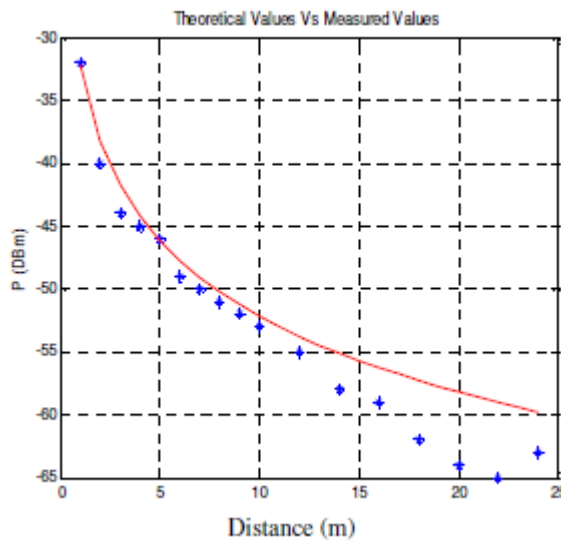


Figure 5.5 Comparison of theoretical and empirical RSS values in outdoor [10]

For indoor environments, log-distance path loss model, among different path loss models, in its simplest form often used for electromagnetic signals, can be expressed as [5]

$$\overline{PL(d)} = \overline{PL(d_0)} + 10 \log \left(\frac{d}{d_0} \right)^n \quad (5.3)$$

where d represents the distance between the transmitter and receiver, $\overline{PL(d)}$ is the average propagation loss (in dB) measured at distance d , n is the path loss exponent which indicates the decreasing rate of signal strength in an environment, d_0 is a reference distance normally chosen close to the transmitter (e.g., 1m), and $\overline{PL(d_0)}$ is usually empirically measured average path loss which occurs at d_0 distance. In general, the exponent n is environment dependent. In free space, n is equal to 2. In more complicated environments, n will generally be larger meaning high signal path loss. n may range from 1.2 to 8 as given in [4]. It must be noted that the model introduced in (5.3) does not consider small scale fading, namely, the variable factors in the surrounding environment such as shadowing. Thus the path loss can only be considered as an average value. Shadowing, also referred to as log-normal shadowing, represents the effects of different propagation paths due to the obstructions, antenna orientation, moving objects in the environment, leading to different RSS measurements at different locations with the same distance to the transmitter. To take these factors into consideration, it has been shown that the received signal strength usually demonstrates a log-normal distribution where it has a mean received power in dBm and standard deviation σ in dB. Hence, we take a probabilistic approach and model the path loss at distance d as a random variable $PL(d)$ as given in (5.4) by using a Gaussian random variable $\mathcal{X}_\sigma \sim N(0, \sigma^2)$ with zero (dBm) mean and standard deviation σ in dB [5].

$$PL(d) = \overline{PL(d)} + \mathcal{X}_\sigma = \overline{PL(d_0)} + 10 \log \left(\frac{d}{d_0} \right) + \mathcal{X}_\sigma \quad (5.4)$$

With a given transmitting antenna power P_t , transmitting antenna gain G_t , and receiving antenna gain G_r , the received signal strength $Pr(d)$ (in dBm) at distance d is given in (5.6) combining (5.5) and (5.4).

$$\Pr(d) = P_t + G_t + G_r - PL(d) \quad (5.5)$$

$$\Pr(d) = P_t + G_t + G_r - \overline{PL(d_0)} - 10n \log\left(\frac{d}{d_0}\right) - \mathcal{X}_\sigma \quad (5.6)$$

We can rewrite (5.6) as in (5.7) since the first four terms are constant for a given transmitter – receiver pair in a certain environment.

$$\Pr(d) = \alpha - 10n \log\left(\frac{d}{d_0}\right) - \mathcal{X}_\sigma \quad (5.7)$$

Here α is a constant in dBm which will be determined empirically in the concerned environment. It is equal to the median received signal power at d_0 which is usually taken to be 1 m. n is also to be determined by a set of calibration measurements since it changes according to the surroundings of the transmitter- receiver pair. In complicated environments n will be larger since the signal will attenuate faster as it travels through obstacles. σ , the standard deviation is also dependent on the environment. The smaller σ is the more accurate the measurements are. In complicated environments σ is expected to be larger. Table 5.1 gives n and σ values in different indoor environments [4].

By using (5.7) we can derive that, given an actual distance d between transmitter and receiver, the received power $\Pr(d)$ is a random variable with log-normal distribution with mean $\alpha - 10n \log\left(\frac{d}{d_0}\right)$ (dBm) and standard deviation σ dB. So the probability distribution model of observing a certain RSSI value at distance d can be written as [5], [2]

$$p(\text{RSSI}|d) = \frac{1}{\sqrt{2\pi}\sigma} \exp \left[-\frac{\left(\text{RSSI} - \alpha + 10\log\left(\frac{d}{d_0}\right) \right)^2}{2\sigma^2} \right] \quad (5.8)$$

where $p(\text{RSSI}|d)$ is the conditional probability density function of the observed RSSI value given the distance d .

Table 5.1 Path Loss Exponent (n) and Standard Deviation (σ) in different indoor environments for log-distance path loss model [4]

Environment	Frequency(MHz)	n	σ (dB)
Retail Store	914	2.2	8.7
Office, hard partition	1500	3.0	7.0
Office, soft partition	1900	2.6	14.1
Chemical factory(obstructed)	4000	2.1	9.7
Chemical factory(LOS)	4000	2.1	7.0
Suburban home	900	3.0	7.0

Floor attenuation factor propagation model takes floors and partitions (i.e., walls) into account as well as the large scale path loss [17]. So it gives more accurate results than the log-distance path loss model. The model is given as [17]

$$\overline{\text{PL}}(d) = \overline{\text{PL}}(d_0) + 10\log\left(\frac{d}{d_0}\right) + \text{FAF} + \sum \text{PAF} \quad (5.9)$$

where FAF is the floor attenuation factor that represents the loss between the floors of the building in dB. PAF is the partition attenuation factor that represents the loss caused by obstructions on the path between the transmitter and the receiver antennas in dB. Some typical FAF and PAF values are given in Table 5.2 [4] and Table 5.3 [36], respectively.

Table 5.2 Average Floor Attenuation Factors in dB in two different buildings [4]

Buildings(Office Building)	FAF(dB) Building 1	FAF(dB) Building 2
Through one floor	16.2	12.9
Through two floors	27.5	18.7
Through three floors	31.6	24.4

Table 5.3 Partition Attenuation Factors for different building materials [36]

	Attenuation (dB)
Elevator	23
Building wall	3
Wooden doors with windows	1
Separating Floors	22

In our work we used an adapted version of this model including only the PAF which consists of wall attenuation factor (WAF) as suggested in [17]. The simplified wall attenuation factor propagation model is

$$\overline{PL}(d) = \overline{PL}(d_0) + 10n \log \left(\frac{d}{d_0} \right) + nW \cdot WAF \quad (5.10)$$

where nW is the number of walls on the path between the transmitter and the receiver and WAF represents the wall attenuation factor in dB. The value of WAF is calculated to be about 3 dB for WLAN applications in the literature [36], [17]. However it may change according to the wall material and thickness as well as the RF signal frequency, so it should be determined empirically.

As a result rewriting (5.8) using WAF propagation model yields

$$p(\text{RSSI}|d) = \frac{1}{\sqrt{2\pi}\sigma} \exp \left[-\frac{\left(\text{RSSI} - \alpha + 10n \log \left(\frac{d}{d_0} \right) - nW \cdot \text{WAF} \right)^2}{2\sigma^2} \right] \quad (5.11)$$

In order to compensate dynamic changes in the environment and to remove the heavy human labor in the training phase, automatic parameter calibration techniques are proposed in the literature [37], [5]. [37] uses IEEE 802.15.4 sensor network in indoor environment and exploits RSSI measurements from pair of anchors to obtain the automatic calibrated parameters. It assumes WAF propagation modeling and calibrates the parameters of n and WAF automatically while obtains α parameter in advance. [5] proposes an outdoor localization method with auto calibration of the parameters and making use of reference tags. In [5] log-distance path loss model is used and the parameters α , n , and σ are estimated automatically.

Details related to our work will be given in Chapter 6.

5.1.3 RSSI Pattern (Map)

For applying nearest neighbor(s) (NN) or probabilistic approaches to the indoor localization problem, RSSI pattern/map of the related environment is usually created in a training phase. The RSSI map represents the signature of the RSSI readings at different locations or continuously distributed in the area. The performance of the

localization algorithm is theoretically limited by the precision and accuracy of RSSI map. There are two different means of creating the map. One method is predicting the propagation behavior to estimate the signal strength over a target area using the detailed floor plan and the propagation models described above. To apply this method, one can carry out empirical measurements to derive $\alpha, n, WAF,$ and σ parameters for probabilistic approaches and α, n, WAF only for NN approaches. It is important to take measurements of RSSI at different distances by considering dynamic environmental changes, target antenna orientation, and other types of ambiguities. These measurements can be averaged for certain distances and curve fitting algorithms can be used to calibrate the related parameters. Alternatively, propagation prediction tools can also be used to estimate these parameters. Then for every location the RSSI map, in fact vector sets of RSSI values, can be created. Other method of RSSI map creation is the empirical method. In this approach signal strength distribution over the area is estimated based on the measured data at different locations. Experimental studies suggest that empirical method is better than the first method in terms of accuracy since propagation models are insufficient in precision to predict the signal propagation behavior [4].

One important step in the empirical method is how to collect the training data over the target area. One way is to take samples of RSSI data at predetermined grid cells that are equal in size forming the target area as in [17] and [13]. In this approach, a number of measurements are taken in an offline training phase to form the signature belonging to that grid. In LANDMARC [11] the RSSI map is created with an online training phase where reference transmitters (tag) are used to obtain the RSSI signature at certain locations. In order to use in probabilistic localization methods, Kernel based approaches [13], [10] or histogram approach [13] can be used to obtain the probabilistic behavior (likelihood) of each grid. In Kernel method [13], a Gaussian probability density of the RSSI observations s is assigned to each grid location l (see (5.12)). The density is a mixture of n_l equally weighted density functions where n_l denotes the number of training RSSI vectors in location l .

$$p(s|l) = \frac{1}{n_l} \sum_{j=1}^{n_l} \frac{1}{\sqrt{2\pi}\sigma} \exp\left[-\frac{(s - s_j)^2}{2\sigma^2}\right] \quad (5.12)$$

In (5.12) σ is an adjustable parameter that determines the width of the density and s_j is each of the observed values of RSSI in the training set at location l . [13] states that, this one dimensional formula can be extended to multivariate observations, e.g., received power from several access points, by multiplying the individual probabilities, which amounts for an assumption of independence of the observations.

In [10], a similar idea is used but this time the RSSI observation density in grid location l is distributed around the sample mean μ_l that is obtained in l . Also RSSI sample std. σ is evaluated by computing the std. for the sample measurements in each grid cell. In order to obtain the likelihood function $p(s|l)$ for multiple dimensions or access points, independence assumption is made and all conditional probabilities are multiplied together. (5.13) is given as an example to a system with 3 access points.

$$p(s|l) = \prod_{i=1}^3 \frac{1}{\sqrt{2\pi}\sigma_{li}} \exp\left[-\frac{(s_i - \mu_{li})^2}{2\sigma_{li}^2}\right] \quad (5.13)$$

The histogram method [13] is closely related to discretization of continuous values to discrete ones. The method requires that we fix a set of bins, i.e., a set of non-overlapping intervals that cover the whole range of the variable from the minimum to the maximum. The number of the bins is an adjustable parameter. The density estimate is then a piecewise constant function where the density is constant within each of the bins that counts the frequency of occurrence of signal samples that fall within the range of each bin. Another way to collect data samples is taking the measurements while walking. In this way only one data sample can be obtained at each location but this time sample locations' precision is higher since many locations are involved. In order to create the area propagation map, the sampled locations are

grouped into clusters where each cluster is composed of a sufficient number of locations [4].

In this thesis we used the method in [17] to create the RSSI map to use for the pattern based NN localization method.

CHAPTER 6

RSSI CALIBRATION IN THE TARGET ENVIRONMENT

In this chapter experimental environment properties will be given and WAF propagation model and calibration of its parameters along with RSSI measurements taken in this environment will be explained. Also the method of automatic calibration of parameters by using reference tags will be proposed and the method of RSSI map creation will be given. The derived parameters and proposed methods will be used in both simulation and experimental phases of the thesis.

The experimental environment consists of two rooms with sizes of 4 m x 3 m and 4m x 6m and 36 m² total area which is shown in Figure 6.1.

The rooms have a bricked wall between and wooden and metal furniture and electrical devices inside. There are 3 RFID readers used in the system one (R3) in the small sized room and two (R1, R2) in the large sized room as shown in Figure 6.1. The readers are placed at the corners of the rooms in order to cover most of the area by the readers' patch antennas. The reference tags (T1, T2, T3, T4) used for automatic calibration and smoothing purposes are distributed in the area two in one and two in the other room towards the central region of the overall area. The used RFID products' RF frequency is 868 MHz, data rate is 250 kbaud, BW is 540 KHz where the tags transmit with 5 dBm output power and readers receive with -90 dBm sensitivity level.

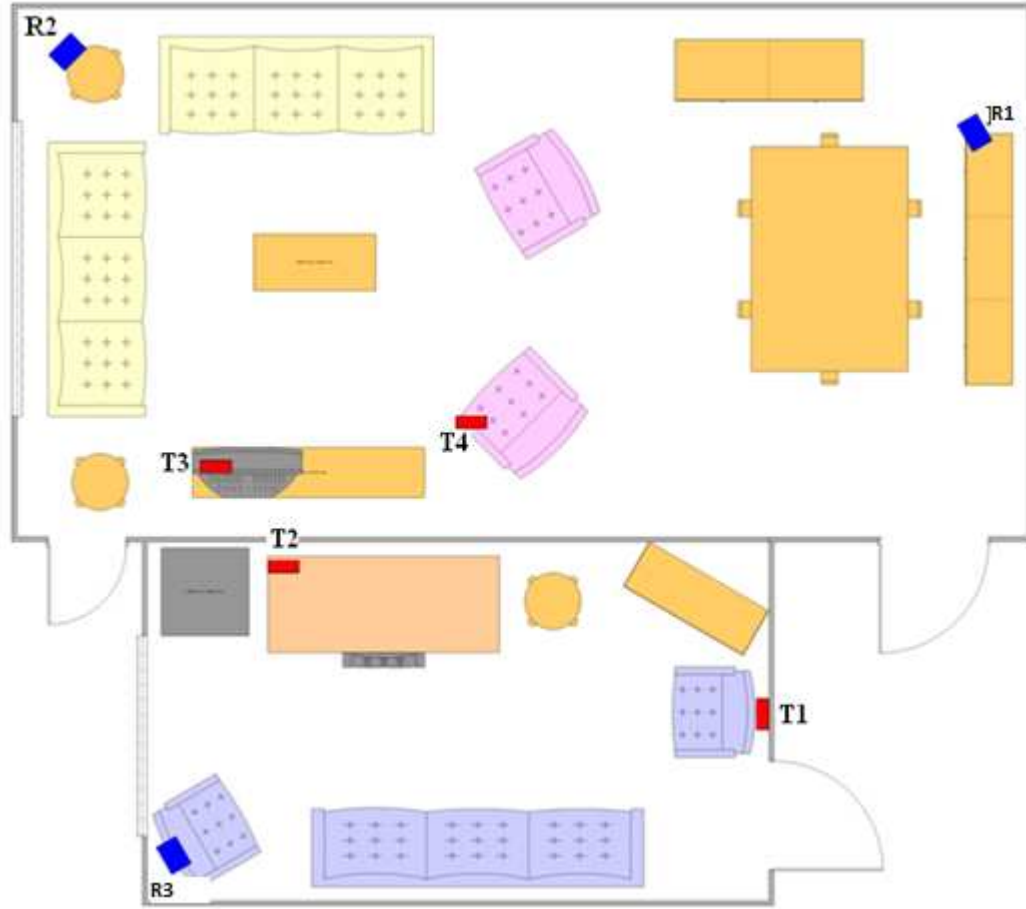


Figure 6.1 Experimental environment

6.1 OFFLINE CALIBRATION OF PARAMETERS

First we rewrite the WAF propagation model for convenience

$$\overline{PL}(d) = \overline{PL}(d_0) + 10n \log\left(\frac{d}{d_0}\right) + nW \cdot WAF \quad (6.1)$$

where d represents the distance between the transmitter and receiver, $\overline{PL}(d)$ is the average propagation loss (in dB) measured at distance d , n is the path loss exponent which indicates the decreasing rate of signal strength in an environment, d_0 is a reference distance normally chosen close to the transmitter (e.g., 1 m), $\overline{PL}(d_0)$ is

usually empirically measured average path loss which occurs at d_0 distance, nW is the number of walls between the receiver and the transmitter, WAF is the wall attenuation factor in dB.

We rewrite (6.2) for convenience for the received signal strength $\text{Pr}(d)$ (in dBm) at distance d

$$\text{Pr}(d) = P_t + G_t + G_r - \text{PL}(d) \quad (6.2)$$

with a given transmitting antenna power P_t , transmitting antenna gain G_t , receiving antenna gain G_r , and path loss $\text{PL}(d)$ at distance d . Then combining with (6.1) by taking d_0 reference distance as 1 m and adding zero (dBm) mean Gaussian noise \mathcal{X}_σ to the received signal power, (6.3) is obtained

$$\text{Pr}(d) = \alpha - 10n\log(d) - nW \cdot \text{WAF} + \mathcal{X}_\sigma \quad (6.3)$$

where $\alpha = P_t + G_t + G_r - \overline{\text{PL}(d_0)}$. Then the mean received power $\overline{\text{Pr}(d)}$ can be written as

$$\overline{\text{Pr}(d)} = \alpha - 10n\log(d) - nW \cdot \text{WAF} \quad (6.4)$$

In the offline training phase the parameters in (6.3) will be found to be used in the experiments and the simulations. α is a constant in dBm that denotes the mean value of received signal power at 1 m distance. It will be found for each reader since it is also affected by the reader and tag antenna gains and antennas may not be identical. n is the mean value of path loss exponent that depends on the propagation environment. It will be found for each reader since the position of the readers and surrounding objects may affect n value. nW is the number of walls between transmitter and receiver (T-R). This will be “0” if the tag and the reader are in the same room and “1” if they are in different rooms in our system. WAF is the wall attenuation factor in dB that is the loss of power when there is a wall between T-R when they are at the same distance. WAF should be equal for all readers since it only

depends on the type of the wall material. \mathcal{X}_σ is the Gaussian assumed [10] RSSI measurement noise with zero (dBm) mean and σ dB standard deviation that stems from signal propagation variations due to multipath effects, antenna orientation, and moving objects in the target area.

For calibrating the parameters mentioned above we have run a set of experiments with one tag at different locations for each reader. The readers were located at the corners of the rooms with a 45° angle to the walls at 1.2 m height. The height was determined so as to have as much as LOS region with the target tag which was located at 1 m height. The height of the tag was determined as 1 m in order to model the case when a person or a medium sized box carrying it. To derive the mean parameters except WAF we took measurements at different distances to the reader in the same room and at line of sight. To find WAF value we took measurements at 3 m distance in the same room with the reader and in the other room. In our experiments, knowing that RSSI at a fixed distance is affected by the location of the tag, orientation of the tag antenna, and moving objects in the surrounding environment, we created these noise sources while measuring RSSI values. We took measurements at fixed distances on a circular radius as illustrated by the stars in Figure 6.2.

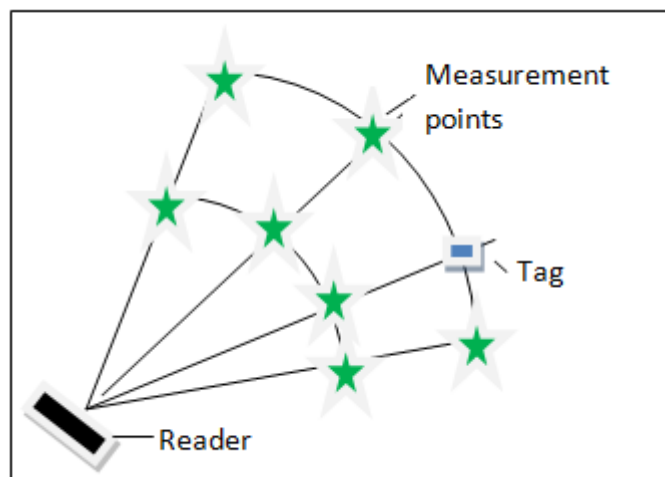


Figure 6.2 Illustration of measurement points for propagation parameter calibration

At each location we took about 100 measurements with 8 different orientation of the tag being vertical while creating random human movements around the tag and the reader. For each distance we experimented at 4 different locations thus having totally 400 measurements for each distance. As an example the histogram of RSSI readings at 1, 2 and 3 m distances are given in Figure 6.3.

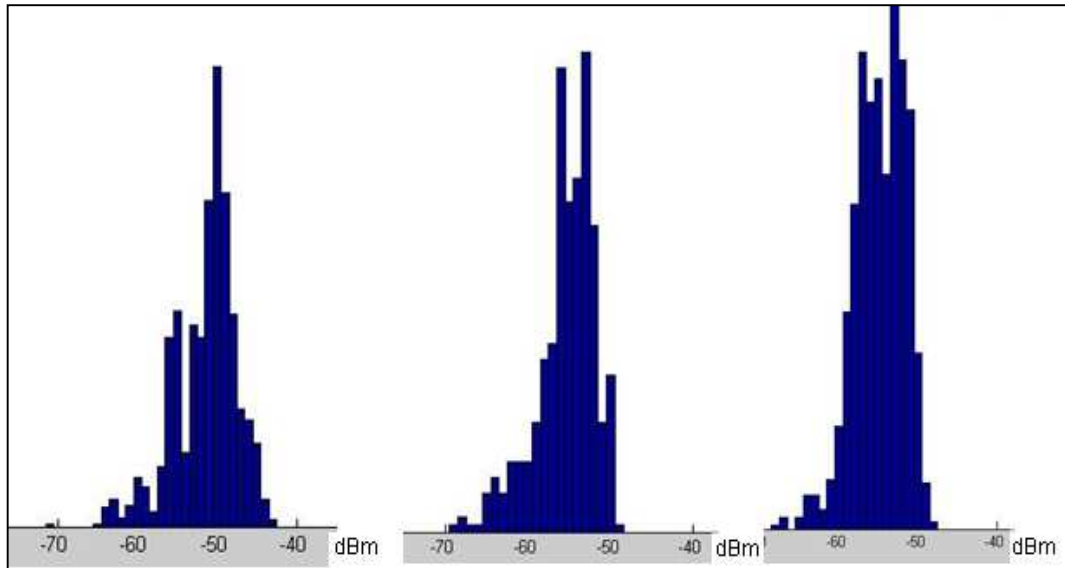


Figure 6.3 RSSI histograms at 1m, 2m, and 3m, respectively.

As can be seen in the above figures RSSI observation varies significantly at the same distances but at different location and orientation. We assume that the RSSI observation at the same distance is Gaussian distributed. By analyzing the 400 measurement data at each distance we find the standard deviation of RSSI readings at that distance. Then taking the average standard deviation values for all of the experimented distances we get the mean standard deviation (std.) value σ over the target area which is approximately 5.2 dBm. [14] reports that σ in a home is 3 dB and [4] reports to be 7 dB in a suburban home. Taking these literature values into consideration, we cannot have a consistent σ value that can be a reference value for us to compare our finding with. That is not surprising in fact because surely, the experimental methods, the antenna type, the physical properties of the environment

are crucial here to get the σ value. Comparing our finding 5.2 dB with the sample literature values we can at least comment that our finding seems reasonable. In order to obtain the other mean propagation parameters we took the average of 400 measurements to give $\overline{\text{Pr}(d)}$ at distance d . After obtaining mean RSSI values at different distance values we used the curve fitting tool of MATLAB exploiting least squares (LS) algorithm to find the n and α parameters in (6.4) for each of the readers. To find WAF we took measurements at the same distances to a reader in two rooms. Then taking the average of the RSSI readings in each room we just took the difference of average RSSI values found in two separate rooms to find WAF value in dB. We found WAF as 2 dB. In [17] it is reported to be 3.3 dB and in [36] 3 dB which are close to our finding. Calculated parameter values for each reader are given in Table 6.1.

Table 6.1 Propagation parameters for 3 readers

	α (dBm)	n	WAF(dB)	σ (dB)
Reader 1	-42	2.3	2	5.3
Reader 2	-52	2.3	2	5.2
Reader 3	-45	2.5	2	5

In Figures 6.4 - 6.6 average RSSI measurement values for each reader at different distances and theoretical path loss model curves with the calculated parameters are given.

In Figure 6.6, measurements taken in the across room of reader 3 are given to show the effect of the wall attenuation. The readings at 1 m, 1.5 m, 2 m, 2.5 m and 3 m are at the same room with the reader where the ones at 3.8 m, 5 m and 6 m are in the other room. So drawing the curve exploiting (6.4) with $n_W=1$ fits well to the real RSSI measurements through the wall.

In our location estimation simulations and experiments we used the parameters given in this section for the methods with offline calibration.

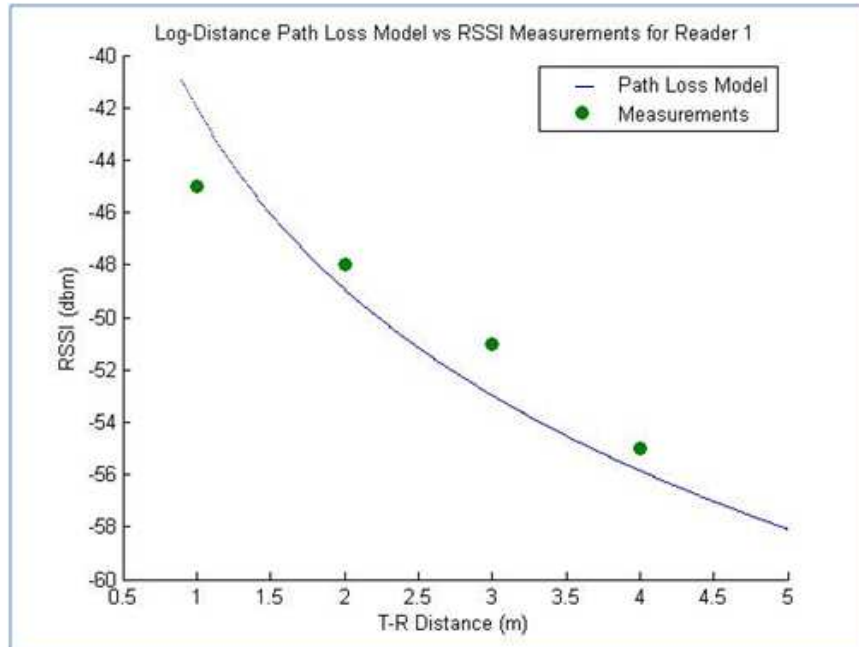


Figure 6.4 Measured and modeled RSSI values for Reader 1

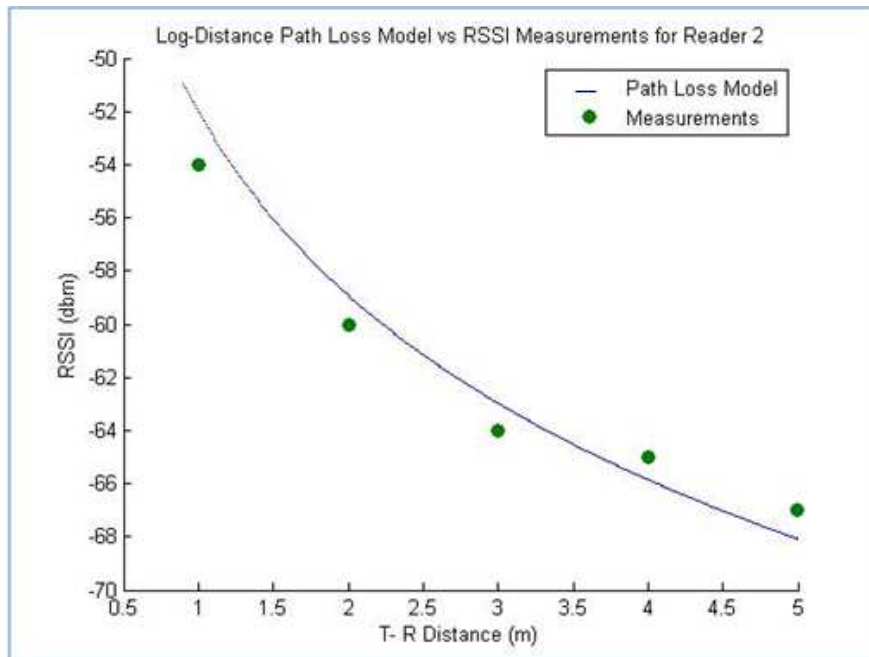


Figure 6.5 Measured and modeled RSSI values for Reader 2

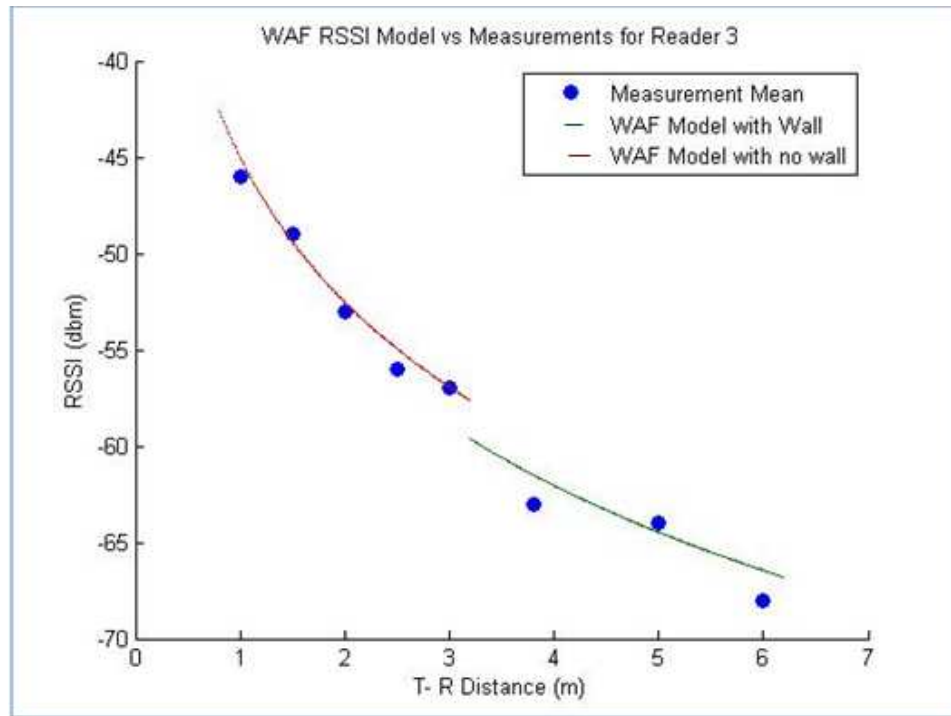


Figure 6.6 Measured and modeled RSSI values for Reader 3

6.2 AUTOMATIC CALIBRATION WITH REFERENCE TAGS

In propagation parameter based localization applications calibration of the propagation parameters is very important in order to decrease the localization error. Usually calibration process is a preliminary offline process that needs human intervention and it suffers from the changes in the environment that may affect the parameters significantly. In order to remove the human intervention and make the parameters adaptive to environmental changes, several automatic calibration procedures are proposed in the literature [38], [39], [40], [16], [5]. These calibration techniques are mostly used for wireless sensor network systems [38], [40], [16]. [5] is the only literature work that exploits automatic calibration for RFID systems but it is proposed for outdoor localization problem. So our work is the only one which uses automatic calibration procedure for indoor localization problem using RFID system. For this purpose we use reference tags that beacon every one second and located at known fixed points in the target environment.

We know that for estimating an accurate propagation parameter set it is important to sample the target area by choosing the experimental grid locations as many as possible. Sufficient sampling gets crucial especially for complicated indoor environments. So for calibrating the parameters we need as many reference tags as possible which is not feasible for real applications. So our one purpose here is to be able to estimate the parameters with an acceptable accuracy with respect to the offline calibration technique using a feasible number of reference tags. In this work we used 4 reference tags in an area of 36 m² including two rooms. We evaluated the accuracy of the parameters by comparing the location estimation results with that of the offline calibrated parameters given in the Section 7.3. Our another aim is to have a flexible system that is adaptive to moving objects, environmental changes or changes in the reader antenna position or orientation that may affect the propagation parameters in the environment. As well as using reference tags for calibration we also used limiting values for α and n parameters (refer to (6.3)) that are obtained by adding a range to the values found by offline calibration.

[16] suggests n and WAF parameters to be automatically calibrated and states that there is no need to calibrate α automatically because it is only affected by the hardware. But in fact α as being the received power at reference distance (e.g., 1 m) it may be affected by the reader antenna orientation and height as well as the surrounding objects or obstacles that affect the signal propagation. So it is necessary to automatically calibrate the α parameter in order to take these effects into account. We calibrated α and n for each reader as proposed in [5]. On the other hand WAF is a parameter that only depends on the wall properties which do not change thus WAF parameter can be obtained a priori and used as a fixed parameter during the application. For probabilistic applications we propose to calibrate the standard deviation of filter measurement model σ by estimating the RSSI measurement noise using reference tags. To sum up, we propose to calibrate the parameters α , n , and σ automatically while using a priori calculated WAF parameter.

Least Squares (LS) or Least Mean Squares (LMS) [38], [39], [40], [16] are suggested in the literature to calibrate the signal propagation parameters. We used LS algorithm to calibrate α and n parameters. For the solution we need to find the parameters that minimize (6.5) for each reader j .

$$F_j = \sum_i (RSSI_{ij} - RSSI'_{ij})^2 \quad (6.5)$$

Where $i=\{1,2,3,4\}$ indicating the reference tag index, $j=\{1,2,3\}$ indicating the reader index, $RSSI_{ij}$ is the RSS value measured from the i^{th} tag at the j^{th} reader and $RSSI'_{ij}$ is the calculated RSS value from the i^{th} tag at the j^{th} reader with the parameters α and n . The equation relating $RSSI'_{ij}$ with α , n parameters, and d_{ij} , that is the known distance from the i^{th} reference tag to the j^{th} reader, is given in (6.6).

$$RSSI'_{ij} = \alpha_j - 10 \cdot n_j \cdot \log(d_{ij}) - nW \cdot WAF \quad (6.6)$$

In order to find the estimates of α_j and n_j for the j^{th} reader we iterate α from -40 dBm to -55 dBm and n from 1.5 to 3.

After estimating the parameters α_j and n_j we can estimate σ by finding the standard deviation of the RSSI readings obtained between each reference tag i and reader j pair as in (6.7). Here we use $RSSI'_{ij}$ as the mean RSSI value from tag i to reader j using (6.6).

$$\sigma = \sqrt{\frac{1}{12} \sum_{j=1}^3 \sum_{i=1}^4 (RSSI_{ij} - RSSI'_{ij})^2} \quad (6.7)$$

By using the proposed methods the calibrated parameters found in the static experiment environment are given in Table 6.2.

Table 6.2 Automatically calibrated propagation parameters and RSSI std.

	α (dBm)	n	σ (dB)
Reader 1	-45	2.3	5.3
Reader 2	-49	2.7	
Reader 3	-42	2.5	

Despite estimated parameters seem quite close to the ones found in the offline calibration, automatic and offline calibrated parameters will be compared in detail in Chapter 7 by using the location estimation error statistics.

6.3 RSSI MAP CREATION

In the propagation pattern based localization method does, we use the method described in [17] that finds the best matches of RSSI pattern (nearest neighbors) stored in the offline training phase. In RADAR mean of RSSI vectors for two different orientations of the transmitters are stored at each training grid location. In our work we store randomly placed tags' RSSI values during the storing process in one grid cell to model as many different orientations' RSSI values as possible. We randomly moved the tag in a 20 cm x 20 cm area and also changed the orientation of the tag placing always vertical to the ground.

At each grid we stored 40 RSSI measurement vectors composing of RSSI observations for the 3 readers. Then we take the mean RSSI values for the corresponding grid cells. We defined 32 furniture dependent grid locations which are approximately 1 m spaced as our training locations in our target area of 36 m². The grids are equally spaced at 1 m distance. In the test set up, readers are placed at 1.2 m height and tags are placed at 1 m height that are also used in the estimation experiments.

CHAPTER 7

SIMULATIONS AND EXPERIMENTAL WORK

In this chapter, first the applied localization and tracking methods both in simulation and experimental work and the proposed contributions are given in Section 7.1. Then the details and results of simulation and experimental work will be explained in Sections 7.2 and 7.3, respectively. To conclude, in Section 7.4, analysis of simulation and experimental work will be given.

7.1 APPLIED LOCALIZATION AND TRACKING METHODS

7.1.1 Propagation Pattern Based Nearest Neighbors (NN) Method

As mentioned in Section 3.1.1 pattern matching algorithms are very successful in location estimation accuracy but have several practical drawbacks. The propagation pattern of the environment can be created in an offline phase storing a large amount of data at densely spaced grid locations or in an online phase using densely spaced reference transmitters in the area. We could not apply and compare the online method because of insufficient number of reference tags. We generated an offline propagation map using 32 grid locations as defined in Section 6.3 and recorded the mean RSSI vector for each grid. After generating the map we applied the method in our experimental work to compare with the other methods. But we do not go into details of this method since we seek a more practical, easy to deploy and cost effective method for real life applications.

7.1.2 Propagation Parameter Based Nearest Neighbors (NN) Method

As mentioned in Section 3.1.2, the propagation pattern of the environment is generated virtually using different propagation models. The used propagation model is often log-distance path loss model which is also used in this work. In this method propagation parameters of the log-distance path loss model (n, α) can be calibrated in an offline training phase (see Section 6.1) or reference transmitters at known locations can be used to automatically calibrate the parameters (see in Section 6.2). We investigate the offline approach in simulations and both approaches in experimental work in details. We especially stress on the automatic calibration approach and use it for the other localization methods in this thesis. In general parameter based NN methods are very simple to set up and implement, but less accurate compared to the pattern based approaches.

7.1.3 Grid Based Bayesian Filtering

Details of the algorithm were given in Section 4.1. It was implemented both in simulation and experimental work and the behaviors of the filter for differing grid resolution, RSSI measurement noise, and process model were investigated and compared with the other methods. Grid based Bayesian filtering is simple and accurate to use for tracking applications with low precision needs in moderate sized environments. But if the size of the area and the precision need increase, the grid resolution and number have to be increased which causes a large load of computational work.

7.1.4 Sampling Importance Resampling (SIR) Particle Filtering

Details of the filter were given in Section 4.2.2. We simulated and implemented the basic SIR filter algorithm experimentally and also applied two different modifications in the resampling stage which were proposed in the literature. One is smoothing the importance factor w at the beginning of the resampling stage by taking

the square root of the importance factor of each current particle. This smoothing avoids sample impoverishment problem. The other improvement is to resample not at every recursion step but when the N_{eff} value is smaller than a threshold N_t value.

We simulated the effects of the proposed improvements for different conditions and also investigated the behavior for different measurement noise, process model, number of particles N , and the N_t value. SIR filter is very easy to apply, computationally more efficient and more accurate for some cases than the grid based Bayesian filter.

7.1.5 Additional Approaches To Conventional Localization Methods

We mainly applied three different approaches to the conventional localization/tracking methods which are detailed below. Automatic calibration of propagation parameters and filter measurement noise std. (σ) approach is proposed in the literature, but this thesis work is the first work that applies this approach to RFID based indoor localization problem as far as we know. RSSI smoothing algorithm using the reference tags can be accepted to be a contribution to the literature since we could not find such an approach in the literature.

7.1.5.1 Automatic and Online Calibration of The Propagation Parameters

We found very little information about the automatic calibration of the propagation model parameters for localization methods in the literature. It is expected that using denser reference transmitters would yield a closer approximation of the real propagation parameters. But we investigated the estimation results when only 4 reference tags were used for calibration. We calibrate the n and α parameters of the log-distance path loss model automatically and also instantaneously at each step of RSSI observation from all of the reference tags so we call it "online calibration" as well as "automatic calibration". The details of the calibration were given in Section 6.2. We apply automatic calibration approach to each of the localization method. But first we apply it to NN method and compare the location estimation results with that

of NN method using offline calibration in experimental work to observe the effects of online calibration.

7.1.5.2 Automatic and Online Calibration of Filter Measurement Noise σ

For the Bayesian filters, using an accurate measurement noise model is important. We assume Gaussian distributed RSSI measurement noise and propose automatic calibration of the standard deviation σ to be used in the measurement model of the Bayesian filter. We calibrate the parameter automatically and online by using the reference tags as explained in Section 6.2. By calibrating σ automatically in an online phase it can adapt to the changes in the environment such as people moving around and so we claim that online calibration of σ may improve estimation accuracy especially in the case of dynamic RSSI measurement errors. Also it is a very simple and practical method to apply. We applied this approach to the grid based Bayesian and SIR filters in the experimental work and tested for different conditions yielding the outperforming estimation results.

7.1.5.3 RSSI Smoothing By Using Reference Tags

Using the RSSI readings from the reference tags with known locations, we propose an algorithm to smooth the RSSI readings from the target tag when it is determined to be in a certain range to one of the reference tags. In order to determine the closeness of the target to the reference tags, we find the Euclidean distance of the target to all of the reference tags and then obtain the weighting factor for each reference tag as also calculated for NN methods. If the weighting factor for any of the reference tags is larger than 0.4, the target is determined to be close to that reference tag. Knowing the real locations, we calculate the expected RSSI vectors of the reference tags using the log-distance path loss propagation model and obtain RSSI error vectors by taking the difference of the expected and observed RSSI vectors. In the last step, if the target is determined to be close to one of the reference tags, the calculated RSSI error vector for that reference tag is multiplied with the

weighting factor and then subtracted from the observed RSSI vector of the target to give the smoothed RSSI vector. The idea is that if the target is close to the reference tag, a correlated measurement error is added to the target RSSI measurement. We claim that for the tested locations of the target tag that are close to the reference tags, the estimation error is decreased significantly by the RSSI smoothing algorithm. To observe the effect we applied this approach to grid based Bayesian and SIR filters in the experimental work and tested with different conditions yielding the improving effect of the algorithm.

7.2 SIMULATIONS

In the simulation phase of our work, several of the localization methods explained in Section 7.1 were applied before the experimental phase in order to compare the methods and investigate the effects of different models and parameters. Since it is sometimes very difficult and time consuming to run experiments to yield statistical data, we have run simulations to determine the detailed plan of our experimental work in advance. It is not possible to model the real environment and noise parameters by simulations but simulation work gives us the theoretical results explaining weak and strong behaviors of localization methods and the behavior of the methods with changing parameters (e.g., grid resolution, number of k_{NN} nearest neighbors, etc.). Simulations of parameter based NN method with offline calibration of the propagation parameters, grid based Bayesian and SIR filtering methods are described in this section.

In Section 7.2.1 we will give details of the environment models and the simulated methods and parameters. In Section 7.2.2 the simulation results of different localization methods with the effects of different parameters, and in Section 7.2.3 comparisons and analysis of the simulated methods will be given.

In Appendix A, the Cramer Rao Lower Bound (CRLB) for our localization problem is derived. Before starting simulation results we will give the important results of the CRLB.

By investigating the resulting equation of the lower bound, it is seen that the location estimation lower bound depends on

- RSSI measurement noise standard deviation σ_0
- Signal propagation log-distance path loss parameter n
- Number of readers k_{RDR} used in the localization system
- The relative target location (x, y) and the reader locations (x_j, y_j) .

We give the CRLB for the RMS distance error with changing RSSI noise std. and number of readers in Figure 7.1.

In the figure it is seen that RMS error lower bound increases with increasing σ and decreasing number of readers as expected.

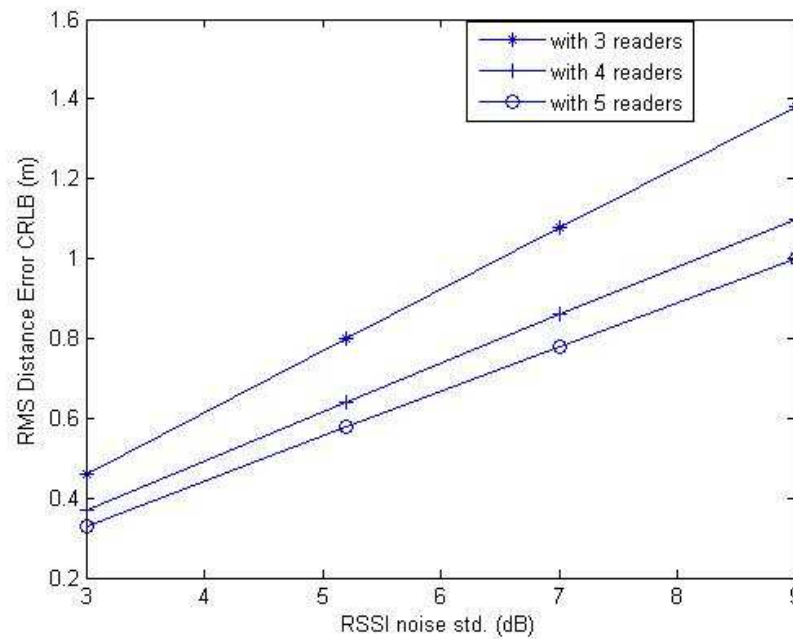


Figure 7.1 RMS error CRLB with changing σ and number of readers

7.2.1 Simulation Setup and Models

For all simulations a single room model with sizes 5 m x 8 m is used. Unless otherwise stated:

For each simulation, 1000 simulation runs were carried out to yield location estimation statistics. The simulated target emits signal with log-distance path loss propagation model with zero mean Gaussian noise added. For each run, the target is placed randomly at any location within the limits of the modeled room. For the Bayesian methods, for each simulation run, location estimation will be done after a certain number of recursions that will be given for the fixed target simulations and estimation will be done for every step if the target is mobile.

Unless otherwise stated the related parameters are used as below:

- Filter measurement model is Gaussian with standard deviation $\sigma=5.2$ dB and RSSI measurement noise is Gaussian with standard deviation $\sigma_0=5.2$ dB
Note: σ is used as a parameter of the filter indicating the measurement model noise std. where σ_0 will denote the std. of the noise added on the RSSI measurement from the target in the following sections.
- Log-distance path loss exponent (n) = 2.3
- Reference RSSI at 1 m distance (α) = -52 dBm
- Number of readers (k_{RDR}): 3 (shown in Figure 7.2)
- Filter process (motion) model is Gaussian with zero mean and std. $D = 0.5$ m and target motion is Gaussian with zero mean and std. $D_0 = 0.5$ m.
- Number of particles in particle filter (N): 250
- Grid spacing of grid cells in NN and grid based methods: 1 m (shown in Figure 7.2.)
- Grid cell size: 1 m² with the centers located on the circles shown in Figure 7.2.
- Number of grid cells (k_{CELL}): 28

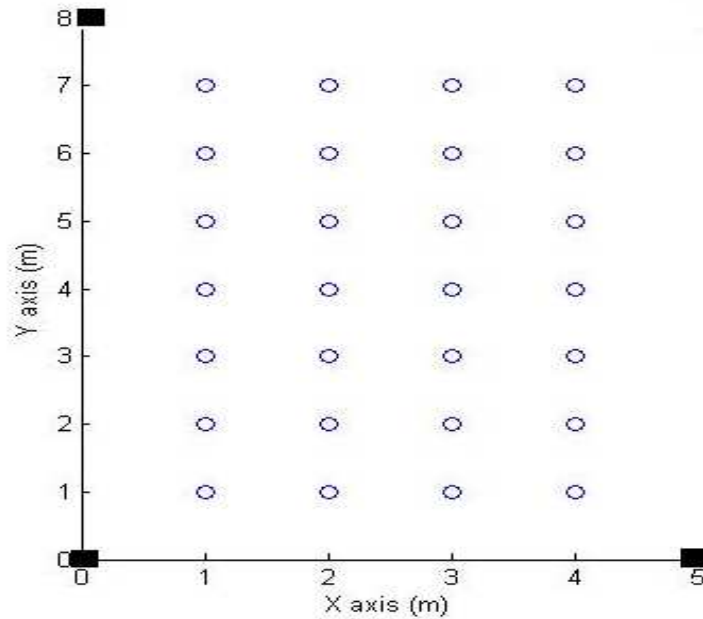


Figure 7.2 Center of grid cells with circles and reader locations with squares

For each simulation run location estimation error is calculated as the Euclidean distance of the estimated (x,y) position to the given target (x,y) position in meters. From total estimation error data we calculate the mean (average) of absolute error, root mean square error (RMSE), and standard deviation (std.) of the error. We also obtain the cumulative distribution function (CDF) of the error distribution which is mostly used for comparison in the literature and using CDF plot we give median (50 percentile) error and 90 percentile error. 50 percentile error can be explained as 50 percent of the total error data is smaller than the given 50 percentile error thus the error is smaller than the given 50 percentile error with probability of 0.5. 90 percentile error can be commented as a measure of the maximum distance error statistics since it means that 90 percent of the total error data is smaller than the given 90 percentile error. In the related literature, one or several of the mentioned statistics is used, so we will give all of the error metrics for each simulation. The error statistics used in this thesis are absolute error statistics.

7.2.2 Simulation Results

In the following sections each simulated method and details will be given. For each simulated localization method different parameters' effects will be investigated.

7.2.2.1 Parameter Based NN Method with Offline Calibration

Parameter based NN method simulations can give us important ideas about the behavior of other types of NN methods. So this simulation is investigated deeply. RSSI measurement noise std. (σ_0), number of readers (k_{RDR}), grid number (k_{CELL}), and number of k nearest neighbors (k_{NN}), target environment area, and reader location configuration are varied to simulate their effects.

A. Changing Number of Grid Cells

The parameters are used as below:

$k_{CELL} = 6, 8, 16, 28, 56, 98, 112$, $k_{NN} = 3, 4, 8, 14, 28, 49, 56$ (respectively for k_{CELL} values), $\sigma_0 = 5.2$ dB, $k_{RDR} = 3$

Changing the number of grid cells, the resulting error statistics are given in Table 7.1 where CRLB=0.80 m.

Table 7.1 Error statistics for changing k_{CELL} for NN method

k_{CELL}	RMSE (m)	Mean error (m)	Median error (m)	90 per. error (m)	Error std. (m)
6	1.87	1.63	1.47	2.89	0.92
8	1.80	1.59	1.48	2.72	0.84
16	1.78	1.57	1.44	2.73	0.84
28	1.79	1.59	1.51	2.65	0.81
56	1.78	1.59	1.49	2.62	0.79
98	1.78	1.59	1.49	2.61	0.80
112	1.77	1.57	1.47	2.66	0.82

It is seen that increasing the grid number, increases the accuracy significantly first. But further increasing the number does not significantly affect the accuracy since increasing grid cell number means only increasing the precision of the location space. So we prefer to use $k_{\text{CELL}}=28$ for our simulation work.

B. Changing The Number of Readers

Changing number of readers, the resulting error statistics are given in Table 7.2.

The parameters are used as below:

$$k_{\text{RDR}} = 3, 4, \sigma_0 = 5.2 \text{ dB}, k_{\text{CELL}} = 28, k_{\text{NN}} = 4$$

Table 7.2 Error statistics for changing number of readers for NN method

k_{RDR}	RMSE (m)	Mean error (m)	Median error (m)	90 per. error (m)	Error std. (m)	CRLB (m)
3	1.95	1.66	1.46	3.09	1.0	0.80
4	1.74	1.49	1.30	2.76	0.91	0.64

For NN methods, increasing number of readers decreases estimation RMS, mean, median, 90 percentile errors and also the std. of the errors as in Table 7.2. This result is an expected result which is also stated by CRLB, since increasing number of readers increases the information that we have about location of the target.

C. Changing RSSI Measurement Noise Std. σ_0

The parameters are used as below:

$$\sigma_0 = 3, 5.2, 7, 9 \text{ dB}, k_{\text{RDR}} = 3, k_{\text{CELL}} = 28, k_{\text{NN}} = 4$$

Changing the σ_0 value, resulting error statistics are given in Table 7.3 and RMS error vs. σ_0 graph is given in Figure 7.3.

Simulation results show that increasing RSSI measurement noise decreases the estimation accuracy as CRLB also states.

Table 7.3 Error statistics for changing RSSI measurement noise std. for NN method

σ_0	RMSE (m)	Mean error (m)	Median error (m)	90 per. error (m)	Error std. (m)	CRLB (m)
3	1.38	1.18	1.01	2.21	0.71	0.46
5.2	1.95	1.66	1.46	3.09	1.0	0.80
7	2.29	1.95	1.74	3.61	1.20	1.08
9	2.57	2.2	2.00	4.10	1.33	1.38

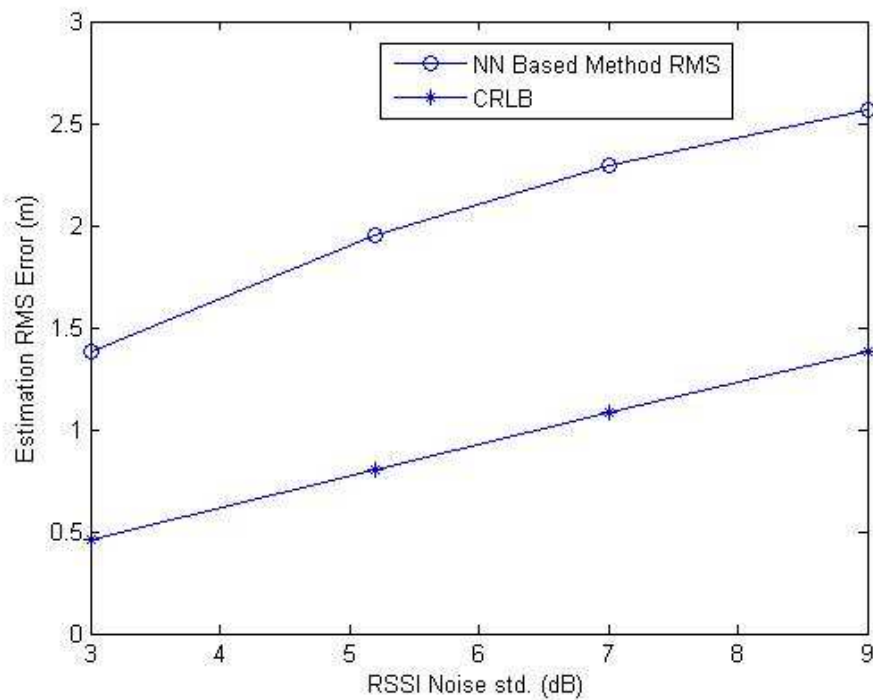


Figure 7.3 Pattern Based NN method RMSE and CRLB with changing σ_0

D. Changing Number of Nearest Neighbors

The parameters are used as below:

$$k_{\text{NN}} = 1, 2, 3, 4, 5, 6, 7, 10, 15, 20, 23, 25, 28, \sigma_0 = 5.2, 11 \text{ dB}, k_{\text{RDR}} = 3, k_{\text{CELL}} = 28$$

Changing the number of nearest neighbors, the resulting error statistics are given in Table 7.4 and Figure 7.4 for $\sigma_0 = 5.2 \text{ dB}$ where $\text{CRLB} = 0.80 \text{ m}$

Table 7.4 Error statistics for changing k_{NN} for NN method with $\sigma_0 = 5.2 \text{ dB}$

k_{NN}	RMSE (m)	Mean error (m)	Median error (m)	90 per. error (m)	Error std. (m)
1	2.17	1.86	1.65	3.3	1.12
2	2.07	1.77	1.55	3.23	1.06
3	2.01	1.73	1.49	3.16	1.03
4	1.95	1.66	1.46	3.09	1.00
5	1.92	1.66	1.44	3.02	0.97
6	1.91	1.65	1.40	2.95	0.96
7	1.89	1.64	1.41	2.87	0.95
10	1.83	1.6	1.44	2.82	0.89
15	1.79	1.6	1.51	2.65	0.81
20	1.79	1.61	1.59	2.64	0.77
23	1.82	1.65	1.60	2.63	0.75
25	1.84	1.68	1.64	2.64	0.75
28	1.87	1.72	1.66	2.69	0.75

Investigating the results in Table 7.4 and Figure 7.4 we notice that RMSE decreases up to a level (1.79 m) with increasing k_{NN} to 15, then RMSE starts to increase as k_{NN} further increases. But, 90 percentile error decreases until we increase k_{NN} up to 23, then 90 percentile error starts to increase as k_{NN} further increases. From these statistics we can conclude that, when k_{NN} increases from 15 to 23, average

estimation error increases slightly while maximum error decreases. So in a real application, it is a matter of choice which error to decrease so as to optimize kNN number.

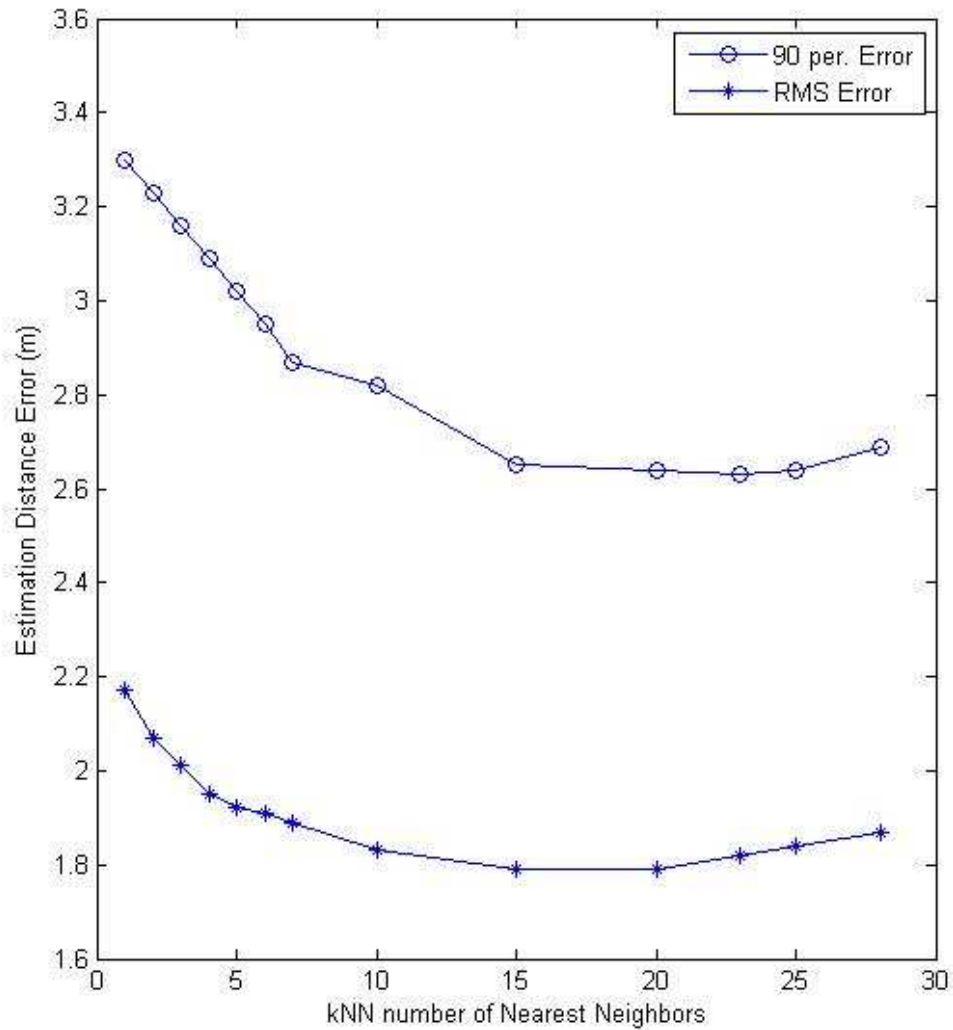


Figure 7.4 RMS error and 90 percentile error with changing k_{NN} for $\sigma_0=5.2$ dB where CRLB=0.80 m

We also simulated the k_{NN} effect with $\sigma_0 =11$ dB in order to see the behavior of the estimation method in more noisy environments where CRLB=1.70 m. The related results are given in Figure 7.5.

In a more complicated environment with $\sigma_0=11$ dB and with 28 grid cells, it is seen that the maximum error is minimum when k_{NN} is 28 (all of the grid cells) where RMS error decreases until k_{NN} reaches 20.

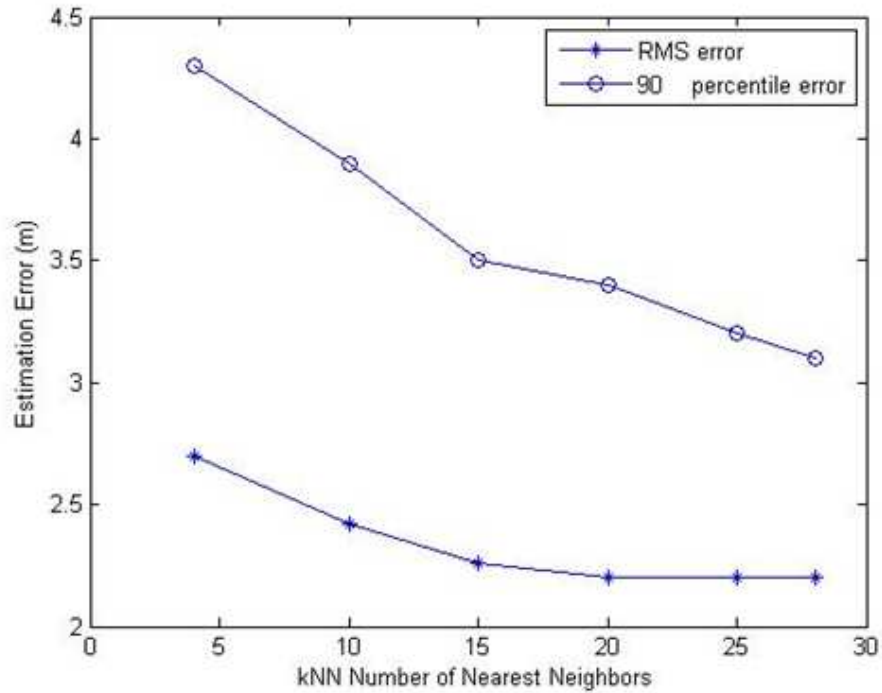


Figure 7.5 RMS error and 90 percentile error with changing k_{NN} for $\sigma_0=11$ dB, where CRLB=1.70 m

The simulations we have run are only for giving idea about how to chose k_{NN} value in an application. We can say that optimum k_{NN} value is affected by different parameters of the localization system and the environment, so it is feasible to determine k_{NN} application specific.

E. Changing the Reader Location Configuration

Our aim is to investigate the estimation accuracy if we place the readers with a different separation in the same target environment. So we chose the separation as half of the default separation as shown in Figure 7.6. Tested readers separations are 2.5 m and 4 m. The error statistics are given in Table 7.5.

The parameters are used as below :

$$k_{\text{CELL}} = 28 \text{ (1m grid spacing)}, k_{\text{NN}} = 14, \sigma_0 = 5.2 \text{ dB}, k_{\text{RDR}} = 3$$

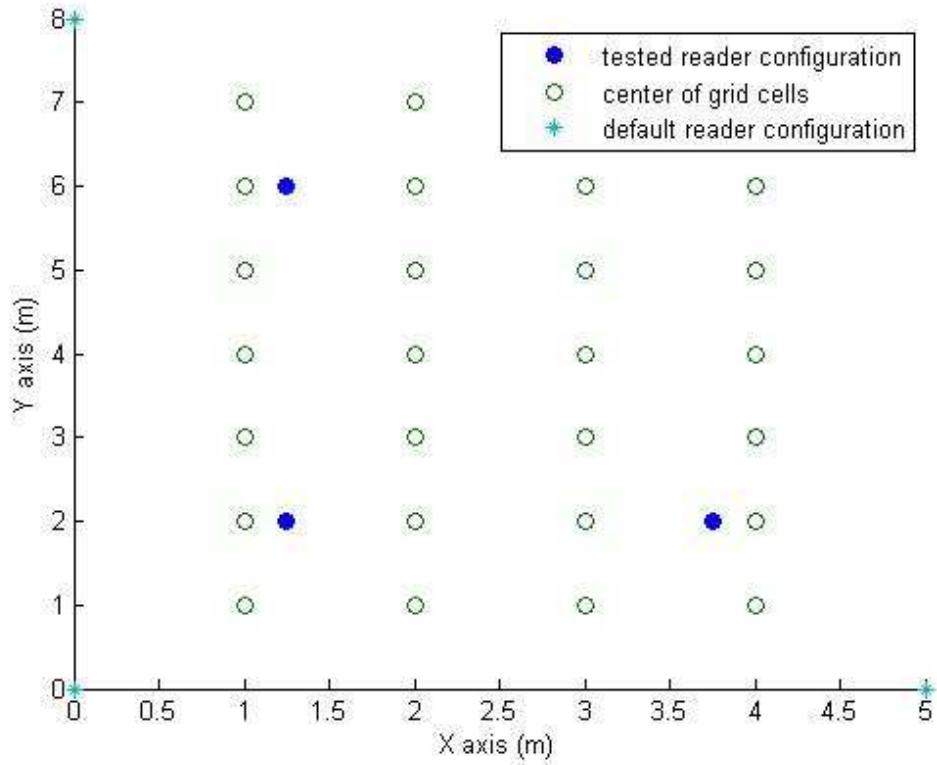


Figure 7.6 Reader configuration with half of the default reader separation

Table 7.5 Error statistics for readers separated with half of the default separations for NN method

Reader sep.	RMSE (m)	Mean error (m)	Median error (m)	90 per. error (m)	Error std. (m)	CRLB (m)
Half of the default	1.52	1.32	1.19	2.32	0.76	0.76
default	1.79	1.59	1.51	2.65	0.81	0.80

It is seen that choosing the reader separations smaller, significantly decreases the estimation error. So in real applications, it is better not to place the readers to the boundaries of the environment but to inner region of the environment if the reader antenna is omnidirectional.

F. Changing the Target Area

Using the parameters below for a larger environment of size 10 m x 16 m the estimation results in Table 7.6 were found.

$$k_{\text{CELL}}=135 \text{ (1m grid spacing)}, k_{\text{NN}}=68, \sigma_0=5.2 \text{ dB}, k_{\text{RDR}}=3,4$$

Table 7.6 Error statistics for a larger area for NN method

Target Area (m ²)	k _{RDR}	RMSE (m)	Mean error (m)	Median error (m)	90 per. error (m)	Error std. (m)	CRLB (m)
160	3	3.73	3.32	3.10	5.58	1.69	1.20
	4	3.39	3.07	2.98	4.92	1.44	0.92
40	3	1.95	1.66	1.46	3.09	1.0	0.80
	4	1.74	1.49	1.30	2.76	0.91	0.64

RFID range is approximately 20 m in indoor environments and for our default environment of 40 m², reader separations are 5 m and 8 m. In real applications, reader separation is chosen up to 20 m in larger environments. So we investigated the behavior of the localization method in a larger area by choosing the reader separation as twice of the default reader separations in a twice sized environment of 10 m x 16 m. As given in the table above, estimation error statistics are also approximately twice of that of default settings.

7.2.2.2 Grid Based Bayesian Filtering

Investigating grid based Bayesian filter characteristics will give us important notion about behavior of overall Bayesian filters including the particle filter. So the simulation results given in this section will also be the basis for the next particle filter section.

In this section we will investigate the effects of important parameters of the grid based Bayesian filters which are

- i. Recursion time (rt)
- ii. Number of readers (k_{RDR})
- iii. Filter measurement model std. (σ) and RSSI measurement noise

Note: σ is used as the filter parameter. RSSI measurement noise is the simulated noise added on the transmit power noise of the target which is also assumed Gaussian but the std. will be denoted as σ_0 and unless otherwise stated $\sigma_0 = \sigma$. For some cases it may be taken zero.

- iv. Filter process (motion) model std. (D) and target motion

Note: D is used as the filter parameter. If the target is simulated mobile, it moves with a Gaussian motion model and the std. will be denoted as D_0 . $D_0=D$ unless otherwise stated.

- v. Number of grid cells (k_{CELL})

The transitional density $p(L_t | L_{t-1})$ forming the process model in our problem is assumed Gaussian with mean L_{t-1} and variance D^2 that means the process noise is Gaussian with zero mean and D standard deviation over the previous location L_{t-1} . $D = 0.5$ m will be used as default parameter for our simulation and empirical work unless otherwise stated.

We will denote recursion time by rt which is the number of times we execute the recursive Bayesian filter to estimate the location of the tracked object. In recursive Bayesian filters D and σ parameters affect the recursion time needed for the filter to

settle which will be called settling time. So, in order to investigate the effects of other parameters, we will start with finding a suitable rt value sufficient for the filter to settle when the target is fixed.

During this section and the next particle filter section, unless otherwise stated, moving target with Gaussian motion model will be assumed with std. $D_0=0.5$ m. The target will start its motion from a randomly chosen location within the area and make 1 motion for each recursion time. At the end of each recursion, estimation will be made and the target will be tracked for rt recursion time. Then the target will start its motion from another randomly chosen location and this sequence will be run for 1000 times. For fixed target cases, first the target is randomly located in the area, then estimation is done at the end of rt recursion time, and the sequence is repeated for 1000 times. Bayesian filtering estimation may diverge from the real location when the target stops moving for few recursion steps for large RSSI measurement noise case. So, in this section and the next particle filter section we also illustrate estimation results for fixed target case which is a worst case scenario in addition to the mobile target cases.

During this section, unless otherwise stated, we use control parameters as given below:

$$k_{RDR} = 3, \sigma = \sigma_0 = 5.2 \text{ dB}, k_{CELL} = 28, D = D_0 = 0.5 \text{ m}, rt = 10$$

But before we start it is necessary to give location estimation results of MAP and MMSE estimates (which are given in Table 7.7) to determine which approach to use throughout simulation and empirical work. For the simulations, we used the control parameters above.

As seen in the table, MAP estimate is worse than MMSE estimate for different measurement noise values, and therefore we use MMSE estimate throughout our simulations and experimental work.

Table 7.7 RMS error for MAP and MMSE estimates of grid based Bayesian filtering

	RMS Error with $\sigma = \sigma_0 = 1$ dB	RMS Error with $\sigma = \sigma_0 = 3$ dB	RMS Error with $\sigma = \sigma_0 = 5.2$ dB
MAP Estimate	0.67	1.06	1.40
MMSE Estimate	0.57	0.97	1.22
CRLB	0.15	0.46	0.80

A. Changing Number of Grid Cells

The parameters are used as below:

$$k_{\text{CELL}} = 8 \text{ (grid spacing 2 m), } 28 \text{ (grid spacing 1 m), } 112 \text{ (grid spacing 0.5 m), } \sigma = \sigma_0 = 5.2 \text{ dB, } k_{\text{RDR}} = 3, D = D_0 = 0.5 \text{ m, } r_t = 10$$

The effect of changing number of grid cells is given in Table 7.8. It is seen that increasing grid cells from 8 to 28 and 112 makes improvement on the estimation accuracy as expected but it also dramatically increases the computation time which makes the grid based Bayesian filtering unfeasible to use in real life applications. So we prefer to use $k_{\text{CELL}} = 28$ for our simulation and experimental work.

Table 7.8 Error statistics with changing number of grid cells where CRLB=0.80 m

k_{CELL}	RMSE (m)	Mean error (m)	Median error (m)	90 per. error (m)	Error std. (m)
8	1.30	1.15	1.11	1.89	0.56
28	1.22	1.09	1.02	1.81	0.54
112	1.16	1.01	0.94	1.72	0.56

B. Recursion Time

Depending on the RSSI measurement noise added on the target transmit power, the location estimation may converge to the target location or diverge from the real location as recursion time increases. So, in order to find the mean recursion time for the filter to settle we add no RSSI noise on the target transmit power and assume target is fixed in this simulation run. For a fixed target, when there is no RSSI measurement noise, the Bayesian filter is expected to converge to the target location as the recursion time increases. Figure 7.7 shows how the mean estimation error varies with increasing rt for randomly placed fixed target all over the area with the parameters $k_{RDR} = 3$, $\sigma = 5.2$ dB, $k_{CELL} = 28$, $D = 0.5$ m, with zero RSSI measurement noise.

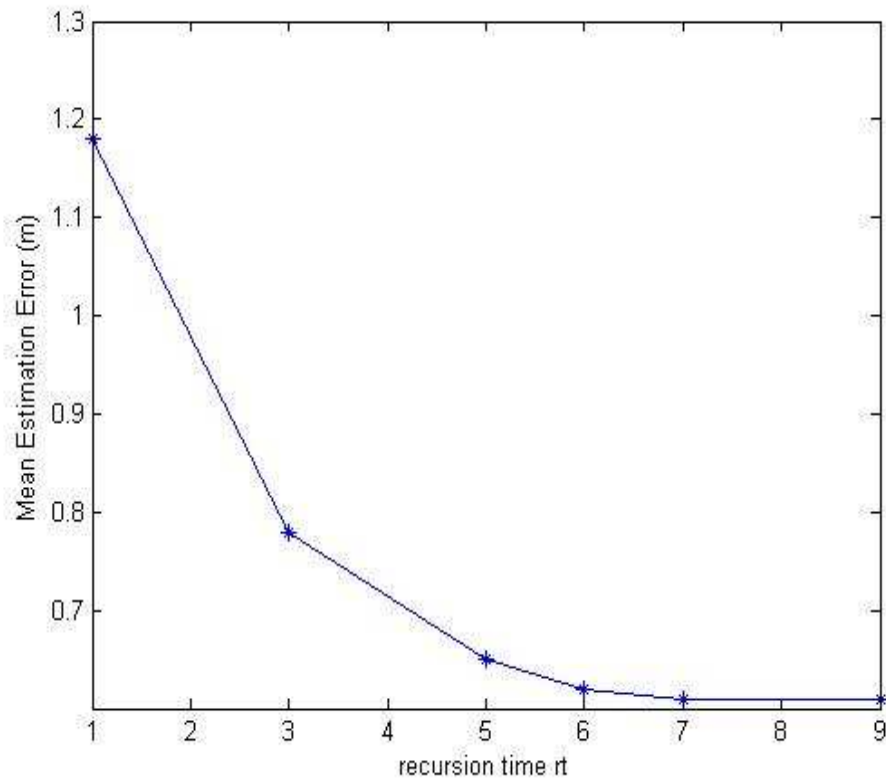


Figure 7.7 Estimation mean error with changing recursion time with no RSSI noise added to the target transmit power and the target is fixed

From Figure 7.7 it can be seen that approximately 6 recursions are sufficient for the estimation to settle for $\sigma=5.2$ dB and $D=0.5$ m. But for obtaining the results in the simulations with $\sigma=5.2$ dB and $D=0.5$ m we use rt as 10 to guarantee the filter to settle.

To investigate the settling time with changing D and σ we simulate a target at a fixed location $(x,y)=(2, 2)$ with zero RSSI measurement noise with the parameters $k_{RDR}=3$, $k_{CELL}=28$. The resulting graphs are given in Figure 7.8 ($\sigma=5.2$ dB) and Figure 7.9 ($D=0.5$ m), respectively.

In Figure 7.8 it can be seen that the settling time increases as D decreases which also means that the filter can track a displacing target more slowly as D gets smaller. Because, D is in fact a parameter inserted in the filter that is proportional to the allowable range for the target to displace so that, a filter with small D value suppresses large displacements in a recursion.

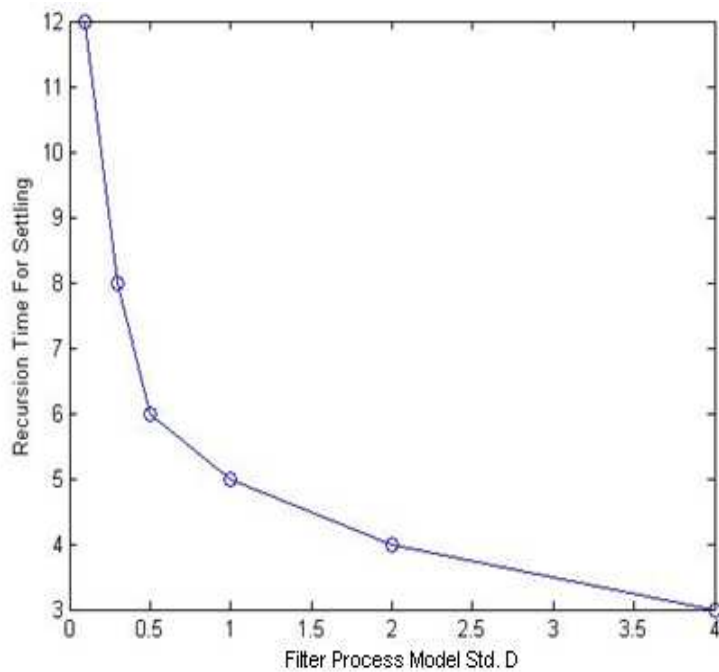


Figure 7.8 Recursion time for settling with changing filter process model std. D

In Figure 7.9 it can be seen that settling time increases with increasing σ value as expected.

In the following simulations, we make use of the results shown in Figure 7.8 and Figure 7.9 to wait for a sufficient recursion time for the filter to settle for different D and σ values.

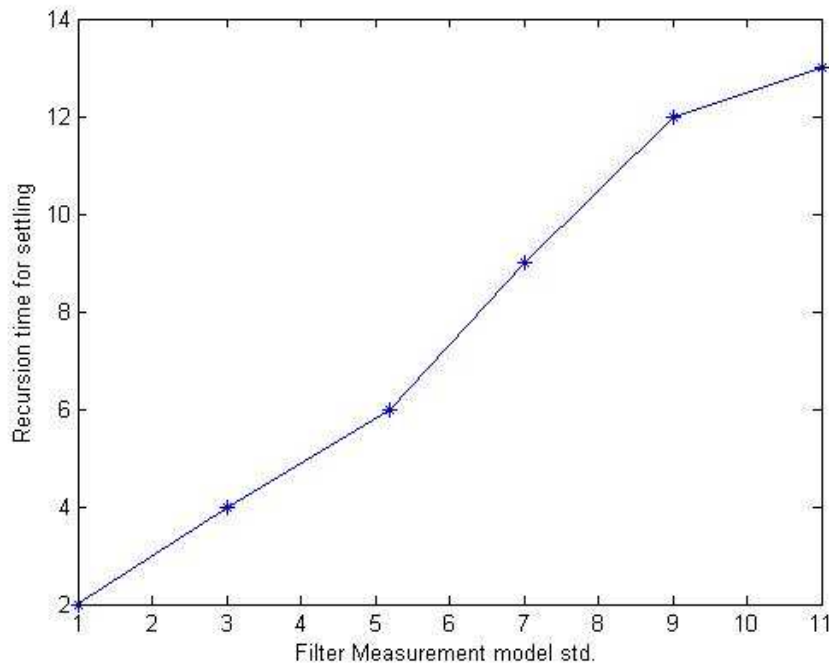


Figure 7.9 Recursion time for settling with changing filter measurement model std. σ

C. Changing Number of Readers

In order to show the effect of number of readers we give the results in Table 7.9 with the parameters below:

$$k_{RDR} = 3, 4, k_{CELL} = 28, \sigma = \sigma_0 = 5.2 \text{ dB}, D = D_0 = 0.5 \text{ m}, rt = 10$$

From Table 7.9, it can be seen that the effect of increasing the number of readers to the estimation accuracy is significant as CRLB states.

Table 7.9 Error statistics for changing k_{RDR} for grid based Bayesian method

k_{RDR}	RMSE (m)	Mean error (m)	Median error (m)	90 per. error (m)	Error std. (m)	CRLB (m)
3	1.22	1.09	1.02	1.81	0.54	0.80
4	1.12	0.97	0.92	1.64	0.49	0.64

D. Changing Filter Measurement Model Std. σ and RSSI Measurement Noise Std. σ_0

The detailed error statistics for a moving target with different $\sigma=\sigma_0$ values are given in Table 7.10 using the parameters below:

$$\sigma=\sigma_0=1, 3, 5.2, 7, 9 \text{ dB, } k_{RDR}=3, k_{CELL}=28, D=D_0=0.5 \text{ m, } rt=8, 8, 10, 12, \\ 16 \text{ (respectively for the given } \sigma \text{ values)}$$

Table 7.10 Error statistics for a mobile target with changing $\sigma=\sigma_0$ values

$\sigma=\sigma_0$	RMSE (m)	Mean error (m)	Median error (m)	90 per. error (m)	Error std. (m)	CRLB (m)
1	0.57	0.49	0.49	0.80	0.24	0.15
3	0.97	0.84	0.77	1.44	0.42	0.46
5.2	1.22	1.09	1.02	1.81	0.54	0.80
7	1.34	1.18	1.12	1.96	0.58	1.08
9	1.51	1.33	1.29	2.20	0.62	1.38

In Table 7.10, estimation error increases as the measurement noise increases as expected.

After giving the results for a mobile target, we also find it notable to give the estimation error statistics in Table 7.11 for a target that is fixed which illustrates the worst case scenario. We use the parameters below:

$$\sigma=\sigma_0=1, 3, 5.2, 7, 9 \text{ dB, } k_{\text{RDR}}=3, k_{\text{CELL}}=28, D=0.5 \text{ m, } r_t=8, 8, 10, 12, 16$$

(respectively for the σ values)

Investigating the results in Table 7.11 we notice that for a fixed target, estimation error drastically increases as measurement noise increases as compared to the mobile target case. It is a known handicap of Bayesian filters.

Table 7.11 Error statistics for a fixed target with changing $\sigma=\sigma_0$ values

σ	RMSE (m)	Mean error (m)	Median error (m)	90 per. error (m)	Error std. (m)	CRLB (m)
1	0.65	0.55	0.47	0.97	0.35	0.15
3	1.36	1.17	1.05	2.13	0.70	0.46
5.2	1.83	1.54	1.34	2.91	0.98	0.80
7	2.07	1.77	1.54	3.33	1.07	1.08
9	2.34	2.00	1.83	3.86	1.21	1.38

E. Changing Filter Process Model Std. D and Target Motion

Table 7.12 gives the estimation results for a mobile target with the parameters $D=D_0=0.1, 0.5, 1 \text{ m, } \sigma=\sigma_0=5.2 \text{ dB, } k_{\text{RDR}}=3, k_{\text{CELL}}=28, r_t=16, 12, 10$ respectively for the given D values.

Results show that increasing the process noise increases the estimation error as expected.

Table 7.12 Error statistics for different $D=D_0$ values where CRLB=0.80 m

$D=D_0$	RMSE (m)	Mean error (m)	Median error (m)	90 per. error (m)	Error std. (m)
0.1	0.79	0.70	0.64	1.23	0.38
0.5	1.22	1.09	1.02	1.81	0.54
1	1.55	1.34	1.25	2.24	0.66

After giving the results for a mobile target, we also give the estimation error statistics with different filter process model std. D in Table 7.13 for a fixed target which illustrates the worst case scenario. We use the parameters below:

$D=0.1, 0.5, 1$ m, infinite, $\sigma=\sigma_0=5.2$ dB, $k_{RDR}=3$, $k_{CELL}=28$, $rt=16, 12, 10, 8$ respectively for the given D values.

Table 7.13 Error statistics for changing filter process model std. D where CRLB=0.80 m

D	RMSE (m)	Mean error (m)	Median error (m)	90 per. error (m)	Error std. (m)
0.1	1.95	1.68	1.50	3.02	0.99
0.5	1.88	1.57	1.34	2.99	1.00
1	1.83	1.54	1.34	2.91	0.98
infinity	1.74	1.55	1.48	2.61	0.79

In Table 7.13 it can be seen that for a fixed target, estimation error decreases as D increases. The best result is obtained when the filter process noise is uniform (where D is infinite) for fixed target case which means that, adding no a priori knowledge to the filter works better if measurement noise is large and the target process noise is small (e.g., it is fixed). This can be explained as follows; for a fixed target with large measurement noise, smaller D value of the filter causes large error in the location

estimation. As a result, we can say that Bayesian filters are suitable to use for tracking mobile targets.

In order to observe the effect of the D parameter of the filter on the dynamic RSSI measurement noise, we simulated a fixed target at only one location with RSSI measurement error applied on the target transmit power at $rt=3$ and $rt=7$. Dynamic RSSI noise means that large changes in RSSI readings occur in time on a fixed target due to the moving objects or people in the environment. We expect that, decreasing D helps better to suppress dynamic RSSI measurement noise since decreasing D does not allow rapid changes in the location estimation as shown in Figure 7.10.

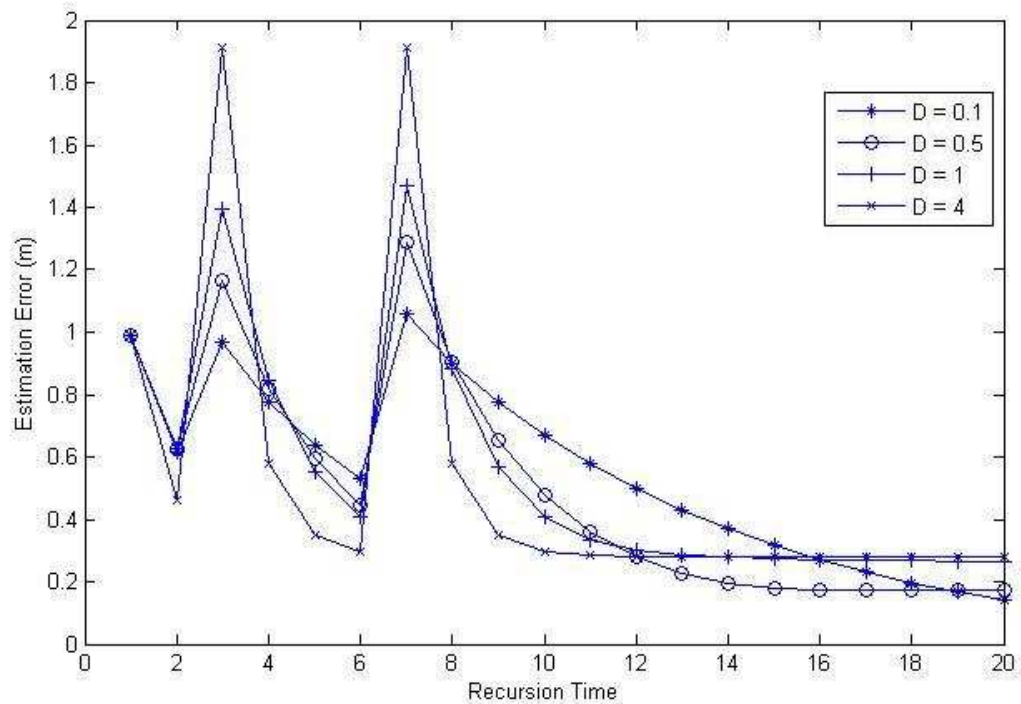


Figure 7.10 Dynamic noise filtering behavior with changing D

In Figure 7.10, at recursion times 3 and 7 it is seen that estimation error jump is larger for larger D values which shows that a filter with smaller D value can filter dynamic RSSI measurement noise better.

7.2.2.3 SIR Particle Filter

In this section, simulation results of basic SIR filtering location estimation with different conditions and parameters will be given first. Then several improvements on the SIR filter will be investigated.

The parameters of SIR filtering that will be investigated are

- i. Number of particles (N)
- ii. Recursion time (rt)
- iii. Filter measurement model std. (σ) and RSSI measurement noise

Note: σ is used as a parameter of the filter. RSSI measurement noise is added on the transmit power of the target which is assumed Gaussian with σ_0 std. or it may be taken zero for some cases. Unless otherwise stated $\sigma=\sigma_0$.

- iv. Filter proposal density (called process model in the general Bayesian case) and target motion

Note: If the proposal density of the filter is assumed to be Gaussian, the std. is denoted as D. If the target moves with a Gaussian proposal distribution, the std. will be denoted as D_0 and $D=D_0$ unless otherwise stated.

For improving the error performance of the basic SIR filter, following approaches will be simulated:

- i. Smoothing the importance factor (w) of each particle in the resampling stage by taking the square root of the current w of each particle and normalizing them to sum up to 1.
- ii. Instead of resampling at every recursion, resampling when the effective sample size N_{eff} is less than a threshold N_t .

During simulations in this section, the control parameters will be used as below unless otherwise stated:

$$k_{\text{RDR}}=3, \sigma=5.2 \text{ dB}, \sigma_0=5.2 \text{ dB}, N=250, \text{rt}=10, D=0.5 \text{ m}, D_0=0.5 \text{ m}$$

Also $\sigma = \sigma_0$ and $D=D_0$ if there is no other explanation.

But before we start, we will give the simulation results of MAP estimate and MMSE estimate of the SIR filter in Table 7.14 in order to determine which one to use for estimation.

Table 7.14 RMS Error for MAP and MMSE Estimate

	RMS Error with $\sigma = \sigma_0 = 1$	RMS Error with $\sigma = \sigma_0 = 3$	RMS Error with $\sigma = \sigma_0 = 5.2$
MAP Estimate	0.64	1.41	2.06
MMSE Estimate	0.53	0.97	1.14
CRLB (m)	0.15	0.46	0.80

Although MAP estimate may converge to the accuracy of MMSE estimate for small $\sigma = \sigma_0$, MMSE estimate's accuracy is always better than that of MAP estimate, so we use MMSE estimate throughout our simulation and empirical applications.

A. Number of Particles (N)

In order to determine the effect of N, we simulated a case where the simulated target is fixed and there is no transmit power noise added. The simulation result of the effect of N on the mean estimation error is given in Figure 7.11.

For our simulation environment and localization problem, mean estimation error decreases as N increases up to 250. So we use N as 250 during our simulation work.

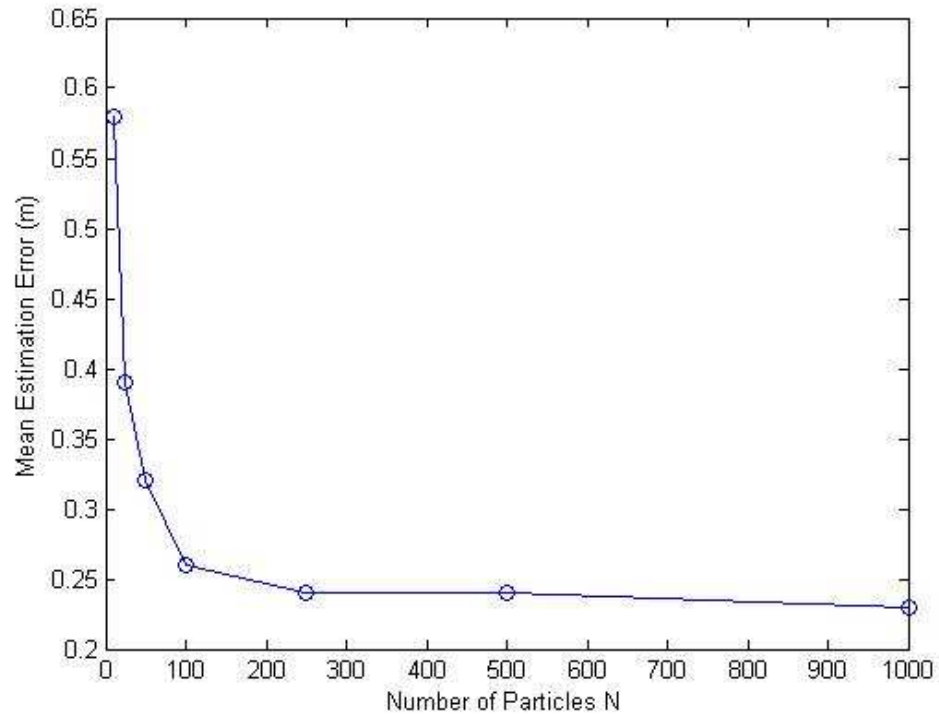


Figure 7.11 Mean estimation error with changing N when the target is at a fixed point with no transmit power noise

B. Recursion Time

In order to determine the effect of recursion time we simulated a fixed target located randomly with no transmit power noise. The relation of the recursion time and mean estimation error is given in Figure 7.12.

Estimation settles after about 7 recursions when the target is fixed. For fixed target simulations we will use rt as 10 to guarantee the filter to settle.

In Figure 7.13 and Figure 7.14 effects of D and σ on settling time are given, respectively.

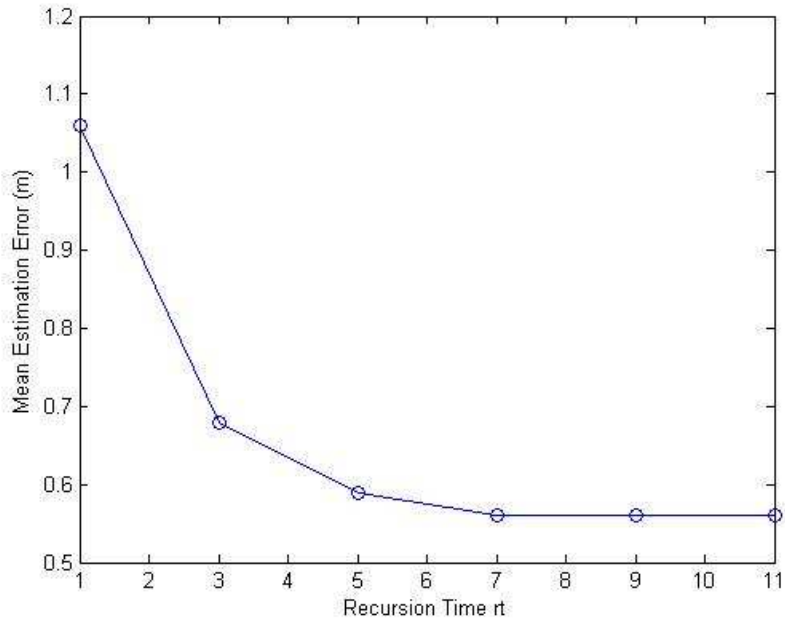


Figure 7.12 Mean estimation error with changing rt when target location is fixed and distributed randomly.

The results in Figure 7.13 and Figure 7.14 are used for determining sufficient rt for different D and σ values in the following simulations.

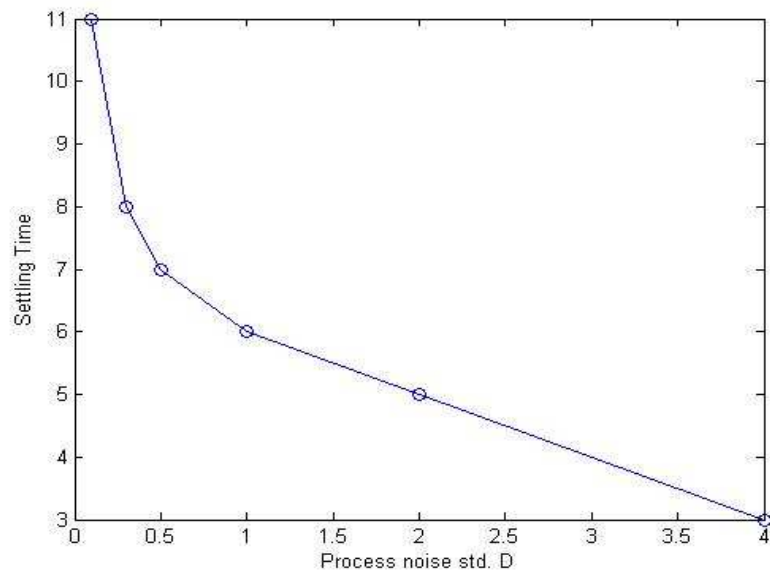


Figure 7.13 Settling time with changing D

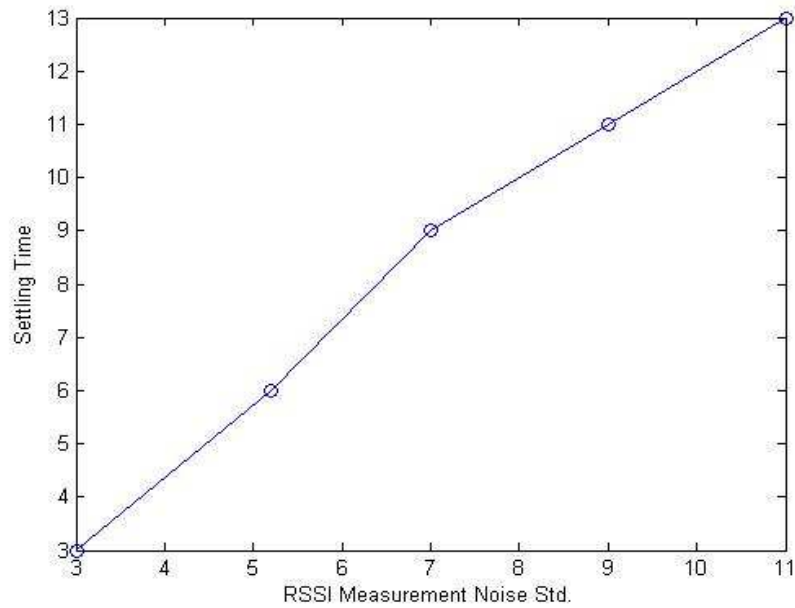


Figure 7.14 Settling time with changing σ

C. Filter Measurement Model Std. σ and RSSI Measurement Noise Std. σ_0

D.

In Table 7.15, estimation results of SIR filter with changing $\sigma = \sigma_0$ values are given when the target is fixed but filter proposal density is assumed Gaussian with $D=0.5$ m. For the simulations, for $\sigma=1, 3, 5.2, 7, 9$ dB, $rt=6, 8, 10, 16, 20$ are used, respectively.

Table 7.15 Error statistics of SIR filter with changing σ when target is fixed

$\sigma = \sigma_0$	RMSE (m)	Mean error (m)	Median error (m)	90 per. error (m)	Error std. (m)	CRLB (m)
1	0.63	0.53	0.46	0.97	0.34	0.15
3	1.48	1.29	1.22	2.23	0.73	0.46
5.2	2.00	1.70	1.51	3.09	1.07	0.80
7	2.38	2.06	1.86	3.65	1.20	1.08
9	2.55	2.18	1.92	4.19	1.32	1.38

Estimation error increases as the measurement noise increases as expected. We know that, for a fixed target with large transmit power noise added, Bayesian filter estimation may diverge from the real target location because Bayesian filters converge to the location where the likelihood of the RSSI measurement is highest for smaller D values and if the measurement is erroneous, estimated location will have a large error. While tracking a mobile target, there is a possibility that the target stops at a location where RSSI measurement has large error with the fading effects. If the target stops at that location for a time, the tracking filter may estimate the location with a large error. So, in the next simulation of a mobile target we will see that the SIR filter gives better results as we stated also in the grid based Bayesian case.

In Table 7.16, error statistics of a randomly moving target with Gaussian proposal distribution of zero mean and D_0 std where $D_0 = D = 0.5$ m. For $\sigma=1, 3, 5.2, 7, 9$ dB, $rt= 6, 8, 10, 16, 20$ are used, respectively.

Table 7.16 Error statistics of SIR filter with changing σ when target moves with Gaussian motion model with D_0

$\sigma = \sigma_0$	RMSE (m)	Mean error (m)	Median error (m)	90 per. error (m)	Error std. (m)	CRLB (m)
1	0.53	0.43	0.37	0.84	0.27	0.15
3	0.97	0.83	0.77	1.44	0.45	0.46
5.2	1.14	0.98	0.88	1.77	0.54	0.80
7	1.38	1.21	1.13	2.11	0.67	1.08
9	1.45	1.27	1.23	2.18	0.68	1.38

When the SIR filter is used for tracking a moving target the results are significantly better than those of the fixed target case. The estimation error increases gradually while σ increases as expected.

E. Filter Proposal Density (Process Model) and Target Motion

In this subsection we investigate

- i. the behavior of SIR filter for two different proposal density models; 1) Gaussian with zero mean and std. D , 2) Gaussian with a mean of known speed in known direction and std. D ,
- ii. the behavior of the filter when target motion is not compatible with the assumed proposal density,
- iii. the behavior of the filter when there is an extra information on the non-accessible target locations,
- iv. the behavior of the filter when there is an extra information on the initial location of the target.

In Table 7.17 proposal density and the target motion are Gaussian with zero mean and changing $D=D_0$.

Table 7.17 Error statistics of SIR filter with changing $D=D_0$ where CRLB=0.80 m

$D=D_0$	RMSE (m)	Mean error (m)	Median error (m)	90 per. error (m)	Error std. (m)
0.1	0.83	0.74	0.65	1.31	0.45
0.5	1.14	0.98	0.88	1.77	0.54
1	1.45	1.24	1.17	2.16	0.65
2	1.73	1.43	1.27	2.65	0.82
4	1.86	1.46	1.32	2.90	0.93

It is seen that as D_0 increases, estimation error increases as expected since the target's location uncertainty increases.

In order to see the effect of D parameter of the filter on the estimation when the target stops, we simulated fixed target and the results are given in Table 7.18. D=infinity illustrates the case where the proposal density is uniformly distributed over the target area meaning there is no a priori information about the motion of the target.

Table 7.18 Error statistics of SIR filter with changing D, when the target is simulated fixed where CRLB=0.80 m

D	RMSE (m)	Mean error (m)	Median error (m)	90 per. error (m)	Error std. (m)
0.1	2.02	1.76	1.57	3.22	1.00
0.5	2.00	1.70	1.51	3.09	1.07
1	1.96	1.67	1.50	3.00	1.02
2	1.93	1.61	1.48	2.96	0.99
infinity	1.67	1.49	1.40	2.48	0.74

As mentioned in the grid based Bayesian filtering, smaller D results in larger errors in estimation when the target stops at a fixed location with large RSSI measurement noise. This is because filter with smaller D can converge closer to the location at which likelihood of the RSSI measurement is highest and if the measurement is faulty, estimated location has a large error in a few recursion time.

In order to see the effect of lack of motion information we give the results in Table 7.19.

Table 7.19 Lack of motion information for Gaussian target motion model

Filter Proposal Density	Target Motion	RMSE (m)	90 per. error (m)
Gaussian with $D=0.5$	Gaussian with $D_0 = 0.5$	1.14	1.77
Uniform over the area	Gaussian with $D_0 = 0.5$	1.32	2.04

Uniform filter proposal density means that there is no a priori information about the motion of the target, i.e, it can be anywhere within the area given the previous location. So this table is given to demonstrate that lacking motion information gives larger estimation error.

In order to see the effect of adding speed and direction information to the estimation system we simulated a target moving with 0.5 m/recursion in y direction. It moves from $y=1$ m to $y=6$ m in 10 rt, starting from a random x coordinate. For the proposal density of the filter we used Gaussian process noise with $D=0.5$ m added to the known speed and direction. To demonstrate the differing effect of adding extra information to the filter model we also simulated the case when the filter has no knowledge of the speed and direction, instead it uses a proposal density model of zero mean Gaussian noise on the previous location with $D=0.5$. The results are given in Table 7.20.

Comparing the first result in the table with that of Gaussian motion model with $D=0.5$ in Table 7.17, it is seen that for target with known speed and direction the filter gives more accurate results than that of when the target moves randomly Gaussian since the uncertainty is larger in the Gaussian case. Comparing the first and second results in Table 7.20, it is seen that lacking information of the speed and direction in the filter proposal density model results in larger estimation error as also illustrated in Table 7.19.

Table 7.20 Target moving with a known speed and direction

Filter Proposal Density	Target Motion	RMSE (m)	Mean error (m)	Median error (m)	90 per. error (m)	Error std. (m)
Gaussian with mean of known velocity and std. D=0.5	Constant velocity	1.09	0.95	0.84	1.63	0.51
Gaussian with zero mean and std. D=0.5	Constant velocity	1.46	1.27	1.21	2.08	0.66

In Table 7.21, target with known initial location was simulated for investigating the effect of additional initial state information. Initial state information is added to two types of target motion models (random Gaussian and constant speed in y direction) to illustrate the effect.

For both motion models, it is evidently seen that, knowing the initial location of the target increases the tracking accuracy of the filter as expected.

If available, adding information of non-accessible regions for the target is also expected to give more accurate estimation results. In order to illustrate this, we simulated a target with the mentioned control parameters with Gaussian motion model where the target is only allowed up to 1 m distance to the surrounding walls. The results are given in Table 7.22.

Table 7.21 Target moving with known initial location

Filter Proposal Density	Target Motion	RMSE (m)	Mean error (m)	Median error (m)	90 per. error (m)	Error std. (m)
Gaussian with zero mean and $D=0.5$	Gaussian with $D_0=0.5$	1.14	0.98	0.88	1.77	0.54
Gaussian with zero mean and $D=0.5$ - knowing the initial location	Gaussian with $D_0=0.5$	1.07	0.93	0.86	1.58	0.50
Gaussian with mean of known velocity and std. $D=0.5$	Constant velocity	1.09	0.95	0.84	1.63	0.51
Gaussian with mean of known velocity and std. $D=0.5$ -knowing the initial location	Constant velocity	1.04	0.90	0.82	1.58	0.47

Table 7.22 Adding non-accessible regions for the moving target with Gaussian model

Filter Burden	Target Motion Burden	RMSE (m)	Mean error (m)	Median error (m)	90 per. error (m)	Error std. (m)
Up to walls	1 m from walls	1.23	1.06	0.97	1.88	0.57
1 m from walls	1 m from walls	1.09	0.93	0.87	1.66	0.51

In the table, it is seen that if the target is allowed up to 1 m distance to the walls and this information is known by the filter, then the estimation accuracy is better than that of the case the information is not known by the filter as expected.

F. Improvements on Particle Filtering

The most important handicap of Bayesian filters is that, if the target stops for a few iteration time, the location estimation may diverge from the real location if the transmit power disturbance is large and the filter process noise is small.

Resampling at every recursion may cause the particles to collapse to a point of location very rapidly if the process noise is small which is called sample impoverishment problem as mentioned earlier. So we applied two different approaches to reduce this problem which are

- i. Resampling not at every recursion but when N_{eff} is smaller than a threshold value N_t so that the impoverishment effect slows down,
- ii. Smoothing the importance factor w by taking the square root so that we avoid the weight of particles to become very large for certain samples and thus avoid collapsing to a single point in the resampling phase.

First we start with giving the results for smoothing the importance factor w for moving and fixed target cases in Table 7.23.

It is seen that smoothing w results in reduction of estimation error for the fixed target case, especially 90 percentile error decreases significantly where estimation error increases slightly for the moving target case when w smoothing is used. Because smoothing w in the resampling stage avoids the particles to collapse to a very small area and in a way has an effect of increasing process noise variation.

Table 7.23 Effect of smoothing w for tracking moving and fixed targets

Filter Proposal Density	Target Motion	RMSE (m)	Mean error (m)	Median error (m)	90 per. error (m)	Error std. (m)
Gaussian with $D=0.5$	Gaussian with $D_0=0.5$	1.14	0.98	0.88	1.77	0.54
Gaussian with $D=0.5$, Smoothed w	Gaussian with $D_0=0.5$	1.21	1.08	0.99	1.83	0.58
Gaussian with $D=0.5$	Fixed	2.00	1.70	1.51	3.09	1.07
Gaussian with $D=0.5$, Smoothed w	Fixed	1.82	1.53	1.43	2.75	0.98

In Table 7.24, effect of resampling using Neff is illustrated for moving and fixed target cases. Also for investigating the effect of N_t value, $N_t=0.5$ and $N_t=0.3$ values are used in the simulations.

For the fixed target case, using $N_t=0.5$ significantly reduces the estimation error especially the 90 percentile error where it slightly increases the error for the moving target case. On the other hand using $N_t=0.3$ does not result in a significant error reduction compared with the results of using $N_t=0.5$, also it increases estimation error significantly for moving target case. Because decreasing N_t causes the filter to resample less often and after a point we observe the unfavorable results of this in the estimation accuracy. As a result we have chosen to use $N_t=0.5$ during our empirical work.

Table 7.24 Effect of resampling when $N_{eff} < N_t$ for tracking moving and fixed targets

Filter Proposal Density	Target Motion	RMSE (m)	Mean error (m)	Median error (m)	90 per. error (m)	Error std. (m)
Gaussian with $D=0.5$	Gaussian with $D_0=0.5$	1.14	0.98	0.88	1.77	0.54
Gaussian with $D=0.5$, Resample when $N_{eff} < 0.5$	Gaussian with $D_0=0.5$	1.17	1.02	0.92	1.79	0.57
Gaussian with $D=0.5$, Resample when $N_{eff} < 0.3$	Gaussian with $D_0=0.5$	1.28	1.10	0.99	1.85	0.64
Gaussian with $D=0.5$	Fixed	2.00	1.70	1.51	3.09	1.07
Gaussian with $D=0.5$, Resample when $N_{eff} < 0.5$	Fixed	1.92	1.62	1.46	2.78	1.03
Gaussian with $D=0.5$, Resample when $N_{eff} < 0.3$	Fixed	1.89	1.59	1.42	2.78	1.02

In Table 7.25, we illustrate the effect of using both approaches for moving and fixed target cases.

Table 7.25 Effect of w smoothing and resampling using N_{eff} for moving and fixed target cases

Filter Proposal Density	Target Motion	RMSE (m)	Mean error (m)	Median error (m)	90 per. error (m)	Error std. (m)
Gaussian with $D=0.5$	Gaussian with $D_0=0.5$	1.14	0.98	0.88	1.77	0.54
Gaussian with $D=0.5$, Resampling when $N_{eff}<0.5$, and w smoothing	Gaussian with $D_0=0.5$	1.37	1.20	1.09	2.04	0.64
Gaussian with $D=0.5$	fixed	2.00	1.70	1.51	3.09	1.07
Gaussian with $D=0.5$, Resampling when $N_{eff}<0.5$, and w smoothing	fixed	1.73	1.51	1.34	2.64	0.83

In the table it is seen that using both approaches in the filter significantly decreases the estimation error for the fixed target case, whereas it significantly increases estimation error for the moving target case. So it is a matter of choice for the implementer to determine which approach to use with which parameter according to the system needs.

7.2.3 Analysis of Simulation Results

In this section we will analyze the simulated methods' weak and strong behaviors and compare them in different aspects.

First we start giving the graphs in Figure 7.15 and Figure 7.16 in order to compare

- i. CRLB,
- ii. Parameter based NN method,
- iii. Grid based Bayesian filter,
- iv. SIR particle filter,
- v. Improved SIR filter by w smoothing and resampling using N_{eff}

for different RSSI measurement noise.

For the simulations the parameters are used as below:

$$k_{\text{RDR}} = 3, k_{\text{CELL}} = 28, k_{\text{NN}} = 14, D = 0.5 \text{ m}, N = 250, N_t = 0.5$$

For Figure 7.15 the target is fixed and for Figure 7.16 the target motion model is zero mean Gaussian with std $D_0 = 0.5 \text{ m}$.

For the fixed target case it is notable that for small (σ_0) measurement noise, Bayesian based methods (grid based Bayesian, SIR and improved SIR particle filters) give better estimation accuracy. But for measurement noise larger than 3 dB improved SIR filter and parameter based NN method have less estimation error than grid based Bayesian and SIR filters and SIR filtering has larger error than the others. Improved SIR filter has significantly less estimation error than the basic SIR filter especially for growing measurement noise.

Switching to the mobile target case, it can be seen that Bayesian based methods give significantly better results for all given measurement noise cases. For $\sigma_0 > 3 \text{ dB}$ cases improved SIR filter is worse than basic SIR and grid based Bayesian filters. SIR and grid based Bayesian filters' estimation results do not differ significantly and converge to the CRLB for growing measurement noise for mobile target case.

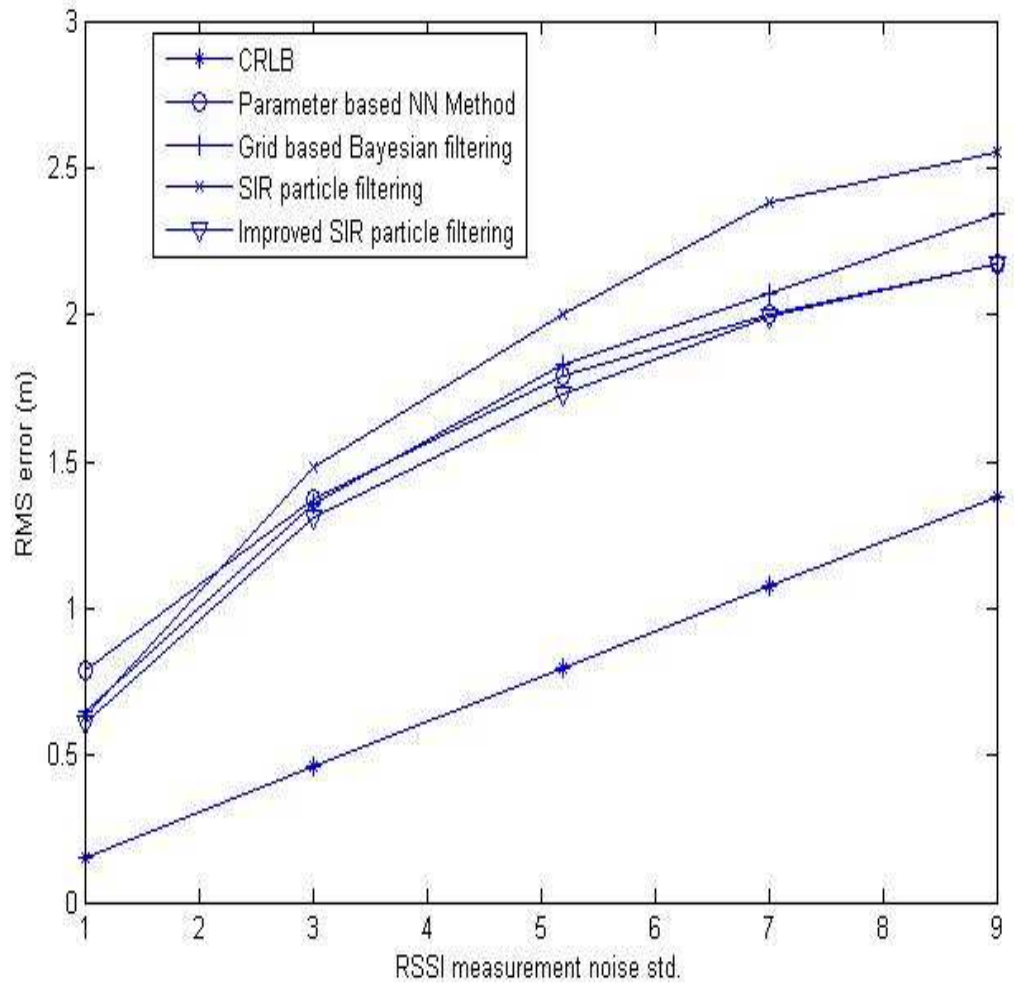


Figure 7.15 RMS error with varying σ_0 for a fixed target

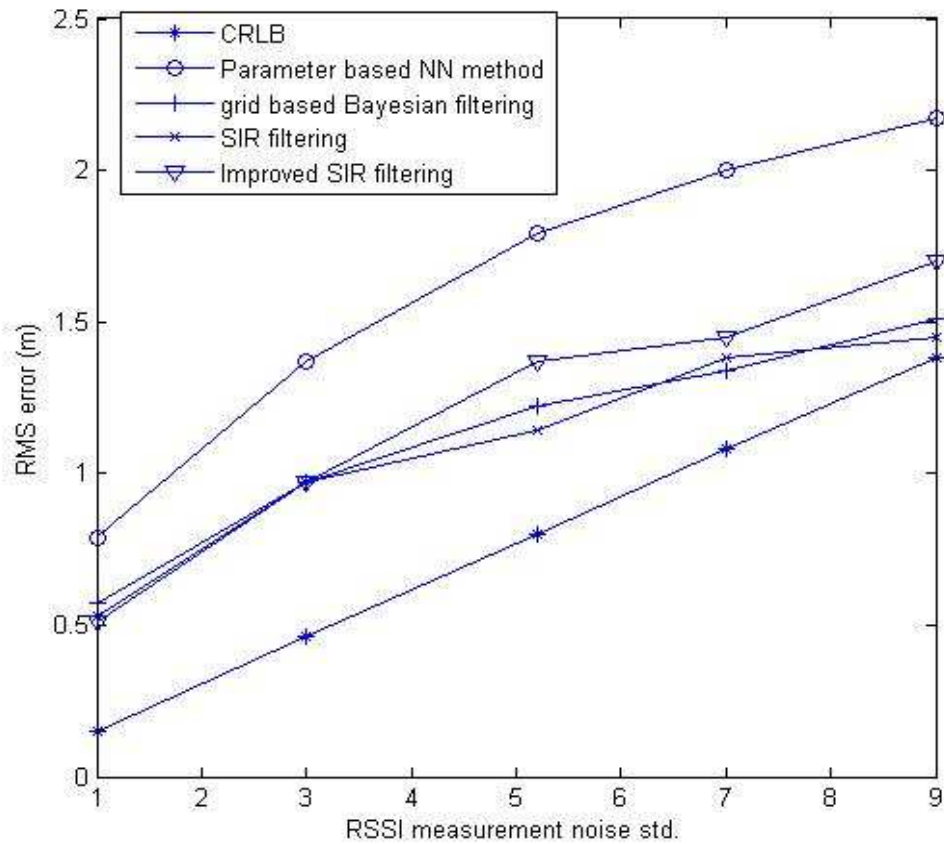


Figure 7.16 RMS error with varying σ_0 for a mobile target

Analyzing the results of the figures given above and the simulation results given in Section 7.2.2 following conclusions can be drawn:

- i. If the target is known to be fixed, using classical Bayesian based methods does not give good results if the measurement noise is large. But if the static measurement noise (σ_0) is small and dynamic noise (e.g., moving people around) is large, using Bayesian filters works well to suppress the dynamic RSSI errors.
- ii. If the target has a known motion characteristic, a Bayesian filter with a good model of motion works well compared to the deterministic (NN) methods.

- iii. The more information the Bayesian filter has the better estimation accuracy we have. Knowing the initial position of the target, knowing the velocity of the target, knowing the non-accessible regions for the target in the area increase the estimation accuracy of the Bayesian filter and for these cases using Bayesian approaches outperforms deterministic approaches.
- iv. Although the estimation performances of basic SIR and grid based Bayesian filters are very similar for mobile targets, SIR filters are simple to apply and need less computation time. Also many different improvements for particle filters are proposed in literature for different applications two of which are illustrated in simulations. So particle filters may be more flexible to adapt to the system needs.
- v. Increasing grid resolution further does not contribute much to the estimation accuracy for our case but increases dramatically computation complexity, so 1 m grid spacing is sufficient to use for NN methods and grid based Bayesian filter in our test configurations.
- vi. Optimum k_{NN} value yielding the best RMS error result changes according to the grid spacing and RSSI measurement noise in the environment. For $\sigma_0=5.2$ dB, optimum k_{NN} is found to be about half the k_{CELL} value for the NN methods.
- vii. MMSE estimate is found to be better than MAP estimate for all localization methods for our test configurations.
- viii. Placing the readers not to the corners but to the inner side of the area making the reader separation smaller yields better estimation accuracy for omnidirectional antenna.
- ix. If the size of the environment area increases, the estimation accuracy decreases when the number of readers is the same. So placing more readers in large environments will increase estimation accuracy in real life applications.

7.3 EXPERIMENTAL WORK

In this section our aims can be emphasized as follows:

- i. To give experimental results of conventional deterministic and probabilistic localization and tracking methods (parameter based NN method, grid based Bayesian filtering, and improved SIR filtering) that were also investigated in Section 7.2.2 via their simulation results,
- ii. To give experimental results of pattern based (empirical) NN method,
- iii. To apply automatic online calibration of propagation parameters using reference tags and to give the resulting effects,
- iv. To apply automatic online calibration of filter measurement noise std. σ using reference tags and to give the resulting effects,
- v. To apply the RSSI smoothing algorithm using the reference tags and to give the resulting effects.

Before giving these results in Section 7.3.2, the experimental environment, hardware and software system setup, and the used localization methods and details of applied experiments will be given in Section 7.3.1.

7.3.1 Experimental Setup

In Section 7.3.1.1 experimental environment properties will be given. In Section 7.3.1.2 details of active RFID hardware and software used in the experimental work will be explained. In Section 7.3.1.3, the localization methods, used parameters, and applied experiments will be detailed.

7.3.1.1 Experimental Environment

For the sake of completeness we give the experimental environment in Figure 7.17 again. Two rooms of 3 m x 4 m and 4 m x 6 m with total area of 36 m² is used for the experiments as shown in Figure 7.17. Whole area is divided into 36 equal grid cells with 1 m grid spacing for the NN methods and grid based Bayesian method. 3

readers are placed at the corners of the rooms with 45° angles with the walls in order to have a sight of approximately all of the target area. Readers are placed at 1.2 m height. The height was determined so as to have as much as line of sight (LOS) region with the target tag which was located at 1 m height. The height of the tag was determined as 1 m in order to model the case when a person or a medium sized box carrying it.

In the figure, R1, R2, and R3 represent the three readers and T1, T2, T3, and T4 are the four reference tags used in the experimental work.

7.3.1.2 System Setup

For the experimental work, active RFID products of EG Elektronik Company shown in Figure 7.18 which were designed and developed with the research fund of TUBITAK were modified to use.

Antenna of each tag must be uniform to transmit at the same power and at the same polarization to have a reliable test bed. In order to achieve this we changed the wired antenna of the tags with PCB mount quarter wave monopole JJB antenna of Antenna Factor Company. After mounting the antennas we tested and calibrated the antenna of each tag to give the same output power and being omnidirectional when the tags are placed perpendicular to the ground.

On the other hand, we determined to design a circularly polarized antenna for the readers in order to be able to compensate for multipath effects and change in the polarization of the tag antenna. So we designed a nearly square shaped patch antenna and manufactured the antenna PCB in electromagnetic laboratory of METU EE department with the great help Prof. Dr. Sencer KOÇ.

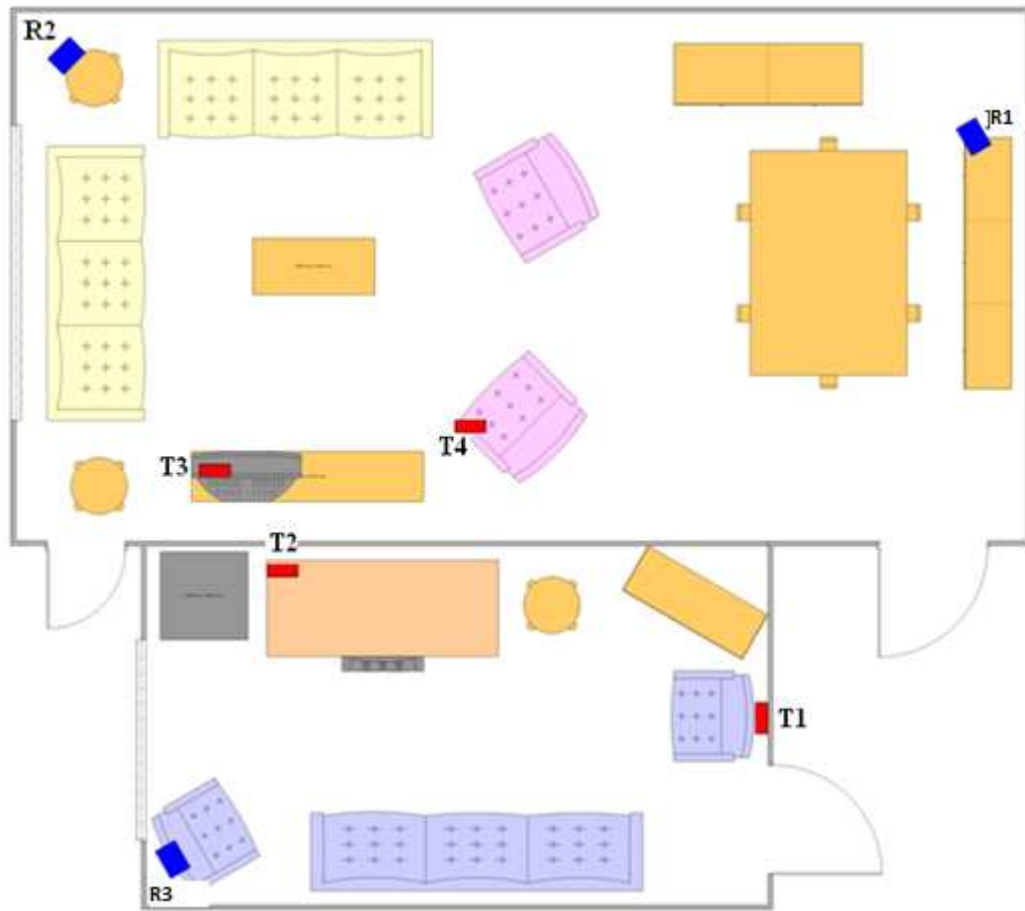


Figure 7.17 Illustration of the experimental environment



Figure 7.18 Active RFID products of EG Elektronik

Information about the used tags and readers are given below:

Tags (shown in Figure 7.19):

- 868 MHz RF frequency
- Manchester coded MSK modulated RF communication
- 250 kbaud RF data rate
- 5 dBm output power
- Listen-before-talk technology
- Beacon ID per 1 second
- 3.3 V coin battery
- 4 years battery life
- Tag antenna: Small JJB antenna-smaller quarter wave monopole antenna, vertically polarized



Figure 7.19 Active RFID tag with JJB antenna attached

Readers (shown in Figure 7.20):

- 868 MHz RF frequency
- -90 dBm RF sensitivity level
- RS485 external communication interface
- Digital RSSI data output with 1 dBm resolution
- 12 V DC input
- Antenna: Nearly square shaped 83 mm x 81.5 mm circularly polarized patch antenna designed and manufactured in the framework of this thesis.



Figure 7.20 Active RFID reader and patch antenna used in the experimental work

In the experimental system we use 3 RFID readers, 1 tag as the target and 4 tags as the reference tags. In order to communicate with the readers we used a USB to RS485 converter that we designed for this thesis work.

For processing and storing the received data from the readers we developed a software and user interface on Microsoft Visual Studio 2008 using C# language. The developed software estimates the current location by running the localization algorithms at each instant when it receives all of the RSSI readings from every reader and every tag. Then it stores the estimated coordinates, received RSSI readings, calculated estimation distance error values, calibrated propagation parameter values, and calibrated measurement noise values.

7.3.1.3 Experimental Methods

Used localization methods in the experimental work are given below:

1. Pattern based (empirical) NN method
2. Parameter based NN method with offline calibration of propagation parameters
3. Parameter based NN method with propagation parameters that are online and automatically calibrated using the reference tags

4. Grid based Bayesian filtering method with online and automatically calibrated propagation parameters
5. Grid based Bayesian filtering method with online and automatically calibrated propagation parameters and with filter measurement noise std. that is automatically calibrated using the reference tags
6. Grid based Bayesian filtering method with online and automatically calibrated propagation parameters and with smoothed RSSI using reference tags
7. Improved SIR particle filter with w smoothing by taking the square root of w and resampling when $N_{\text{eff}} < N_t$.

Used parameters are as below unless otherwise stated:

$k_{\text{NN}} = 36$ (1 m grid spacing), $k_{\text{CELL}} = 36$, $\sigma = 5.2$, $N = 10000$, $N_t = 0.5$, process noise is zero mean Gaussian with std. $D = 0.5$, for mobile target experiment process noise is Gaussian with mean 0.5 m/rt and std. $D_0 = 0.5$ m.

The error statistics given in this work are absolute error statistics. CRLB for the experimented system setup is 0.76 m.

Following experiments were implemented in order to be able to compare the localization methods in different aspects.

Fixed target experiments:

The experimental results are obtained for the fixed target at 25 different points which are furniture dependent covering the target area as shown in Figure 7.21. Locations of reference tags and the readers can also be seen in the figure.

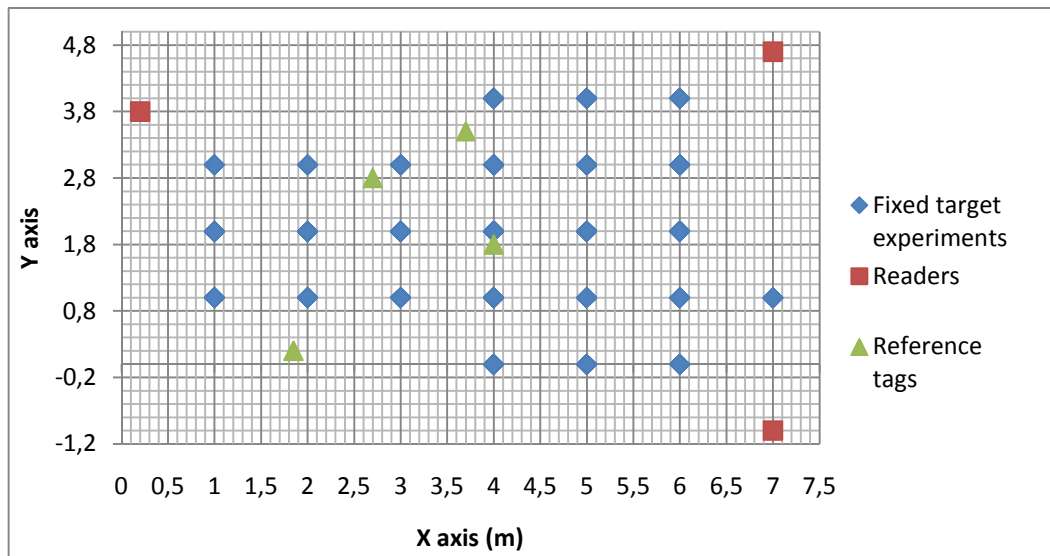


Figure 7.21 Coordinate axis illustration of the experimental environment, locations of fixed target experiments, location of readers and reference tags

At each point, 30 estimations were made with randomly oriented target but the antenna being always vertically polarized. Also at the time of experiments there exists a random dynamic RSSI noise in the environment caused by the movements of experimenter person within the target area. The statistics were drawn from a total of 750 estimation data. The experimented points start from 1 m distance from the surrounding walls.

Mobile target experiments:

For investigating the behavior of Bayesian we moved the target with constant velocity of 0.5 m/rt in y direction from $y=0$ m to $y=3.5$ m in the small sized room, and from $y=0$ m to $y=4$ m in the large sized room as shown in Figure 7.22. It was very challenging to move the target with zero mean Gaussian process noise and inputting the real target location at each time instant to the PC software in order to calculate the estimation errors. That is why we used constant velocity process model for the experimental work.

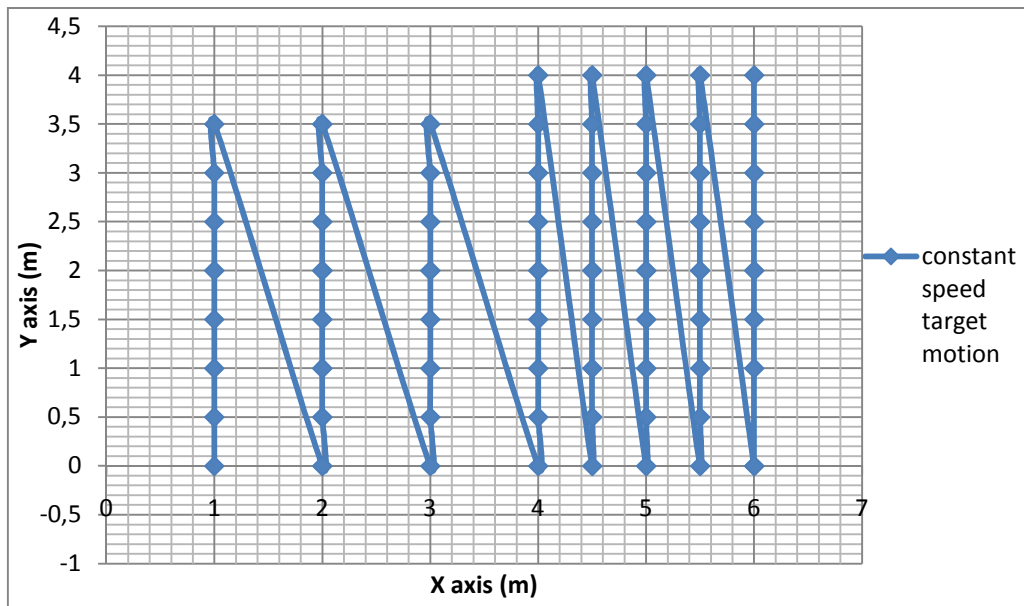


Figure 7.22 Target moving with constant velocity (0.5 m/rt) for mobile target experiment

Dynamic RSSI measurement error experiment:

In order to investigate the behavior of automatic propagation parameter calibration, automatic σ calibration, and conventional Bayesian filters for the case of dynamic measurement errors we made an individual experiment where the target is fixed in the central location of the area. Then dynamic measurement error was generated with moving people around the target and the readers. We repeated this experiment for 3 different target locations. After obtaining 30 estimation results at each location we obtain the statistics for 90 estimation data.

Obstructed reader experiment:

We prepared another individual test setup for searching the effects of online calibration of propagation parameters (n , α) and RSSI smoothing on estimation accuracy in case of environmental changes, e.g., changing the position of an object in the target environment. In order to test this effect, we placed large metal based

objects in front of each 3 readers and we repeated the experiment for 3 different target locations and obtained 30 for each and a total of 90 estimation data.

7.3.2 Experimental Results

In this section, the results of localization methods for different experiments mentioned in Section 7.3.1.3 will be detailed.

7.3.2.1 Deterministic Localization Methods

In this section comparison of pattern based and parameter based NN localization methods will be given and effect of k_{NN} value for NN methods will be investigated.

7.3.2.1.1 Pattern Based (Empirical) vs. Parameter Based (offline) NN Methods

Empirical pattern based NN method proposed in RADAR is compared to the offline calibrated parameter based NN method which was also proposed in RADAR. The estimation results of both methods for fixed target experiment is given in Table 7.26. $k_{NN} = 36$ is used for this experiment.

Table 7.26 Experimental results of pattern based and offline parameter based NN methods for fixed target

Method	RMSE (m)	Mean error (m)	Median error (m)	90 per. error (m)	Error std. (m)
Pattern Based NN	1.32	1.16	0.9	2.0	0.67
Offline Parameter based NN	1.68	1.46	1.4	2.8	0.83

Pattern based approach is seen to outperform the parameter based approach for our environment as also stated in RADAR. This is an expected result since the obtained

propagation map/pattern contains a large information of the continuous space propagation behavior of the environment. Known localization methods with the best error performance are based on this technique. But since our aim is to find ways of simple, affordable, applicable, and flexible localization solutions we do not prefer to use pattern based solutions and so we do not search it in details.

7.3.2.1.2 Effect of k_{NN} parameter for NN methods

In the simulation work for $\sigma_0=5.2$ dB, k_{NN} value giving the best RMS error was found to be approximately half of the number of k_{CELL} value. For the experimental work we tested the effect of k_{NN} value by fixed target experiments and obtained the results in Table 7.27.

Table 7.27 Effect of k_{NN} on estimation error using offline parameter based NN method for the fixed target case

k_{NN}	RMSE (m)	Mean error (m)	Median error (m)	90 per. error (m)	Error std. (m)
4	2.2	1.85	1.5	3.6	1.2
18	1.70	1.46	1.3	2.95	0.95
36	1.68	1.46	1.4	2.8	0.83

Experimental results are not matching with the simulation results for k_{NN} value. In the experimental work the RMS errors are approximately the same for $k_{NN}=18$ and $k_{NN}=36$ whereas 90 percentile error is significantly better for $k_{NN}=36$. The differing results of simulation and experimental work may stem from the misestimating the RSSI measurement noise of the environment. Because the measurement error is in fact not an exact Gaussian distribution, but we assume it to be Gaussian as it is commonly used in the literature.

After evaluating these results we used $k_{NN}=36$ for the rest of our experimental work.

7.3.2.1.3 Effect of Automatic Online Calibration of Propagation Parameters (n , α) Using Reference Tags

By automatically and online calibrating the propagation parameters n and α , it is expected that the parameters are adapted according to the changing environment (e.g., a new obstacle placed in the room, change in the position of the reader, moving people around, etc.). Therefore, localization methods using online calibrated parameters are expected to give better estimation results than that of offline calibrated parameters in an environment with dynamic RSSI measurement error and obstructed readers. But for a static environment, offline calibration methods are expected to give better results since many samples of RSSI measurements are taken for offline calibration where only 4 samples are taken for the online calibration.

For investigating the general effect of online calibration, a comparison of parameter based NN method with offline calibrated parameters and parameter based NN method with online calibrated parameters is given in Table 7.28.

Table 7.28 Effect of automatic online calibration of propagation parameters for fixed target experiment

Method	RMSE (m)	Mean error (m)	Median error (m)	90 per. error (m)	Error std. (m)
Offline NN	1.68	1.46	1.4	2.8	0.83
Online NN	1.63	1.44	1.3	2.5	0.76

It is seen that 90 percentile error for online calibrated NN method is significantly smaller than that of offline calibrated method for the fixed target experiments. If the fixed target experiments would have been made in static environment we could not explain this improved effect. But, since there exists randomly generated dynamic RSSI noise at the time of experiments caused by the movements of the experimenter

person, it can be explained as that online method is able to adaptively calibrate the parameters so as to decrease estimation errors.

For dynamic measurement error experiments, the obtained mean standard deviation of the estimation errors is 0.50 m for online method and 0.57 m for offline method. This result shows that, localization methods using online calibration of propagation parameters are less affected by the dynamic RSSI errors compared to offline calibration methods.

In addition, for obstructed reader experiment, the mean error for online calibration NN method is 1.35 m where it is 1.62 m for offline calibration method. This result shows that online calibration is also useful for adapting the parameters to work in changing environmental conditions.

After testing automatic calibration method by using parameter based NN approach we used online calibrated propagation parameters for the other estimation methods in the experimental work.

7.3.2.2 Probabilistic Localization Methods

In this section we will investigate the behavior of deterministic and probabilistic localization approaches in different cases. For comparison we will give the estimation results in fixed target case, mobile target case, and dynamic RSSI measurement error case. We expect that probabilistic methods are worse than the deterministic methods for fixed target cases, but they outperform deterministic methods for tracking mobile target and dynamic errors in RSSI measurement cases. In order to compare deterministic and probabilistic methods we will give the results of online calibrated parameter based NN as a deterministic method and grid based Bayesian and improved SIR filters as probabilistic methods.

We start by giving the estimation results of fixed target experiments in Table 7.29.

Table 7.29 Comparison of parameter based NN, grid based Bayesian and improved SIR particle filter for fixed target case

Method	RMSE (m)	Mean error (m)	Median error (m)	90 per. error (m)	Error std. (m)
Parameter based Online NN	1.63	1.44	1.3	2.5	0.76
Grid Based Bayesian	2.04	1.77	1.6	3.1	1.03
Improved SIR	1.72	1.48	1.3	2.6	0.87

It is seen that for fixed target case deterministic method outperforms the probabilistic methods as expected, but improved SIR filter estimation errors are close to the NN method's errors as given in the simulations.

The results of mobile target experiments are given in Table 7.30.

Table 7.30 Comparison of parameter based NN, grid based Bayesian and improved SIR particle filter for moving target with known velocity

Method	RMSE (m)	Mean error (m)	Median error (m)	90 per. error (m)	Error std. (m)
Parameter based Online NN	1.73	1.53	1.49	2.50	0.82
Grid Based Bayesian	1.58	1.37	1.22	2.39	0.8
Improved SIR	1.32	1.16	1.10	2.09	0.64

For the mobile target experiments it is seen that probabilistic methods outperform the deterministic method. In addition improved SIR filter performs better than the grid based Bayesian filter for mobile target tracking.

To illustrate the tracking performance of a deterministic localization method and a probabilistic filter we give a graphical illustration of parameter based NN method and grid based Bayesian filter in Figure 7.23 when they are used to track a constant velocity target which is one of the applied mobile target experiments. It is seen that the Bayesian filter tracks the route while the NN method may make random estimations away from the target route.

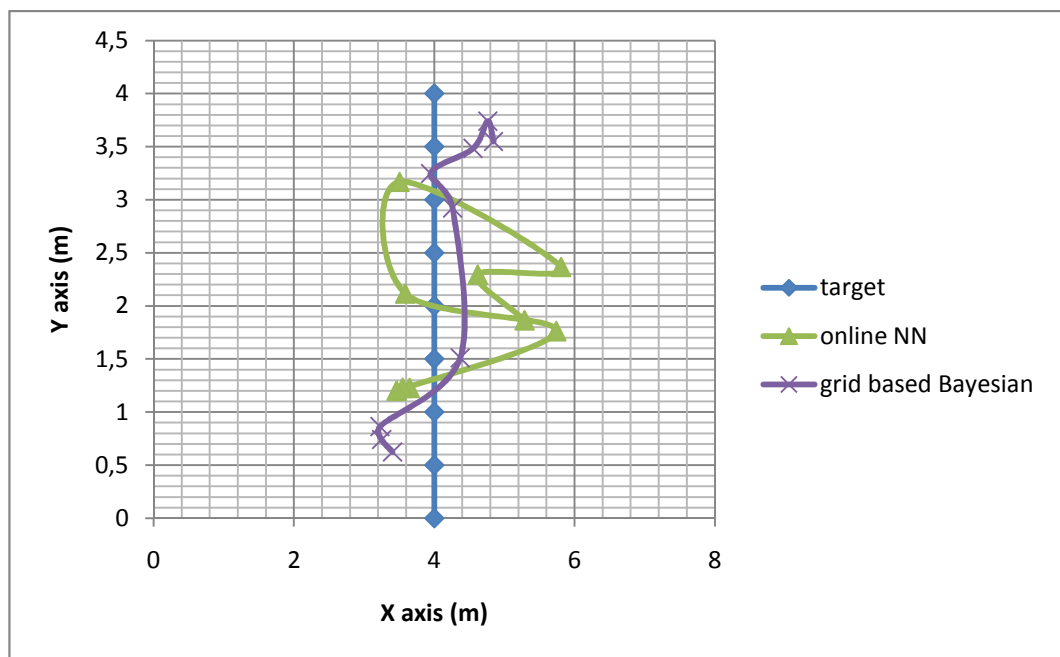


Figure 7.23 Graphical illustration of NN based method vs. Bayesian filtering for target tracking

In order to investigate the behavior of probabilistic methods in environments with dynamic RSSI noise we give the results of the dynamic RSSI measurement error experiments in Table 7.31.

Table 7.31 Error std. comparison of parameter based NN, grid based Bayesian and improved SIR particle filter for dynamic measurement noise experiment

	Parameter based Online NN	Grid Based Bayesian	Improved SIR
Error Std. (m)	0,50	0,41	0,36

Error standard deviation gives us an idea about the deviation of the estimation error from the mean so that smaller std can be commented as that method is less affected by the dynamic noise giving a more stable estimation result. Also, an example illustration of the dynamic noise experiments is given in Figure 7.24 where the target is fixed at only one location and RSSI error is generated randomly in time. As a result, it is seen that probabilistic localization methods give more stable estimation results in environments of dynamic measurement noise and improved SIR is slightly better than the grid based Bayesian filter.

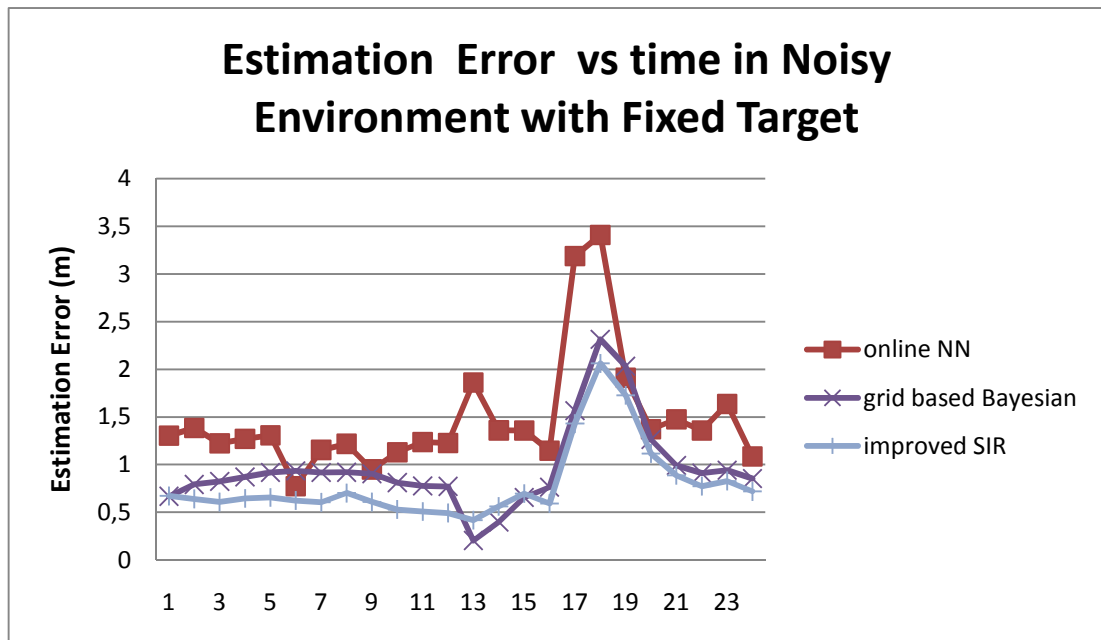


Figure 7.24 Graphical illustration of parameter based NN, grid based Bayesian and improved SIR particle filter for dynamic measurement noise experiment

7.3.2.3 Effect of Automatic Online Calibration of Filter Measurement Noise Std. (σ) Using Reference Tags

In order to investigate the effect of automatic and online calibration of σ we applied this technique to grid based Bayesian filtering and in this section basic grid based Bayesian filter will be compared to the Bayesian filter with online calibrated σ for fixed target case, mobile target case and dynamic RSSI error case.

In Table 7.32, estimation results of the mentioned methods are given for the fixed target experiments.

For the fixed target case, online calibration of σ slightly increases the overall estimation accuracy.

Table 7.32 Effect of automatic calibration of filter measurement noise σ for fixed target case

Method	RMSE (m)	Mean error (m)	Median error (m)	90 per. error (m)	Error std. (m)
Grid Based Bayesian	2.04	1.77	1.6	3.1	1.03
Grid Based Bayesian with auto σ	1.98	1.70	1.5	3.0	1.02

Table 7.33 gives the estimation error statistics of the grid based Bayesian and online calibration of σ methods for mobile target case.

Similar to the fixed target case, online calibration of σ gives slightly better estimation results for mobile target case.

Table 7.33 Effect of automatic calibration of σ for mobile target case

Method	RMSE (m)	Mean error (m)	Median error (m)	90 per. error (m)	Error std. (m)
Grid Based Bayesian	1.58	1.37	1.22	2.39	0.8
Grid Based Bayesian with auto σ	1.50	1.30	1.20	2.20	0.75

Table 7.34 and Figure 7.25 are given to illustrate the effect of online calibrated σ method in environments with dynamic RSSI measurement error. In Figure 7.25, an experiment result with the target fixed at only one location is given as an illustrative example.

Table 7.34 Error std. comparison of grid based Bayesian and grid based Bayesian with automatic calibration of σ for dynamic RSSI measurement error experiment

	Grid Based Bayesian	Grid Based Bayesian with auto σ
Error Std. (m)	0.41	0.34

For the dynamic RSSI measurement error experiments online calibration of σ gives more stable estimation results.

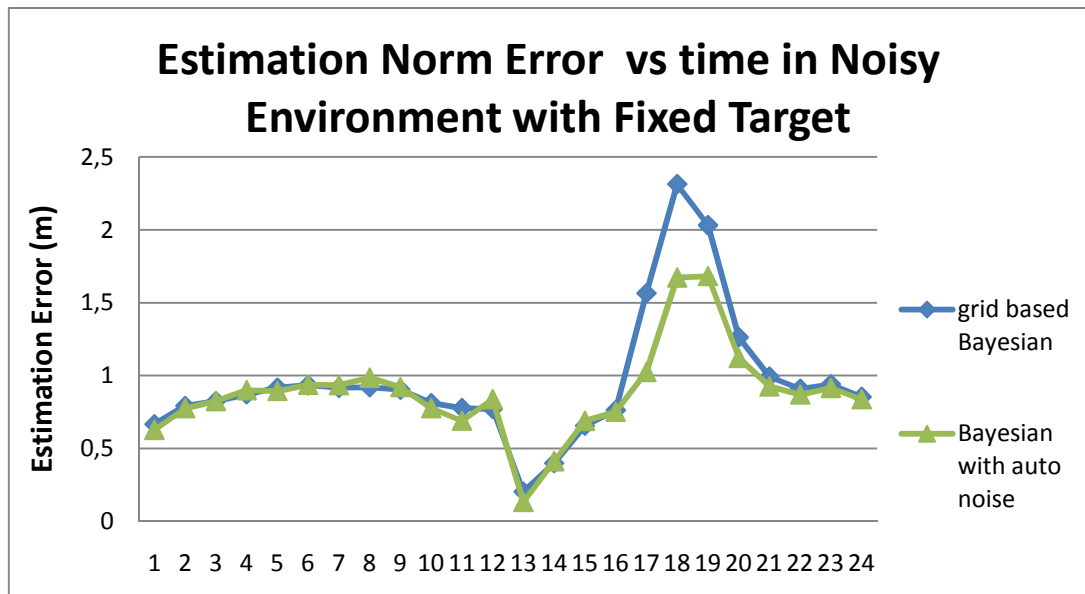


Figure 7.25 Graphical illustration of effect of automatic calibration of σ for dynamic RSSI measurement error

7.3.2.4 Effect of Online RSSI Smoothing Using Reference Tags

In order to investigate the effect of RSSI smoothing algorithm we applied the algorithm to the grid based Bayesian filtering, so we will give results and comparison of simple grid based Bayesian filter and grid based Bayesian with RSSI smoothing in this section. It is expected that the smoothing gives better estimation accuracy for the experimented target locations that are close to the reference tag locations.

Results of fixed target experiments are given in Table 7.35 and it is seen that the overall error performance of the localization method with RSSI smoothing algorithm is better for the fixed target case.

From the fixed target experiments, the results of the experimented points in 1.5 m neighborhood of the reference tags are chosen to give the mean errors in Table 7.36. It is seen that the smoothing algorithm is very successful near the reference tags. So,

it can be noted that, in order to increase the overall estimation error accuracy more reference tags can be used.

Table 7.35 Effect of online RSSI smoothing using reference tags for fixed target case

Method	RMSE (m)	Mean error (m)	Median error (m)	90 per. error (m)	Error std. (m)
Grid Based Bayesian	2.04	1.77	1.6	3.1	1.03
Grid Based Bayesian with RSSI Smoothing	1.87	1.58	1.3	3.0	0.99

Table 7.36 Effect of RSSI smoothing at locations near the reference tags for the fixed target case

	Grid Based Bayesian	Grid Based Bayesian with RSSI smoothing
Mean Estimation Error (m)	2.13	1.55

In Table 7.37, it is seen that smoothing algorithm has also improving effect on the estimation accuracy for the mobile target case.

Obstructed reader experiments of the RSSI smoothing algorithm support the above results. 2 of the 3 experimented target locations in obstructed reader experiments are the neighbor locations of reference tags. So in the obstructed reader case, the results in Table 7.38 show the predominating effect of RSSI smoothing.

Table 7.37 Effect of online RSSI smoothing using reference tags for mobile target case

Method	RMSE (m)	Mean error (m)	Median error (m)	90 per. error (m)	Error std. (m)
Grid Based Bayesian	1.58	1.37	1.22	2.39	0.8
Grid Based Bayesian with RSSI smoothing	1.37	1.21	1.05	1.98	0.66

Table 7.38 Effect of RSSI smoothing for obstructed reader case

	Grid Based Bayesian	Grid Based Bayesian with RSSI smoothing
Mean Estimation Error (m)	1.55	1.20

7.3.2.5 Effect of Online Calibration of σ and RSSI Smoothing Using Reference Tags

After giving the effects of online calibration of σ and RSSI smoothing individually by applying them to the grid based Bayesian filter, now we will give the results of improved SIR filter with online calibration of σ and RSSI smoothing applied together for mobile target experiments. In Table 7.39, results of the application are given with comparison of grid based Bayesian and improved SIR filters.

As seen in the table application of both approaches to the improved SIR filter makes a further improvement to the improved SIR filter for mobile target experiments. Especially the 90 percentile error decreases significantly with the application. As a result we can claim that improved SIR method with online calibration of σ and RSSI

smoothing gives outperforming results for mobile target case as compared with all the other methods we investigated.

Table 7.39 Effect of online calibration of σ and RSSI smoothing together for mobile target case

Method	RMSE (m)	Mean error (m)	Median error (m)	90 per. error (m)	Error std. (m)
Grid Based Bayesian	1.58	1.37	1.22	2.39	0.8
Improved SIR	1.32	1.16	1.10	2.09	0.64
Improved SIR with online σ and RSSI smoothing	1.25	1.12	1.05	1.82	0.56

7.3.2.6 Using Monopole Antenna For The Readers Instead of Patch Antenna

At the beginning of our thesis work we proposed to use circularly polarized reader antenna instead of monopole antenna for decreasing RSSI measurement errors that are caused by multipath effect and unmatched polarization of the target and reference tags' antennas. After obtaining our results by using the patch antenna, we switched to the monopole antenna which is vertically polarized to observe the difference in estimation accuracy. So we tested only the mobile target experiments with the monopole antenna to show the difference. The estimation results are seen in Table 7.40.

Table 7.40 Effect of reader antenna on localization accuracy: monopole antenna vs. patch antenna for mobile target case

Reader Antenna	Method	RMSE (m)	Mean error (m)	Median error (m)	90 per. error (m)	Error std. (m)
Circularly polarized patch	Parameter based Online NN	1.73	1.53	1.49	2.50	0.82
	Grid Based Bayesian	1.58	1.37	1.22	2.39	0.8
	Grid Based Bayesian with online σ	1.50	1.30	1.20	2.20	0.75
	Improved SIR	1.32	1.16	1.10	2.09	0.64
	Improved SIR with online σ and RSSI smoothing	1.25	1.12	1.05	1.82	0.56
	Vertically polarized monopole	Parameter based Online NN	1.86	1.64	1.62	2.96
Vertically polarized monopole	Grid Based Bayesian	1.93	1.74	1.62	2.76	0.82
	Grid Based Bayesian with online σ	1.57	1.42	1.44	2.20	0.66
	Improved SIR	1.73	1.56	1.50	2.54	0.75
	Improved SIR with online σ and RSSI smoothing	1.49	1.33	1.26	2.16	0.67

Investigating the results, estimation accuracy for all of the localization methods are seen to be worse for the monopole antenna case. Also note that, for the monopole antenna case grid based Bayesian estimation error is larger than that of the NN

method where it is vice versa for the patch antenna case. Searching the reason we noticed that σ_0 found by auto calibration had an average of 7.5 dB for the monopole antenna experiments thus σ parameter was calibrated to an average value of 7.5 dB where it was about 5.2 dB for the patch antenna case. But we used $\sigma = 5.2$ dB for the grid based Bayesian and the improved SIR filters for the monopole antenna experiments. That is why there is a significant decrease in the estimation error for the methods using online calibration of σ for the monopole antenna experiments. To sum up, we can say that using monopole antenna for the readers when the tag antenna is also monopole, causes larger RSSI measurement noise resulting in larger estimation error. But since the monopole antenna is omnidirectional and the patch antenna is directional, for a larger area that we need more than 3 readers, we must use more patch antennas than monopole antennas to cover the whole area as shown in Figure 7.26 and Figure 7.27.

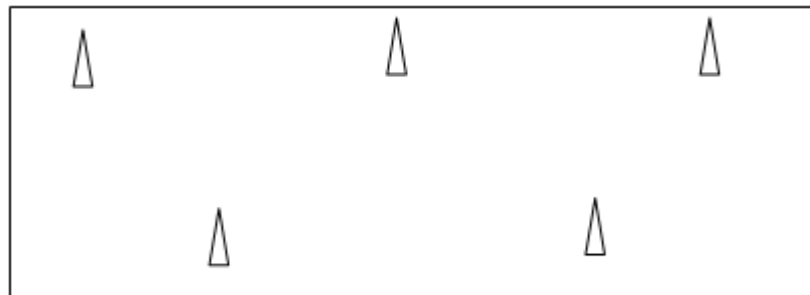


Figure 7.26 Sample monopole antenna placement configuration

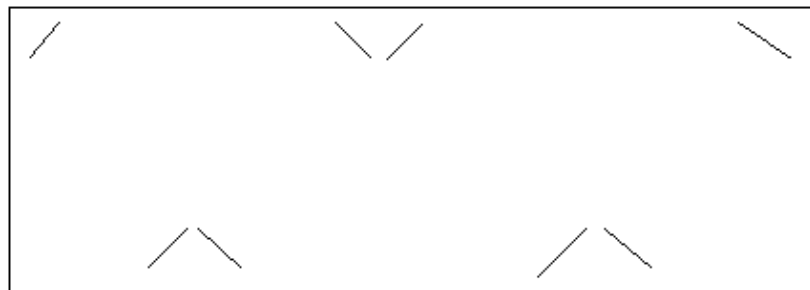


Figure 7.27 Sample patch antenna placement configuration

For the illustrated environment, 5 monopole antennas are used whereas 8 patch antennas are needed to cover the whole target area which increase the system cost. So the implementer should choose which type to use according the system needs.

A summary and analysis of the experimental results will be given in the next section with comparison of the simulation results.

7.4 ANALYSIS OF SIMULATION AND EXPERIMENTAL RESULTS

In this section experimental and simulation results of the applied localization methods are given together in order to be able to see the behavior of the methods as a whole in differing experimental conditions. Experimental results of fixed target experiments (Table 7.41), mobile target experiments (Table 7.42), dynamic RSSI measurement error experiments (Table 7.43), and obscured reader experiments (Table 7.44) are given below individually. Simulation results of fixed target case (Table 7.45) and mobile target case (Table 7.46) are given again for completeness. In the experimental and simulation work, all of the experimental conditions were not applied to all of the localization methods. So, in the tables, only the related methods mentioned in the simulation results section of 7.2 and experimental results section of 7.3 are given. For the experimental and simulation work, improved SIR filter contains the improvements by w smoothing and resampling when $N_{eff} < 0.5$.

First evaluating the pattern based and parameter based NN methods in the experimental work we verified that pattern based approaches outperform parameter based approaches as stated in the literature. But for the NN method and probabilistic localization methods we used parameter based approach to obtain the environment signal propagation behavior in order to use simple, affordable, fast solutions for real applications. We preferred not to simulate the pattern based NN method since it is very challenging to have an accurate model.

For improving parameter calibration and make it simpler we proposed the approach of automatic and online calibration of propagation parameters and tested this approach by applying it to the NN method and claimed several advantages over the

offline calibration approach. The advantages can be seen in Table 7.41 to Table 7.44 for all of the experimented conditions by comparing offline and online NN methods. To sum up, it can be claimed that for dynamic RSSI measurement errors and changing environments, adaptively calibrating the parameters in online phase improves the estimation accuracy and also it is much simpler than the offline calibration method despite an added system cost by using the reference tags.

Table 7.41 Experimental error statistics for all used localization methods for fixed target experiments where CRLB=0.76 m

Method	RMSE (m)	Mean error (m)	Median error (m)	90 per. error (m)	Error std. (m)
Pattern Based NN	1.32	1.16	0.9	2.0	0.67
Parameter based Offline NN	1.68	1.46	1.4	2.8	0.83
Parameter based Online NN	1.63	1.44	1.3	2.5	0.76
Grid Based Bayesian	2.04	1.77	1.6	3.1	1.03
Grid Based Bayesian with auto σ	1.98	1.70	1.5	3.0	1.02
Grid Based Bayesian with RSSI Smoothing	1.87	1.58	1.3	3.0	0.99
Improved SIR	1.72	1.48	1.3	2.6	0.87

Table 7.42 Experimental error statistics for all used localization methods for mobile target experiments where CRLB=0.76 m

Method	RMSE (m)	Mean error (m)	Median error (m)	90 per. error (m)	Error std. (m)
Parameter based Offline NN	1.84	1.61	1.59	2.87	0.84
Parameter based Online NN	1.73	1.53	1.49	2.50	0.82
Grid Based Bayesian	1.58	1.37	1.22	2.39	0.8
Grid Based Bayesian with auto σ	1.50	1.30	1.20	2.20	0.75
Grid Based Bayesian with RSSI Smoothing	1.37	1.21	1.05	1.98	0.66
Improved SIR	1.32	1.16	1.10	2.09	0.64
Improved SIR with online σ and RSSI smoothing	1.25	1.12	1.05	1.82	0.56

Table 7.43 Experimental error std for all localization methods for dynamic RSSI measurement error experiments

	Parameter based Offline NN	Parameter based Online NN	Grid Based Bayesian	Grid Based Bayesian with auto σ	Grid Based Bayesian with RSSI Smoothing	Improved SIR
Error Std. (m)	0.57	0.50	0.41	0.34	0.39	0.36

Table 7.44 Mean estimation error for related localization methods for obstructed reader experiments

	Parameter based Offline NN	Parameter based Online NN	Grid Based Bayesian	Grid Based Bayesian with RSSI smoothing
Mean Estimation Error (m)	1.62	1.35	1.55	1.20

Table 7.45 Simulation results of all simulated localization methods for fixed target case where CRLB=0.80 m

Method	RMSE (m)	Mean error (m)	Median error (m)	90 per. error (m)	Error std. (m)
Parameter based Offline NN	1.79	1.59	1.51	2.65	0.81
Grid Based Bayesian	1.83	1.54	1.34	2.91	0.98
Basic SIR	2.00	1.70	1.51	3.09	1.07
Improved SIR	1.73	1.51	1.34	2.64	0.83

Table 7.46 Simulation results of simulated probabilistic localization methods for mobile target case where CRLB=0.80 m

Method	RMSE (m)	Mean error (m)	Median error (m)	90 per. error (m)	Error std. (m)
Grid Based Bayesian	1.22	1.09	1.02	1.81	0.54
Basic SIR	1.14	0.98	0.88	1.77	0.54
Improved SIR	1.37	1.20	1.09	2.04	0.64

Then we proposed to use probabilistic localization/tracking methods for mobile targets and for environments with dynamic RSSI noise. Improved SIR filter is more successful for both mobile target tracking and for the estimation stability in noisy environments. But for mobile target case, simulation results show that grid based Bayesian filter is better than the improved SIR filter. Simulation results also show that basic SIR filter is the best of Bayesian filters for mobile target case. We did not experimented basic SIR filter since the estimation results for the fixed target case are not satisfactory, but if it is known that the target does not stop while moving in the real application then using basic SIR filter may give more accurate results. For the fixed target case the estimation error of improved SIR filter is close to that of NN method and grid based Bayesian filtering has larger estimation errors both for simulation and experimental work. In addition to these results, as the simulation suggests, the more information the Bayesian filters have the better estimation accuracy we have. Knowing the initial position of the target, knowing the speed and direction of the target, knowing the non-accessible regions for the target in the area increase the estimation accuracy of the Bayesian filters and for these cases using Bayesian approaches outperforms deterministic approaches.

By using the reference tags we also proposed to calibrate σ of the Bayesian filters automatically and online at each step of estimation. We applied this approach to grid based Bayesian filter individually in the experimental work to investigate the effect. After experimenting we claim that online calibration of σ improves the estimation accuracy for fixed and mobile target cases and it improves the estimation stability in noisy environment. This approach is applied to the improved SIR filtering along with the RSSI smoothing approach.

We propose to add an extra information to the estimation system by calibrating the RSSI readings of the target by using the RSSI readings of reference tags. This approach is a contribution of this thesis as far as we know. We applied this approach again to the grid based Bayesian filter individually and we claim that using this smoothing can improve the estimation accuracy significantly for the near locations of the reference tags for any applied experimental condition. The overall effect could be

improved by adding more reference tags and this approach can be applied to the other localization methods easily.

Online calibration of σ and RSSI smoothing approaches were applied together to the improved SIR filter and tested with the mobile target experiment. Comparing with the other applied localization methods, this approach gives the best estimation accuracy.

In the simulation work it was given that the separation of the readers and thus the size of the environment affect the estimation accuracy very significantly. Increasing the separation between the readers increases the estimation error. Also we showed that the antenna type of the readers is another important factor which affects the estimation accuracy. In our experiments using circularly polarized reader antenna increased the estimation accuracy while increasing the system cost. So, type of the antenna and reader separation are to be determined according to the system needs and the system cost.

In conclusion, it can be claimed that, application of the automatic calibration of σ and other propagation parameters, RSSI smoothing algorithm, and any other information about the behavior of the target motion to the Bayesian filters would yield an outperforming result for all of the experimental conditions. Also it is seen that applying these approaches to the improved SIR filter would yield more robust and accurate estimation results.

CHAPTER 8

CONCLUSIONS

The need for indoor localizing and tracking people or objects in real time has been grown recently especially in manufacturing, healthcare, and logistics. As these needs grow, real time locating and tracking systems (RTLS) gain great importance and different solutions using especially Wi-Fi devices, wireless sensor networks (WSN), and radio frequency identification (RFID) devices exploiting received signal strength indication (RSSI) have been proposed and developed in both academic and business world. Investigating the proposed techniques in the literature we have noticed the lack of information on the advantages and disadvantages of these techniques which are applied in the same test bed for different test conditions. Also, since indoor environment is usually a complicated environment causing multipath and fading effects on the RF signal, location estimation has still problems to be worked on. We think that two important of them are i) increasing the estimation accuracy ii) decreasing the system complexity and time consumption and hence decreasing the system cost of the RTLS system. Therefore, our aim in this thesis work was to evaluate the most common localization methods on the same test bed both with simulation and experimental analyses and yield their weak and strong behaviors in different test conditions. Also we propose an integrated and modified method that is simple to install, cost effective, and moderately accurate to use for real life applications.

We used an active RFID system composed of 3 readers, 1 target tag, and 4 reference tags in an environment of two rooms with 12 m² and 24 m² areas in a home where the RSSI measurement noise standard deviation is found to be 5.2 dB for our experimental work. RFID is a small sized, cost effective, and commonly used system for real life RTLS applications. We designed and produced circularly polarized patch antenna for the readers in order to decrease RSSI measurement errors caused by the multipath effect and mis-orientation effect of the monopole tag antenna. For developing the PC software that processes and stores the data and for developing the user interface we used C#.

We mainly applied and tested pattern/map based nearest neighbors (NN) (also called pattern matching or fingerprinting) and parameter based NN approaches (in this approach pattern matching method is used but the pattern is generated virtually by using the signal propagation models) as deterministic localization methods, and grid based Bayesian filter and sampling importance resampling (SIR) particle filter as probabilistic localization methods which are studied in the literature for localization and tracking purposes. We investigated the behaviors of each for different environmental and system parameters and compared them with each other on the same test bed for using in RFID based localization and tracking system. For the NN methods we investigated the effects of number of nearest neighbors used for location estimation and grid resolution are investigated. For the grid based Bayesian filtering effect of grid resolution on the estimation accuracy is investigated. For SIR filtering effect of number of particles is investigated and two improvements proposed in the literature are implemented to the basic SIR filter to observe their effects. One is resampling not at every recursion step but when the effective sample size N_{eff} is smaller than a threshold N_t . Second one is smoothing the importance factor w by taking the square root of the current w at the beginning of each resampling stage. For the general location estimation problem we tested the effects of number of readers and separation between the readers used for the localization system, size of the target environment, RSSI measurement noise of the environment, and target motion characteristics by using simulation analysis. For the Bayesian methods, we also searched the effects of filter process noise model and filter measurement noise

model. We also tested the behaviors of the Bayesian filters if additional information about the target motion is added to the filter models such as the velocity of the target, initial location of the target, and non-accessible locations in the area. For real life applications we tested the effect of the used reader antenna (patch antenna and monopole antenna) in the system.

Our simulation and experimental work yielded that deterministic methods are usually better to localize a fixed target than the Bayesian methods if the RSSI measurement noise of the environment is large (> 3 dB). Results of the deterministic methods showed that empirical pattern based NN method outperforms the parameter based NN method since it has a more accurate propagation map of the environment. But pattern based approaches need an important amount of human labor and time for the system setup for especially large sized environments and if there is a change in the environment (e.g., changing the location of an obstacle in the environment) or system setup (e.g., location of a reader) the system has to be reinstalled. So we preferred not to search details of pattern based approaches. For mobile target scenarios, both simulation and experimental work showed that Bayesian methods outperform the deterministic methods and SIR particle filter generally works better than the grid based Bayesian filter. The advantage of the Bayesian filters is that any information about the environment and the motion of the target can be added to the estimation system and results in an increased estimation accuracy. For example, for a production control case, the initial location and the route of the goods in production are known which will yield the Bayesian filters work very well, outperforming the deterministic methods. Another advantage of the Bayesian filters is that the estimation is more stable in environments with dynamic RSSI noise compared to the deterministic localization methods.

We assumed large-scale log-distance path loss signal propagation model for the environment. In order to obtain the signal propagation parameters of the log-distance model and the measurement noise std. σ for the Bayesian filters we made offline calibration experiments and also implemented an automatic calibration system using reference tags. This is the only work in the literature using automatic calibration of

the propagation parameters and measurement noise for indoor localization using an RFID system as far as we know. After testing both approaches in the experimental phase with different test conditions, we claim that the localization methods using automatic calibration give better estimation results than the offline calibrated methods for the environments with dynamic RSSI measurement errors (e.g., people moving around). Since the system is adaptive, if there is a change in the environment there is no need to calibrate the propagation parameters again as in the case of offline calibration.

We propose to add an extra information to the estimation system by calibrating the RSSI readings of the target by using the RSSI readings of reference tags. We call this algorithm RSSI smoothing and this is the only work in the literature using such an approach for localization purpose. The experimental results showed that using this smoothing can improve the estimation accuracy significantly for the near locations of the reference tags for any applied experimental condition. The overall effect could be improved by adding more reference tags and this approach can be applied to both deterministic and probabilistic localization methods easily.

In addition to these results, a few more words should be mentioned about real life applications. First of all, the experimental results that we give in this thesis are only for illustrating the comparison of the localization methods and the effects of the environmental and system parameters on the localization accuracy. Using the same methods one can obtain different results in another application since the estimation results are very much affected by the environment properties and the antenna of the RF devices.

In conclusion, we claim that, implementation of the automatic calibration of σ and other propagation parameters, RSSI smoothing algorithm, and adding any other information about the behavior of the target motion to the Bayesian filters, especially, to the improved SIR filter yield an outperforming result for mobile target cases and it also works robust for fixed target cases compared to the grid based Bayesian filter.

As a future work, this study can be implemented in a larger experimental environment and by using different number of readers with different reader separations to yield the estimation accuracy of the localization methods in a more real application environment. Also, using multiple directional (patch) antennas for each reader can be studied which is expected to improve the estimation accuracy by adding the direction information of the target. Increasing the number of reference tags can be implemented as a future work to increase the accuracy.

Antenna diversity is known to improve the quality and reliability of the wireless link. So, for further development in the estimation accuracy, different antenna diversity techniques (e.g., spatial diversity, polarization diversity) can be used to decrease the multipath distortion in indoor environments inspite of increased system cost. For such a system the readers must have at least two antennas seperated from each other by a certain distance. But it must be noted that such a system requires additional hardware and processing complexity on the receiver.

REFERENCES

1. **Dixit, V. V.** *A Particle Filter Based Framework For Indoor Wireless Localization Using Custom IEEE 802.15.4 Nodes*, Arlington : M.Sc. Thesis, The University of Texas, 2008.
2. **E. Aydın, and R. Öktem.** *An RFID Based Indoor Tracking Method for Navigating Visually Impaired People*, Turk J Elec Eng & Comp Sci, Vol. 18, No. 2, pp. 1-12, 2010.
3. **Lim, J.** *Tracking A Variable Number Of Targets Based On RSS Measurements In Wireless Sensor Networks*, New York : PhD Thesis, Stony Brook University, 2007.
4. **Yeap, T. H.** *Analysis and Design of Neural Network- Based WLAN Indoor Location System*, Ottawa : M. Sc. Thesis, University of Ottawa, 2007.
5. **X. Huang, R. Janaswamy, and A. Ganz.** *Scout: Outdoor localization using active RFID technology*, 3rd Int. Conf. on Broadband Com., Networks and Systems, pp. 1-10, 2006.
6. **Sanpechuda, T. K.** *A Review of RFID Localization: Applications and Techniques*, 5th International Conference on Electrical Engineering/Electronics, Computer, Telecommunications and Information Technology, Vol. 2, pp. 769-772, 2008.
7. **M. Bouet, and A. L. dos Santos.** *RFID Tags: Positioning Principles and Localization Techniques*, 2nd International Home Networking Conference, pp. 1-5, 2008.
8. **A. Bekkali, H. Sanson, and M. Matsumoto.** *RFID Indoor Positioning based on Probabilistic RFID Map and Kalman Filtering*, 3rd IEEE International Conference

on Wireless and Mobile Computing, Networking and Communications, pp. 21-27, 2007.

9. **A. D. Koutsou, F. Seco, A. R. Jimenez, J. O. Roa, J. L. Ealo, C. Prieto, and J. Guevara.** *Preliminary Localization Results With An RFID Based Indoor Guiding System*, IEEE International Symposium on Intelligent Signal Processing, pp. 1-6, 2007.

10. **E. Aydin, R. Oktem, Z. Dincer, and I. K. Akbulut.** *Study of an RFID Based Moving Object Tracking System*, RFID Eurasia, pp. 1-5, 2007.

11. **L.M. Ni, Y. Liu., Y.C. Lau, and A.P. Patil.** *LANDMARC: Indoor Location Sensing Using Active RFID*, 1st IEEE International Conference on Pervasive Computing and Communications, 2003.

12. **S. I. Soonjun, D. Boontri, and P. Cherntanomwong.** *A Novel Approach of RFID Based Indoor Localization Using Fingerprinting Techniques*, 15th Asia-Pacific Conference on Communications, pp. 475-478, 2009.

13. **T. Roos, P. Myllymaki, H. Tirri, P. Misikangas, and J. Sievanen.** *A Probabilistic Approach to WLAN User Location Estimation*, International Journal of Wireless Information Networks, Vol. 9, No. 3, pp. 155-164, 2002.

14. **G. V. Z'aruba, M. Huber, F. A. Kamangar, and I. Chlamtac.** *Indoor Location Tracking Using RSSI Readings From A Single Wi-Fi Access Point*, Wireless Networks, Vol. 13, No. 2, pp. 221-235, 2002.

15. **A. M. Ladd, K. E. Bekris, A. P. Rudys, D. S. Wallach, and L. E. Kavraki.** *On the Feasibility of Using Wireless Ethernet for Indoor Localization*, IEEE Transactions on Robotics and Automation, 2004, Vol. 20, pp. 555-559.

16. **P. Barsocchi, S. Lenzi, S. Chessa, and G. Giunta.** *A Novel Approach to Indoor RSSI Localization by Automatic Calibration of the Wireless Propagation Model*, IEEE 69th Vehicular Technology Conference, pp. 1-5, 2009.

17. **P. Bahl, and V. N. Padmanbhan.** *RADAR: An In-Building RF-based User Location and Tracking System*, *IEEE INFOCOM*, Vol. 2, pp. 776-784, 2000.
18. **J. Hightower, R. Want, and G. Borriello.** *SpotON: An Indoor 3D Location Sensing Technology Based on RF Signal Strength*, UW CSE Technical Report, 2000.
19. **R. Huang, and G. V. Záruba.** *Location Tracking in Mobile Ad Hoc Networks Using Particle Filters*, *Journal of Discrete Algorithms*, Vol. 5, pp. 455–470, 2007.
20. **D. Haehnel, W. Burgard, D. Fox, K. Fishkin, and M. Philipose.** *Mapping and Localization with RFID Technology*, *IEEE International Conference on Robotics and Automation*, Vol. 1, pp. 1015-1020, 2004.
21. **Skellam, J.G.** *Studies in Statistical Ecology: Spatial Pattern*, *Biometrika*, Vol. 39, pp. 346-362, 1952.
22. **M. Saxena, P. Gupta, and B.N. Jain.** *Experimental Analysis of RSSI-Based Location Estimation in Wireless Sensor Networks*, 3rd International ICST Conference on Communication, 2008.
23. **B. Ristic, S. Arulmpalam, and N. Gordon.** *Beyond The Kalman Filter: Particle Filters for Tracking Applications*, Artech House Publishers, 2004.
24. **W. Burgard, A. Den Dieter, F. Armin, and B. Cremers.** *Integrating Global Position Estimation and Position Tracking for Mobile Robots: The Dynamic Markov Localization Approach*, *IEEE/RSJ International Conference on Intelligent Robots and Systems*, 1998.
25. **D. Fox, W. Burgard, and F. Dellaert.** *Robust Monte Carlo Localization For Mobile Robots*, *Artificial Intelligence*, Vol. 128, pp. 99-141, 2000.
26. **Zorych, I.** *A Bayesian Approach to Wireless Location Problems*, Newark : PhD. Thesis, The State University of New Jersey, 2005.
27. **Copsey, K.** *Tutorial On Particle Filters*, Birmingham : NCAF January Meeting, Aston University, 2001.

28. **M. S. Arulampalam, S. Maskell, N. Gordon, and T. Clapp.** *A Tutorial on Particle Filters for Online Nonlinear/ Non-Gaussian Bayesian Tracking*, IEEE Transactions on Signal Processing, Vol. 50, pp. 174-188, 2002.
29. **A. Doucet, S. Godsill, and C. Andrieu.** *On Sequential Monte Carlo Sampling Methods for Bayesian Filtering*, Statistics and Computing, Vol. 10, pp. 197–208, 2000.
30. **S. Godsil, A. Doucet, M. West.** *Methodology for Monte Carlo Smoothing With Application To Time-Varying Autoregression*, International Symposium on Frontiers of Time Series Modelling, 2000.
31. **B. P. Carlin, N. G. Polson, D. S. Stoffer.** *A Monte Carlo Approach To Nonnormal and Nonlinear State-Space Modeling*, Journal of The American Statistical Association, Vol. 87, No. 148, 1992.
32. **F. Gunnarsson, N. Bergman, U. Forssell, J. Jansson, R. Karlsson, and P. Nordlund.** *Particle Filters for Positioning, Navigation and Tracking*, IEEE Transactions on Signal Processing, Vol. 50, pp. 425-437, 2002.
33. **Chen, Z.** *Bayesian Filtering: From Kalman Filters to Particle Filters, and Beyond*, 2003.
34. **Pupala, R. N.** *Introduction To Wireless Electromagnetic Channels & Large Scale Fading*, 2005.
35. **Felloni, B.** *Fading Models*. Espoo : Helsinki University of Technology, 2004.
36. **I. Guvenc, C.T. Abdallah, R. Jordan, and O. Dedeoglu.** *Enhancements to RSS Based Indoor Tracking Systems Using Kalman Filters*, GSPx and International Signal Processing Conference, 2003.
37. **P. Barsocchi, S. Lenzi, S. Chessa, and G. Giunta.** *Virtual Calibration for RSSI-Based Indoor Localization with IEEE 802.15.4*, ICC, pp. 1 - 5, 2009.

38. **K. Whitehouse, and D. Culler.** *Calibration As Parameter Estimation In Sensor Networks*, WSNA, pp. 59-67, 2002.
39. **D. A. Faihan, and A. A. Adel.** *Tuning Of Lee Path Loss Model Based On Recent RF Measurements In 400 MHz Conducted In Riyadh City, Saudi Arabia*, Arabian J. Science and Eng., Vol. 33, pp. 145-152, 2008.
40. **G. Mao, D. O. Anderson, and B. Fidan.** *Path Loss Exponent Estimation For Wireless Sensor Network Localization*, The International Journal of Computer and Telecommunications Networking, Vol. 51, pp. 2467-2483, 2007.
41. **Trees, H. L. Van.** *Detection, Estimation, and Modulation Theory*, New York : John Wiley and Sons, 1968.

APPENDICES

APPENDIX A: CRAMER-RAO LOWER BOUND (CRLB) FOR LOCALIZATION

In Appendix A we derive CRLB for comparison reason. We will only give the derivation of the important steps, not the intermediate steps. For the detailed information and derivation refer to [3], [41].

CRLB provides a lower bound on the covariance matrix of any estimator of parameter θ . CRLB is the inverse of the Fisher information matrix $\mathbf{F}(\theta)$. In our case the parameter $\theta = l = [x \ y]$ is the (x,y) coordinate location of the target and \hat{l} can be estimated from the observations s_j that are the RSSI measurements from the target to the j th reader in our localization problem.

Then the Fisher information matrix can be written as

$$\mathbf{F}(l) = \begin{bmatrix} F_{xx} & F_{xy} \\ F_{yx} & F_{yy} \end{bmatrix} \quad (\text{A.1})$$

For our case Fisher information matrix is calculated as

$$\mathbf{F}(l) = \begin{bmatrix} -E \left(\frac{\partial^2 \ln p(s|l)}{\partial x \partial x} \right) & -E \left(\frac{\partial^2 \ln p(s|l)}{\partial x \partial y} \right) \\ -E \left(\frac{\partial^2 \ln p(s|l)}{\partial y \partial x} \right) & -E \left(\frac{\partial^2 \ln p(s|l)}{\partial y \partial y} \right) \end{bmatrix} \quad (\text{A.2})$$

where $p(s|l)$ is the probability density of the observation vector s conditioned on the target location l that is to be estimated. The observation vector is $s = \{s_1, \dots, s_r\}$, where r is the number of RFID readers in the system.

For x coordinate of the target, CRLB states the inequality

$$\text{var}(\hat{x}) \geq [\mathbf{F}(l)^{-1}]_{xx} = \frac{F_{xx}}{F_{xx}F_{yy} - F_{xy}^2} \quad (\text{A.3})$$

For y coordinate of the target, CRLB states the inequality

$$\text{var}(\hat{y}) \geq [\mathbf{F}(l)^{-1}]_{yy} = \frac{F_{yy}}{F_{xx}F_{yy} - F_{xy}^2} \quad (\text{A.4})$$

For l location of the target, CRLB states the inequality

$$\text{var}(\hat{l}) = \text{var}(\hat{y}) + \text{var}(\hat{x}) \geq \frac{F_{xx} + F_{yy}}{F_{xx}F_{yy} - F_{xy}^2} \quad (\text{A.5})$$

So, in order to calculate the elements of Fisher information matrix in (9.2) that are F_{xx} , F_{yy} , and F_{xy} we start with writing the density $p(s|l)$.

$$p(s|l) = \prod_{j=1}^r \frac{1}{\sqrt{2\pi}\sigma} \exp \left[-\frac{\left(s_j - \alpha + 10 \log \left(\frac{d_j}{d_0} \right) \right)^2}{2\sigma^2} \right] \quad (\text{A.6})$$

where d_j is the distance from the target location (x, y) to the j th reader location (x_j, y_j) .

$$d_j = \sqrt{(x_j - x)^2 + (y_j - y)^2} \quad (\text{A.7})$$

We denote the mean value of the RSSI observation from the j th reader as \bar{s}_j .

$$\bar{s}_j = \alpha - 10n \log \left(\frac{d_j}{d_0} \right) \quad (\text{A.8})$$

Taking the natural logarithm of the density $p(s|l)$ we get

$$\ln p(s|l) = \ln \left(\frac{1}{\sqrt{2\pi}\sigma} \right)^3 - \frac{1}{2\sigma^2} \sum_{j=1}^r (s_j - \bar{s}_j)^2 \quad (\text{A.9})$$

Then we find the expected value of the second derivatives of the natural logarithm to give the Fisher information matrix elements as:

$$F_{xx} = -E \left(\frac{\partial^2 \ln p(s|l)}{\partial x \partial x} \right) = \left(\frac{10n}{\sigma \ln 10} \right)^2 \sum_{j=1}^r \left[\frac{(x_j - x)^2}{(x_j - x)^2 + (y_j - y)^2} \right] \quad (\text{A.10})$$

$$F_{yy} = -E \left(\frac{\partial^2 \ln p(s|l)}{\partial y \partial y} \right) = \left(\frac{10n}{\sigma \ln 10} \right)^2 \sum_{j=1}^r \left[\frac{(y_j - y)^2}{(x_j - x)^2 + (y_j - y)^2} \right] \quad (\text{A.11})$$

$$F_{xy} = F_{yx} = -E \left(\frac{\partial^2 \ln p(s|l)}{\partial x \partial y} \right) = \left(\frac{10n}{\sigma \ln 10} \right)^2 \sum_{j=1}^r \left[\frac{(x_j - x)(y_j - y)}{(x_j - x)^2 + (y_j - y)^2} \right] \quad (\text{A.12})$$

$$\text{var}(\hat{l}) \geq \frac{\left(\frac{\sigma \ln 10}{10n} \right)^2 \left(\sum \left[\frac{(x_j - x)^2}{(x_j - x)^2 + (y_j - y)^2} \right] + \sum \left[\frac{(y_j - y)^2}{(x_j - x)^2 + (y_j - y)^2} \right] \right)}{\sum \left[\frac{(x_j - x)^2}{(x_j - x)^2 + (y_j - y)^2} \right] \sum \left[\frac{(y_j - y)^2}{(x_j - x)^2 + (y_j - y)^2} \right] - \left\{ \sum \left[\frac{(x_j - x)(y_j - y)}{(x_j - x)^2 + (y_j - y)^2} \right] \right\}^2} \quad (\text{A.13})$$

By the equations of CRLB it is seen that the location estimation lower bound depends on

- RSSI measurement noise standard deviation σ_0
- Signal propagation log-distance path loss parameter n
- Number of readers k_{RDR} used in the localization system
- The relative target location (x, y) and the reader locations (x_j, y_j) .

Square root of (A.13) is used in the thesis to compare with RMS error.